SIMULATING THE HYDROLOGICAL RESPONSE TO CLIMATE CHANGE IN A SOUTHERN ALBERTA WATERSHED

KATHARINE A. FORBES
B.Sc., University of Lethbridge, 2005

A Thesis
Submitted to the School of Graduate Studies
of the University of Lethbridge
in Partial Fulfillment of the
Requirements for the Degree

MASTER OF SCIENCE

Department of Geography
University of Lethbridge
LETHBRIDGE, ALBERTA, CANADA

ABSTRACT

The current body of research in western North America indicates that water resources in the Oldman Basin are vulnerable to the impacts of climate change. The objectives of this thesis were to parameterize and verify the ACRU hydrological modelling system for the 256 km^2 Beaver Creek watershed, a tributary to the Oldman River. The ACRU model successfully simulated monthly volumes of the observed hydrological record (r^2 =0.78), and simulated the behaviour of the mean annual hydrograph with sufficient accuracy to assess the mean change in future hydrological response over 30-year simulation periods. A range of global climate model (GCM) projections were used to perturb the 1961-1990 baseline climate record using the delta downscaling technique, which resulted in the input for future hydrological simulations. Five potential future hydrological regimes were compared to the 1961-1990 baseline conditions to determine the net effect of climate change on the hydrological regime of the Beaver Creek catchment over three time periods of 2020, 2050 and 2080. Despite annual projections for a warmer and wetter climate in this region, the majority of the simulations indicated that the seasonal changes in climate resulted in a shift of the seasonal streamflow distribution. The results indicated an increase in winter and spring streamflow volumes and a reduction of summer and fall streamflow volumes over all time periods, relative to the baseline conditions (1961-1990) in 4 of the 5 scenarios.

ACKNOWLEGEMENTS

This research was generously supported by grants held by Dr. Stefan Kienzle from the Alberta Ingenuity Centre for Water Research (AICWR). Additional financial support was provided by the University of Lethbridge School of Graduate Studies and the Dean of Arts and Science. I have had the privilege to be guided by a team of scientists who have enriched my academic experience beyond my expectations and provided me with many wonderful memories and lessons that I will not soon forget. I would like to extend my gratitude to Dr. Joe Rasmussen for his contributions and insight on this project. A very special thank you to Dr. Jim Byrne for the thoughtful guidance and encouragement throughout this project, and in particular the trip to the American Geophysical Meeting. I also gratefully acknowledge the commentary and helpful suggestions from Dr. Daniel Fagre in the final stages of the thesis. Finally to my supervisors, Dr. Stefan Kienzle and Dr. Craig Coburn, who successfully provided me with two entirely complimentary perspectives and a continuous source of energy and inspiration. I would also like to thank the Department of Geography and in particular Matthew Letts, Suzan Lapp, Jackie Montain, Guy Duke and Margaret Cooke.

A significant part of my graduate experience has been influenced by the graduate student community and in particular the "boys of W565B" Franco, Kean, Ryan and Rob who made each day an adventure. I would also like to thank my friends and family whom without I would surely have spontaneously combusted. As a final thought, the years between 2005 and 2007 saw me retire from a 10-year track and field career and complete a Master of Science, both of which, three years ago I would have told you would never happen. So, the adage is true…*anything* is possible.

TABLE OF CONTENTS

LIST OF FIGURES

LIST OF TABLES

LIST OF EQUATIONS

CHAPTER 1

Introduction

1.1 Introduction

Fresh water is essential to societies and ecosystems (Gleick, 1993), the supply and demand of future water resources will be directly affected by the impacts of climate change (IPCC, 1997; Arnell, 1999). The projected changes in global climate may cause significant alterations to regional hydrological regimes (Loaiciga *et al.,* 1996; Xu, 2000), potentially reducing the availability of fresh water resources (Gleick, 1993). Changes in regional hydrology could have far reaching implications for agricultural production, fish and wildlife and municipal and industrial water supplies (Xu, 2000; Field *et al.,* 2007).

The Intergovernmental Panel on Climate Change (IPCC) has declared that water quantity and quality in North America are particularly vulnerable to the effects of climate change (IPCC, 1997; Field *et al.,* 2007). In midcontinental, semi-arid regions, temperature driven increases in evapotranspiration may result in reductions of surface and groundwater stores (IPCC, 1997). Snowmelt dominated regions are also particularly vulnerable to the effects of increased temperatures as they affect snowpack accumulation and melt rate (Barnett *et al.,* 2005).

Water resources in the semi-arid Canadian Prairies are vulnerable to the impacts of climate change as a significant volume of the annual runoff is derived from mountain snowmelt. In the westernmost province of Alberta, water supply is under increasing pressure due to population growth as well as increasing agricultural and industrial demands (AENV, 2003; Schindler and Donahue, 2006). Over the past century, streamflows have declined in the major rivers throughout the province over the summer

months when agriculture and industry demands are greatest. Subsequent low flows over this period can have serious implications for aquatic species as in-stream flows are in insufficient to meet ecosystem needs (Schindler and Donahue, 2006). Previous research which examined the effects of climate change on the mountain headwaters of the Oldman Basin indicated that water supply may be reduced due to a reduction of snowpack (Lapp *et al.,* 2005).

Hydrological models provide a means to evaluate the relationship between the hydrology and climate in a catchment (Leavesley, 1994). Modelling the effects of climate change on the hydrology of a catchment governed by snowmelt and rainfall precipitation, a diversity of land uses, soil types and topography will improve the understanding of future climate change impacts in the Oldman Basin. Simulating the response of hydrology to future climate hinges on the accuracy of modelling current conditions (Whitfield *et al.,* 2003). If sufficient model accuracy is obtained in simulating observed streamflow records, the model can be run with scenarios representing potential future climates (Leavesley, 1994).

The impacts of climate change on regional hydrology are most commonly assessed by combining the output from general circulation models (GCMs) with a physically-based hydrological model (Xu, 1999a; Loukas *et al.,* 2002). Scenarios derived from GCMs provide the only projection of changes in climate due to changing atmospheric composition (IPCC-TGICA, 1999). While GCMs are proficient at simulating large-scale continental and hemispheric processes, they are unable to generate projections of future climate at the scale required for regional hydrological studies (Carter *et al.,* 1994). Regionalization techniques are used to transfer the signal from large-scale

GCMs to a local scale climate in order to provide regionally representative input into a hydrological model (Wood *et al.,* 1997). Results of hydrological simulations will provide a projection of the impacts of changing atmospheric composition on the hydrological regime in a southern Alberta catchment.

1.2 Research Objectives

The principal objective of this thesis was to quantify the impact that changes in future climate on the hydrology of a small catchment with a diversity of land uses, topography, soils and thus hydrological processes. The impact of climate change on hydrology was investigated using the ACRU hydrological modelling system (Schulze, 1995), which was run with five GCM-derived scenarios of future climate. This research was the initial step in a larger research project with the objective of modelling the impacts of climate change throughout the Oldman Basin. This research also provided the first application of the ACRU model in Canada. The results of the thesis were achieved through the completion of two primary sub-objectives.

The initial sub-objective was to parameterize the hydrological modelling system for a small catchment in the Oldman Basin. The majority of this research involved the application of a spatially distributed modelling approach by delineating hydrological response units. All climate, land use and soils data were spatially parameterized to reflect spatial and temporal accuracy of runoff in the catchment. Once the parameterization was complete, the modelling system was verified against streamflow observations to evaluate modelling accuracy.

The second research sub-objective was to derive scenarios of future climate for the investigation of streamflow response to climate change. This objective involved the regionalization of large-scale GCM output to represent catchment-scale changes in climate. Five scenarios of future climate derived from GCMs were used to estimate the range of plausible future regional climate changes. Simulations of future hydrological conditions for the time periods 2020, 2050 and 2080 were compared to a baseline (1961-1990) simulation to determine the net change of hydrological processes in the catchment.

1.3 Thesis Structure

The organization of this thesis is presented as a sequence of five chapters that explain, in a journal paper format, the two major objectives of the thesis. Beginning with this chapter, the thesis topic and main objectives are introduced. The second chapter consists of a review of literature pertaining to the major concepts, methods and information required for the completion of this thesis. The literature reviewed covers the subjects of global climate change and the hydrological cycle, climate change and the western Prairie Provinces, hydrological modelling, climate scenario development and regionalization techniques.

The third chapter, and first journal paper, explains in detail the parameterization methods and verification results of the modelling system. The fourth chapter, and second journal paper, is an application of the parameterized modelling system to five scenarios of future climate. The results of the fourth chapter indicate the range of changes to future hydrology that could be expected in the study area. The final chapter provides a synthesis of the conclusions that can be drawn from this research. Also included in this chapter are

recommendations for future research directions. The format of this thesis required some repetition, as the two journal papers were written as stand-alone articles.

CHAPTER 2

Literature Review

2.1 Introduction

The scientific literature regarding the concepts and methods pertaining to the application of GCM-derived climate scenarios in a hydrological model for the investigation of the impacts of climate change on hydrology are reviewed in this chapter. The topics of global climate change and the hydrological cycle are explained, followed by a review of observations and projections of future climate and hydrology in southern Alberta. This information was reviewed to provide a background on the study of climate change and how deviations in climate may affect water availability in the study area. Also reviewed are hydrological modelling principles, relevant processes and the modelling system used in this thesis. This is followed by a description of the general circulation models, climate scenario selection and techniques for regional downscaling. The final section provides a summary of the topics reviewed. The references included in this chapter refer to key contributions in the science, which support the selection of the research questions, methods and techniques applied in this thesis.

2.2 Climate Change

2.2.1 Global Climate Change and the Hydrological Cycle

The most recent report by the Intergovernmental Panel on Climate Change (IPCC) made several conclusions based on climate change observations reported by recent scientific research (IPCC, 2007). The previous IPCC assessment in 2001 concluded that a global surface warming of 0.6°C occurred between the years 1901 and

2000. The most recent 100-year linear trend (1906-2005) indicated an increase in global average temperature of 0.74°C, likely influenced by the record-breaking temperatures in 11 of the last 12 years. Model projections indicate that global average temperature is likely to increase by 0.2°C (mean model projection) per decade over the next twenty years, and hydrological systems have been identified as one of the most vulnerable systems to increasing temperatures (IPCC, 2007).

A warmer atmosphere is capable of holding a greater amount of water vapor, and accordingly the link has been made between the projected increase in atmospheric temperature and a potential intensification of the hydrological cycle (Arnell, 1999; Held and Soden, 2000; IPCC, 2001; Douville *et al.,* 2002). Recent observations of atmospheric water vapour have indicated an increase at the surface and in the upper troposphere since the 1980s (IPCC, 2007). The theoretical assumption of this change in the global hydrological cycle is that temperature enhanced evapotranspiration rates will increase the precipitable water in the atmosphere leading to increased global average precipitation (Loaiciga *et al.,* 1996; Kundzewicz and Somlyody, 1997; Dore, 2005). However, it is a combination of atmospheric circulation, latitude, regional physiography, climatic and land use conditions that determine the regional hydrologic regime (Loaiciga *et al.,* 1996). Thus the effect of warming on the hydrological cycle results in a regionally variable distribution of precipitation (Loaiciga *et al.,* 1996; Andreasson *et al.,* 2004).

There is considerable uncertainty about the impacts of climate change on hydrological processes at the regional and watershed scales (Loaiciga *et al.,* 1996; Arnell, 1999; IPCC, 2001; Douville *et al.,* 2002). Observed global precipitation patterns have shown a reallocation of precipitation, indicating that dry areas have become drier and wet

areas are receiving more precipitation (Dore, 2005). It is anticipated that warming in the mid- and high – latitudes could affect soil moisture, groundwater levels and the timing of runoff due to the effects of increased temperatures on evapotranspiration and precipitation (Dore, 2005).

2.2.2 The Water Balance Equation

The linkage between the global hydrological cycle and regional scale processes poses a considerable challenge for hydrologists (Dingman, 2002). The water balance equation provides a quantitative means to evaluate hydrological regime of a region (Leavesley, 1994; Dingman, 2002). The quantification of runoff provides an indication of available water resources in a region (Dingman, 2002).

$$P + G_{in} - (Q + ET + G_{out}) = \Delta S \qquad \text{[Eq. 2.1]}$$

Where P is precipitation (liquid and solid), G_{in} is ground-water inflow (liquid), Q is stream outflow (liquid), ET is actual evapotranspiration (vapour), G_{out} is groundwater outflow (liquid) and ΔS is the change in storage (liquid and solid) (Dingman, 2002). The water balance equation is the common conceptual foundation of many hydrological models (Leavesley, 1994). This equation also forms a logical framework for the assessment of the impacts of climate change on water resources within a region.

2.2.3 Climate Change and the Regional Hydrological Balance

The impact of climate change on freshwater resources in North America is expected to be regionally variable (Field *et al.,* 2007). Consistent with their 1997 report on the regional impacts of climate change, the IPCC conclude, with very high confidence that warming will result in a reduction of snowpack and earlier release of snowmelt in western mountainous basins (Field *et al.,* 2007). Similar conclusions were made by Barnett *et al.* (2005), who further illustrated that water availability in the Canadian Prairies will be compromised due to the effect of higher temperatures on snowpack accumulation, snowmelt and soil moisture. The changes in climate and the impact on hydrology in snowmelt-dominated regions, specifically the Canadian Prairies, have been examined in the climate and hydrologic records (e.g. Burn, 1994; Akinremi *et al.,* 1999; Zhang *et al.,* 2000, 2001a). Observed records of climate and hydrology illustrate the regional interactions between variables of the water balance and provide an estimate of potential future changes in the hydrological regime (Yue *et al.,* 2001; Zhang *et al.,* 2001a).

2.2.4 Observations of Climate and Hydrology in Western Canada

2.2.4.1 Temperature

In a recent analysis of historical climate observations, Schindler and Donahue (2006) concluded that the western Prairies have warmed between 1°C and 4°C since the turn of the 20th century. Gan (1998) found that, between the years of 1949 and 1989, four of the seven climate stations examined in southern Alberta showed a significant increasing trend (α=0.05) in the months between November and June. Warming trends

over recent decades (1949-1989) were also found by Gan (1995) in the winter months throughout western Canada. The trends in the historical observations of temperature in the Prairies, and in particular the western Prairies, reveal that the climate is warming; less certain are the trends in precipitation and the concomitant effects on hydrology.

2.2.4.2 Precipitation

Mekis and Hogg (1999) and Zhang *et al.* (2000) both concluded that annual precipitation in Canada has increased over the 20th century. However, observations in the Prairie Provinces have not indicated a consistent direction in the precipitation trend. Akinremi *et al.* (1999) conclude that, between the years 1921-1995, precipitation in the Prairies has increased on average by 0.60mm/year. They note that the beginning of the time series may be influenced by the extreme drought between the years 1929-1938 which would exaggerate the slope of the time series. Gan (1998) found that between the months of November to June (1949-1989), trends in monthly precipitation were scattered with some stations indicating decreasing trends in one or two months while other stations exhibited no trend (α=0.05). Climate observations in southern Alberta (Lethbridge) indicated that between the years 1909-2003 there was a reduction of 18.2% in total accumulated precipitation over the period (Schindler and Donahue, 2006). They also found that over half of the stations analyzed in the western Prairies exhibited between a 14 and 24% total reduction in precipitation over the same 95-year period.

Akinremi *et al.* (1999) determined that snow cover on the Prairies decreased significantly over the period 1961-1995. Akinremi *et al.* (2001) conclude that annual rainfall has increased by 16% (51mm) over the 40-year period between 1956 and 1995

and the number of rainfall events has increased by 29% annually. They also concluded that the largest increase in rainfall volume and number of events occurred between the months of January to April and speculated that this trend may be attributed to warming. The spatial distribution of the trends indicated that the western Prairies experienced the largest increase in both amount and number of events over the 40-year analysis. Brown and Goodison (1996) reconstructed snow cover for southern Canada and concluded that since 1970, winter and spring snow cover in the prairies has decreased. They further concluded that the decreases are within the range of natural variability.

Both studies by Akinremi *et al.* (1999) and Brown and Goodison (1996) indicated trends of decreasing snow cover, yet the trends of annual precipitation volume are dissimilar. The disparity of the trends may be influenced by beginning the trend analysis during a period of drought as indicated by Akinremi *et al.* (1999) or conversely in a wet period. Also, large-scale, multi-decadal indices such as the Pacific North America and Pacific Decadal Oscillation have been shown to influence precipitation behaviour in western Canada (Brown and Goodison, 1996; Bonsal *et al.,* 1999; Bonsal and Wheaton, 2005). The spatial and temporal scales as well as the size of the samples are different and thus, conflicting results between studies are not necessarily illogical.

2.2.4.3 Evapotranspiration and Soil Moisture

Gan (1998) modelled evapotranspiration in the Canadian Prairies, over a 40-year period (1949-1989), and found decreasing trends of actual evapotranspiration. They concluded that this trend might be attributable to a reduction of soil moisture. In the months of April, May, July and August, potential evapotranspiration exceeded actual

evapotranspiration, illustrating the limiting effects of soil moisture in this region. The study also found that in Alberta, at 13 sites, mean annual evapotranspiration was 350mm/year while mean annual precipitation was only 450mm/year, which illustrated the significance of evapotranspiration in the water balance of this region (Gan, 1998; 2000). In a recent study, Burn and Hesch (2007) concluded that in the southern Prairies, modelled lake evaporation decreased over the 30-year period predating the year 2000, and indicated that wind speed had a greater effect on the trends than vapour pressure deficit. Overall, the studies of Burn and Hesch (2007) and Gan (1998) illustrate that evapotranspiration plays a complex role in the water balance of the Prairies and is influenced by regional changes in climate and the availability of moisture.

2.2.4.4 Hydrology

Several studies have indicated that, over recent decades, streamflow has declined in several western Canadian waterways (Westmacott and Burn, 1997; Gan, 1998; Zhang *et al.*, 2001a; Burn and Hag Elnur, 2002). Rood *et al.* (2005) examined streamflow observations in western North America and concluded that 21 of 26 river systems in the province of Alberta exhibited negative trends in discharge over the past century, a mean annual reduction of 0.22% per year. Zhang *et al.* (2001a) also found declining trends in annual streamflow in southern Alberta between the years 1947-1996. They postulate that the trends in southern Alberta as well as declining trends observed throughout southern Canada were attributed to warming and the associated increase in evaporation. Correlations of temperature and streamflow records in the Prairies led Westmacott and

Burn (1997) to conclude that southern Alberta is an area of concern for future declines in streamflow.

The effects of increased temperatures have also influenced the timing of hydrological response. Burn and Hag Elnur (2002) found that maximum flows in April exhibited an increasing trend and October flows showed a decreasing trend (1969-1997) in southern Canadian rivers. Burn (1994) studied the peak runoff events in western Canada and concluded that the onset of the freshet is occurring earlier in recent years and that this trend is likely attributable to climate change. The historical record of the Bow River in southern Alberta has the longest peak streamflow data set in Alberta (beginning in the early 1900's). The advancement of the peak spring snowmelt date on the Bow River was found to have an inverse relationship with the temperature record suggesting that the timing of the peak flood events in the Bow River may be related to air temperature. In the southwestern portion of the Prairies, Zhang *et al.* (2001a) found similar positive trends in streamflow for the month of March (1947-1996).

These trends in the climate indicate that the Prairies have experienced warming throughout the most recent century (Gan 1995; Gan 1998; Schindler and Donahue, 2006). The trends in precipitation volume are difficult to compare due to the variable lengths of observed records. However, the change in precipitation from snow to rain, particularly in the winter and spring months is more consistent in the available literature (Brown and Goodison, 1996; Akinremi *et al.,* 1999; Akinremi *et al.,* 2001). Studies of evaporation trends indicated that changes in climate variables have a considerable impact on the evapotranspiration rate and play a major role in the water balance of this region (Gan 1998; Burn and Hesch, 2007). Hydrometric records have revealed decreasing trends in

annual flow volumes in western Prairie rivers (Rood *et al.,* 2005; Schindler and Donahue, 2006), while a change in the seasonal variability of streamflow has been linked to surface air temperatures (Burn 1994; Zhang *et al.,* 2001a).

Overall, the trends in the current body of research indicate that warming has an impact on the water balance in this region. While the trends are difficult to interpret, they illustrate the potential for climate change to have a significant impact on water availability in this region. To examine the impact of future climate change on Prairie climate and future water availability, studies have used data from GCMs to establish the projected future impacts on climate and water resources.

2.2.5 Future Trends in Climate

Modelled projections of climate change indicate that temperatures in the interior plains of southern Canada will experience the greatest warming (Boer *et al.,* 2000). Verification studies of GCMs in simulating present climate (1961-1990) have indicated considerable variation between the GCMs at simulating seasonal temperature and precipitation over the western cordillera of Canada (Bonsal *et al.,* 2003). To account for the large variability of climate projections for the province of Alberta, Barrow and Yu (2005) examined the range of GCM projections assuming that all model projections were equally uncertain. They concluded that warming by as much as 3°C to 5°C could occur by the 2050s (2040-2069). The projections for future precipitation are less certain in the direction and magnitude of change, as the modelled range extends from -10% to +15% over the 2050 period. The impact of these changes on other components of the water

balance is a critical link to understanding the implications for future water availability in this region.

2.2.6 Physiological Response of Vegetation

In addition to radiative forcing, changing plant physiology associated with elevated CO_2 concentrations could have an impact on the climate system (Betts *et al.,* 2000, 2007; Forster *et al.,* 2007). Enhanced atmospheric CO_2 concentrations are associated with an increase in stomatal conductance and a corresponding suppression of transpiration in plants (Drake *et al.,* 1997; Schulze and Perks, 2003). This has been shown to increase water use efficiency in plants resulting in less demand on soil water storages (Drake *et al.,* 1997; Betts *et al.,* 2007). The effect of enhanced CO_2 concentrations on the water consumption of vegetation is an important feedback in the assessment of the future regional water balance, and remains a key uncertainty in the interpretation of hydrological impact studies.

2.2.7 Potential Impacts for Water Availability

It is expected that climate change will affect the regional water balance through changes in the timing, form and volume of precipitation, rate of evapotranspiration and volume of soil moisture (Regonda *et al.,* 2005; Dore, 2005; Merritt *et al.,* 2006). A focus of recent research has been on mountainous basins and semi-arid regions, as water availability in these areas is expected to be vulnerable to climate change (IPCC, 1997). A significant portion of the surface water resources in the Oldman Basin are generated from snowmelt originating in the eastern slopes of the Rocky Mountains.

The effects of warming on mountainous regions are well documented (Mote, 2003; Barnett *et al.,* 2005; Regonda *et al.,* 2005; Stewart *et al.,* 2005). In western North America, 75% of monitored climate stations report a decline in snow water equivalent (Solomon *et al.,* 2007). The impacts of warming on snowpack accumulation are more sensitive in temperate, lower elevation ranges where the freezing line is in close association with altitude (Solomon *et al.,* 2007). Lapp *et al.* (2005) concluded that, in scenarios of future climate, the most dramatic reductions in snowpack occurred at lower elevations in the mountain headwaters of the Oldman Basin. Therefore, it is plausible that changes in snowpack accumulation may also affect prairie catchments, particularly those with montane headwaters. In comparison with rainfall, snow is less susceptible to being sublimated and thus is an effective source for soil and ground water recharge (Dingman, 2002). Research in the eastern slopes of the Rocky Mountains indicated that due to higher winter temperatures, the projected increases in winter precipitation (Lapp *et al.,* 2002) would not compensate for the decline in winter snowpack and that this may culminate in a decline in surface water supply in the Oldman Basin (Lapp *et al.,* 2005).

Nemec and Schaake (1982) evaluated the effect of perturbed climate variables on runoff and found that arid climates were sensitive to changes in temperature and precipitation. Elevated temperatures are assumed to increase the rate of evapotranspiration (Middelkoop *et al.,* 2001). This may hold true for potential evapotranspiration, which is determined by the atmospheric demand. However, actual evapotranspiration, particularly in arid regions, is regulated by the availability of soil moisture (Dingman, 2002).

Despite expected increases in future precipitation, Sauchyn *et al.* (2000) projected increasing aridity in the Canadian Plains due to higher potential evapotranspiration. Soil moisture in the Prairies is an effective indicator of changes in surface hydrology and is important for evaluating the vulnerability of the Prairies to climate change (McGinn *et al.,* 2001). Using a climate change scenario, which projected warming with no increase in precipitation, McGinn *et al.* (2001) modelled soil moisture in the province of Alberta and found a reduction of 10% relative to baseline conditions.

2.2.8 Synthesis

The trends in the observed records and the projections from GCMs illustrate the potential for climate change to cause a decrease in water availability in the Prairie Provinces, and southern Alberta in particular. It is beneficial to examine the trends in the observations of climate variables and streamflow as they illustrate the general hydrological behaviour of a region (Dingman, 2002). However, observations cannot account for future changes in atmospheric composition. Projections of future hydrological conditions based on scenarios from GCMs provide an indication of the future response to climate change (IPCC-TGCIA, 1998). However, the scale and uncertainty of these models is simply too large to project changes in future hydrological processes at the regional and local scales (Loaiciga *et al.,* 1996; Kundzewicz and Somlyody, 1997; Dingman, 2002).

Predicting future water availability requires the quantification of runoff at the watershed scale (Dingman, 2002). The hydrology of arid and semi-arid regions has a higher sensitivity to changes in climate because the ratio of precipitation to runoff is

lower relative to humid climates (Wigley and Jones, 1985). The temporal variability of precipitation in a semi-arid climate emphasizes the importance of soil and groundwater storages. These non-linear interactions between the regional water balance components increase the complexity in quantifying water balance processes (Beven, 2001; Bronstert *et al.*, 2002). The sensitivities and complex interactions between the variables of the water balance can be more accurately quantified by modelling the processes of the regional water balance.

2.3 Hydrological Modelling

Within the context of hydrology, modelling can be used to conceptualize the physical processes of the hydrological cycle (Dooge, 1992; Viessman and Lewis, 2003). Hydrological models are integral to hydrological sciences as they are an effective means to 1. understand complex hydrological process and their inter-behavior, 2. quantify hydrological processes that are otherwise difficult to monitor, 3. extend hydrological science to ungauged catchments and 4. assess future hydrological change (Beven, 2002). Of particular importance, hydrological models provide a quantitative framework to assess the interaction between hydrology and climate (Leavesley, 1994). Scenarios of future climate change can be simulated by hydrological models to examine the effects of future climate on the hydrological regime (Xu, 1999b).

2.3.1 Classification of Hydrological Models

Hydrological models can be classified according to their structure (i.e. simulation basis), spatial and temporal scales (Leavesley, 1994; Dingman, 2002). The modelling

approach is a major consideration in the applicability of a hydrological model to a research problem. Several classifications of models have been applied to water resources research, each with a specific approach to the mathematical representation of hydrological processes.

2.3.1.1 Conceptual Models

Conceptual models use simplified, a priori relationships of physical processes to represent the interactions in the hydrological cycle (Leavesley, 1994; Dingman, 2002). The parameterization of these models typically requires calibration using observed data and can be difficult to obtain for complex catchments (Boyle *et al.,* 2001). The calibration process often requires lengthy observed records, therefore, limiting their transferability to many catchments (Abbott *et al.,* 1986). Furthermore, it is possible to achieve a reasonable simulation of the observed hydrograph while misrepresenting the actual hydrological processes that govern the catchment (Gan *et al.,* 1997). While conceptual models have proven successful in verification studies of streamflow observations, their parameters are not necessarily directly related to the physical characteristics of the catchment (Refsgaard and Knudsen, 1996). Consequently, the utility of such a model in climate change studies is limited due to a significant amount of uncertainty with respect to the interaction of model inputs. A solution to this problem would be to ensure that all conceptually described processes are explicitly represented as physical processes (Schulze, 1995).

2.3.1.2 Empirical Models

Empirical hydrological models, such as those based on linear regression, use relationships between observed data sets (Leavesley, 1994; Dingman, 2002). The mathematical representation of the hydrological system in empirical models is based on experimental data and thus is highly dependent on data for calibration (Viessman and Lewis, 2003). They also do not consider the physical processes and laws that govern the processes of the hydrological cycle (Leavesley, 1994). Therefore, the transferability and applicability of these models to future climate conditions is constrained by the conditions of the investigated catchment at the time they were developed (Leavesley, 1994).

2.3.1.3 Physically-Based Models

The final major type of hydrological model is physically-based or process-based, which quantify processes of the hydrological cycle through the application of the physical laws of hydrology (Leavesley, 1994; Dingman, 2002). The parameters of physically based models represent physical catchment characteristics such as topography, soils, vegetation and geology (Refsgaard and Knudsen, 1996). The advent of the physically-based approach to hydrological modelling was in response to the need for modelling in complex catchments and transferability of these models to similar catchments without prior gauging (Todini, 1988). These models are designed to overcome the deficiencies of other modelling approaches (Abbott *et al.,* 1986).

Physically-based models have the highest requirements for input data, limiting their application to basins with available physiographical and hydroclimatical data (Leavesley, 1994; Liu and Todini, 2002; Romero *et al.,* 2002). Physically-based models

are well suited to climate change impact studies as they capture the interaction of key climate variables with the physiography of the catchment (Liu and Todini, 2002). Through mathematical representations of interception, infiltration, soil-water redistribution, evaporation, transpiration, snowmelt, surface, subsurface and groundwater flows, these models capture the nonlinear transformation of precipitation to streamflow (Leavesley, 1994).

2.3.2 Spatial Representation of Hydrological Processes

Major challenges in hydrological simulation stem from the non-linear responses influenced by antecedent conditions and spatially heterogeneous topography, land cover, soils and the stochastic nature of precipitation (Beven, 2001). Watershed processes can be represented as a single homogenized unit in a lumped hydrological model. The spatially distributed behaviour of precipitation and heterogeneous catchment processes may limit the application of lumped models in complex catchments (Kite and Kouwen, 1992). Distributed hydrological modelling provides a means to capture the spatial variability within a catchment by dividing the catchment into smaller units (Kaleris *et al.,* 2001; Dingman, 2002). By increasing the spatial representation of catchment processes, both the understanding of catchment dynamics and simulation accuracy are improved (Boyle *et al.,* 2001).

Distributed hydrological modelling can be approached by subdividing the catchment into units of homogenous hydrological response. Hydrological response units (HRUs) represent areas of soils, topography and vegetation that have a homogeneous hydrological response to precipitation (Limaye *et al.,* 1996; Beven, 2002). Several studies

have used GIS modelling techniques to delineate HRUs (Flugel, 1997; Arnold *et al.,* 1998), establishing the fundamental units for spatial distribution of hydrological processes within the catchment.

The application of process-based, distributed hydrological models is well suited to studying the hydrological response to a changing environment (Bitfu and Gan, 2001). While the intensive data inputs and detailed parameterization of sub-grid processes have been criticized (Beven, 1989; 1996), the distributed nature of physical processes is required for simulation of non-stationary conditions (e.g. climate change) in complex catchments (Refsgaard *et al.,* 1996). Furthermore, the assessment of future climate changes in water availability requires a hydrological model capable of simulating the spatial and temporal interactions of precipitation (rainfall and snowmelt), topography and soil storage (Gleick, 1986).

2.3.3 The ACRU Agro-hydrological Modelling System

The ACRU agro-hydrological modelling system was developed by the Department of Agricultural Engineering (now the School of Bioresources Engineering and Environmental Hydrology) at the University of KwaZulu-Natal, Republic of South Africa, in the late 1970s, and has since been revised and updated for more extensive applications. The ACRU model is a physical-conceptual, multi-purpose, multi-level, model that can simulate total evaporation, soil water and reservoir storages, land cover and abstraction impacts on water resources, and streamflow at a daily time step (Schulze, 1995; Smithers and Schulze, 1995). The most recent version of the ACRU model (V. 334) includes the simulation of rain and snow precipitation to broaden the application of

the ACRU model to environments where snowmelt is a major contributor to local hydrology.

2.3.3.1 Theoretical Principles of ACRU

The structure of the ACRU model is conceptual in that it theorizes the processes that govern the hydrological cycle, and is physical in that the physical laws of hydrology are mathematically represented within the conceptual framework (Schulze, 1995). The ACRU model is based upon a multi-layer soil water budget with specific variables governing the atmosphere-plant-soil water interfaces. The current version of ACRU simulates the principal hydrological processes of rain and snow interception, infiltration, snowpack accumulation and soil water storages, unsaturated and saturated soil water redistribution, total evaporation (a daily summation of snow sublimation, plant transpiration from rooting zone (s) and evaporation from the soil surface) and temporally discrete runoff generation.

The spatial representation of precipitation, soils and land cover is facilitated by operating ACRU as a distributed model, where the modelled catchment is subdivided into either subcatchments or HRUs. Precipitation, the most important and sensitive input (Schulze, 1995), can be distributed spatially by interpolating values using surfacing techniques in a GIS.

2.3.3.2 Physical Processes of the ACRU Model

The ACRU model applies a generalized daily water budget approach and considers the spatially and temporally variable response of hydrological processes within

the watershed. Daily precipitation events are assessed for each HRU individually, beginning with initial abstractions by canopy interception and stormflow (runoff) production. The resulting volume can be conceptualized as the net daily precipitation available for infiltration or runoff.

The snow routine, recently adapted into the latest version of ACRU, follows a water retention concept where the storage capacity of liquid water in the snowpack regulates the quantity and timing of water release from the snow storages. The physically-based sub-modules consider the form of precipitation, i.e. rain versus snow, evaporation, snowpack accumulation, metamorphosis and melt. The form of precipitation is determined by a curvilinear calibration method of local observations, which include two principal variables: the threshold mean daily temperature where 50% of the precipitation occurs as snow, and the range of temperatures within which mixed precipitation occurs.

On a daily basis, snow accumulation, snowmelt, sublimation and snow density are calculated. Snowmelt is defaulted to initiate above the 0°C threshold temperature. The rate of melt is increased after rain-on-snow events, when maximum compaction is achieved or when the retention capacity of free water in the snowpack is met. Alternatively, the rate is decreased under forested canopies to account for slower ablation dynamics in the forested environment. Water is released from the snow cover based on the threshold maximum retention capacity for liquid water in the snowpack.

The ACRU method for runoff production is divided into rapid and delayed flows and is labeled stormflow for ease of explanation. The estimation of stormflow depth is adapted from the Soil Conservation Service (SCS) method (United States Department of

Agriculture, 1985) which relates runoff potential to the soils relative wetness. Stormflow is generated if net daily precipitation (gross precipitation minus interception loss) exceeds the daily soil water deficit for stormflow production. The deficit is the difference between the soil water content at porosity and the volume of water in the soil column of the critical depth for runoff production (Schulze, 1995).

This depth is estimated from recommended values in the user documentation, and often the first approximation is defaulted to the depth of the A-horizon. These values are estimated from a matrix of the dominant runoff producing mechanism of the HRU (subcatchment) and consider climate, soil properties and vegetation density. The apportionment of stormflow between same day response and delayed stormflow (interflow) is controlled by the interflow potential of the HRU, and is quantified by the stormflow response coefficient. This is based on the soil and slope characteristics of the HRU/subcatchment (Schulze, 1995).

Soil water redistribution is categorized as saturated or unsaturated soil water movement. After infiltration, soil water in a soil horizon in excess of the field capacity percolates downward at the saturated rate determined by the soils wetness and texture. The rate of unsaturated soil water movement is determined by the wetness of the surrounding soil horizons. If the water volume in the subsoil store exceeds the field capacity, it is allocated to the groundwater store. Baseflows are generated from the groundwater store at an exponentially declining rate, which can be estimated from streamflow recession analysis.

The ACRU total evaporation method involves the application of a meteorologically determined reference potential evaporation with empirically-derived

crop coefficients (Doorenbruis and Pruit, 1977) to approximate the daily water used by the vegetation. Daily potential reference evaporation is determined by the application of one of the several available reference evaporation methods ranging from the United States Weather Bureau Class A evaporation pan, to physically-based methods such as the Penman equation (Penman, 1948). Due to the availability of A-pan data in South Africa, the ACRU model uses the A-pan as the reference evaporation to which all other methods are internally adjusted.

ACRU partitions daily evaporation and transpiration relative to the vegetations phenology (i.e. biomass) expressed by the LAI. The apportionment of transpiration between soil horizons is controlled by the root mass distribution between the respective horizons. Soil water in excess of the permanent wilting point is considered available for transpiration by plants. Evaporation of snow is estimated from both intercepted snow and snow which reaches the ground (throughfall).

2.3.3.3 ACRU and Climate Change

As the model was designed to be highly responsive to changes in land use and climate it is well suited to climate change impact studies (Schulze and Smithers, 2000). When accurately calibrated and verified, the ACRU model was capable of simulating all the elements of the hydrological cycle, and thereby establishing the fundamental basis for hydrologic impact studies (Schulze and Perks, 2003).

ACRU has been used extensively in South Africa for water resource assessments (Everson, 2001; Kienzle *et al.*, 1997; Schulze *et al.*, 2004), flood estimation (Smithers *et al.*, 1997; 2001), land use impacts (Kienzle and Schulze, 1991; Tarboton and Schulze,

1993), nutrient loading (Mtetwa *et al.*, 2003) and irrigation supply (Dent, 1988). The ACRU model was applied by Schulze and Perks (2003) to investigate the impacts of climate change impacts on hydrology and water resources in South Africa. They utilized scenarios of future climate to drive the ACRU model to make projections of future hydrological conditions and availability of water resources.

2.4 Climate Scenario Development

2.4.1 Climate Scenarios

The assessment of the regional impacts of climate change requires the use of climate scenarios (IPCC-TGCIA, 1999). Climate scenarios are considered plausible representations of the impact that future greenhouse gas concentrations will have on the climate (Carter *et al.,* 1994; Mearns *et al.*, 2001,). The climate scenarios themselves have a large impact on the outcome of the impact study (Wood *et al.,* 1997).

Impact assessments make use of three main types of climate scenarios; incremental, analogue and those derived from GCMs (Feenstra *et al.,* 1998; Hulme *et al.*, 1999; IPCC-TGCIA, 1999). Incremental (synthetic or arbitrary) scenarios apply incremental changes in meteorological variables and are typically combined with observation over a baseline period (Feenstra *et al.,* 1998; IPCC-TGCIA, 1999). Incremental scenarios are typically applied in sensitivity and threshold analyses however these scenarios can be potentially unrealistic as they may not produce physically reasonable estimates of future climate (Mearns *et al.,* 2001).

Analogue scenarios make use of observed historical data (e.g. paleoclimatic) as a scenario for future climate (Feenstra *et al.,* 1998; IPCC-TGCIA, 1999). However,

scenarios based on relationships in the historical period may not necessarily reflect changes associated with greenhouse gas forcing of the future climate (IPCC-TGCIA, 1999, Mearns *et al.,* 2001). More common are the application of scenarios derived from climate models, in particular general circulation models (GCMs), as they simulate the climatic response to changing greenhouse gas concentrations (Feenstra *et al.,* 1998; IPCC-TGCIA, 1999; Mearns *et al.,* 2001).

2.4.2 General Circulation Model Scenarios

The impacts of climate change on regional hydrology are most commonly assessed by combining the output from GCMs with a physically-based hydrological model (Gleick, 1986; Xu, 1999a; Loukas *et al.,* 2002). Coupled, atmosphere-ocean GCMs are a highly complex, mathematical representation of atmosphere, ocean, ice cap, and land surface processes based on physical laws and physically-based empirical relationships (IPCC, 1997; Feenstra *et al.,* 1998; Mearns *et al.,* 2001). Presently, GCMs are the most advanced tool for evaluating the changes in climate associated with changing concentrations of atmospheric gasses (IPCC-TGCIA, 1999; Xu, 1999a; Mearns *et al.,* 2001; Meehl *et al.,* 2007).

2.4.2.1 Climate Change Experiments

Previous modelling of global climate by GCMs applied equilibrium-response experiments where an abrupt doubling of atmospheric CO_2 was used to simulate the response of the climate to elevated greenhouse gas concentrations (Carter *et al.,* 1994; IPCC-TGCIA, 1999). These experiments have since been replaced by transient

experiments, which simulate the dynamic processes, both spatially and temporally, of heat and moisture exchange from the ocean to the atmosphere. This simulates a more realistic lag between changing atmospheric composition and climate (Feenstra *et al.,* 1998; IPCC-TGCIA, 1999; Mearns *et al.*, 2001).

In recognition of the gradual increase of greenhouse gas and aerosol concentrations in the atmosphere over the industrial period, warm start experiments simulate the historical evolution of atmospheric composition (IPCC-TGCIA, 1999; Mearns *et al.,* 2001). The current simulations of future climate change are determined by socio-economic experiments, which represent plausible future changes in human economic behaviour, specifically the projected future greenhouse gas and aerosol emissions and land cover change (IPCC-TGCIA, 1999; Mearns *et al.,* 2001).

The IPCC generated a group of emissions scenarios (SRES) (Nakicenovic *et al.,* 2000) to represent future demographic, politico-economic, societal and technological changes (IPCC-TGCIA, 1999; Mearns *et al.*, 2001; Barrow and Yu, 2005). The SRES emissions scenarios are grouped into four families representing the principal driving focus; these being either global or regional and environmental or economic (Nakicenovic *et al.,* 2000). Six illustrative scenarios (marker scenarios) have been chosen to represent equally plausible future anthropogenic behaviour (Nakicenovic *et al.*, 2000). These scenarios of future greenhouse gas and aerosol emissions determine the radiative forcing on the energy balance of the Earth-atmosphere-ocean system and thus, through their application in GCMs, determine the effects on global climate (Nakicenovic *et al.,* 2000; Barrow and Yu, 2005).

2.4.3 Regionalisation Techniques

While GCMs are proficient at simulating upper level circulation on a global or continental scale (von Storch *et al.,* 1993), they are often inaccurate at simulating regional climate (Wood *et al.,* 1997). The most practical application of climate scenarios would be to use raw GCM output in a hydrological model (Xu, 1999a). However, the large areal coverage of GCMs, typically between 250 x 250 km and 600 x 600km per gridcell (IPCC-TGICA, 1999), are not well suited to the needs of impact modelling (Cohen, 1990; Von Storch *et al.,* 1993; Epstein and Ramirez, 1994; Xu, 1999a; Xu 1999b; Hay *et al.,* 2000; Mearns *et al.*, 2001). Factors influencing the regional accuracy of GCMs include the size of the region, location and the variables required (IPCC-TGICA, 1999).

Several techniques have been developed to resolve the disparity of scales between GCMs and the needs of impact modelling commonly referred to as the process of "downscaling" or "regionalisation" (Giorgi and Mearns, 1991; IPCC-TGICA, 1999). Regionalization techniques commonly used in hydrological assessments of climate change impacts include statistical downscaling, dynamic downscaling and perturbation methods (Xu, 1999b).

2.4.3.1 Statistical and Dynamic Downscaling

Statistical downscaling refers to the empirical process of correlating synoptic scale GCM outputs to local climate observations (Xu, 1999b; Hay *et al.,* 2000). Dynamic downscaling is an alternative method, which uses higher resolution, limited-area models or regional climate models driven by the boundary conditions of the GCM (Wood *et al.,*

1997; Xu, 1999b). Wilby *et al.* (1999) conclude that statistical downscaling is advantageous compared to dynamic downscaling as it is considerably less computationally intensive, and higher resolution (point) climate records can be obtained. The dynamic method still results in resolution, which may not be sufficient for hydrological applications and may require further downscaling (Xu, 1999b). The final, and most simplistic, method involves the construction of change fields that represent the difference (or ratio) between the control simulation (1961-1990) of the GCM and that of a future period (Wood *et al.,* 1997).

2.4.3.2 The Delta Method

The delta method involves constructing a perturbed climate record by applying monthly change fields derived from GCM output, to an observed climate record (Wood *et al.,* 1997; Xu, 1999a). These change fields reflect the difference between future climate projection from the GCM and the baseline simulation. The assumption of this method is that the GCM is more effective at capturing the relative signal of climate change and not the absolute changes in future climate (Hay *et al.,* 2000). For the simulation of future precipitation it does not allow for any change in future variability (i.e. number of raindays) (Andreasson *et al.,* 2004). However, this method is advantageous as the monthly mean of the observations are perturbed, while preserving the local and regional variability of the climate station (Leavesley, 1994; Hamlet and Lettenmaier, 1999; Loukas *et al.,* 2004).

In a comparison of statistical downscaling and the delta technique in mountainous catchments, Hay *et al.,* (2000) concluded that both methods exhibit similar seasonal

trends (precipitation and temperature) but the delta method resulted in more conservative simulations of future runoff. Hamlet and Lettenmaier (1999) elected to use the delta technique in a hydrological simulation of the Columbia Basin as they concluded that neither statistical nor dynamical downscaling were able to resolve decadal and inter-annual climate variability. Although the most simplistic, the delta method has been applied in several recent climate change impact assessments on hydrology involving a physically-based hydrological model (Morrison *et al.*, 2002; Miller *et al.,* 2003; Schulze and Perks, 2003; Andreasson *et al.,* 2004; Cohen *et al.,* 2006; Merritt *et al.*, 2006; Belatos *et al.,* 2006).

2.5 Summary

The simulation of climate change impacts on regional hydrology requires a broad range of knowledge on the pertinent scientific principals and methods employed in past and present research. A fundamental understanding of the impacts of climate change on hydrology, and the current trends in the climate and hydrological regime of the southern Alberta are required for the selection of methods and techniques used to construct the scenarios and simulate the regional hydrology. Furthermore, a thorough understanding of the physical processes simulated by the hydrological model and techniques of scenario development qualify the assumptions and limitations of the method, making the interpretation of the results all the more robust.

CHAPTER 3

Parameterization and verification of the ACRU hydrological modelling system for a catchment in southern Alberta, Canada

3.1 Introduction

Changes in global climate could have serious implications for ecosystems and societies due to increased variability of regional water supply (Gleick, 1986; Xu, 1999b). Concerns for water supply in Alberta, Canada, have grown in importance due to the increased demands from a rapidly growing population and economy, and the threat of increased climate variability in the near future (AENV, 2003). Trends observed in the hydrometric records over the last century have indicated declining annual, and specifically summer season, flows in rivers reaching east of the Rocky Mountains (Rood *et al.,* 2005; Schindler and Donahue, 2006). These trends illustrate the necessity for the quantification of hydrology in this region and, in particular, the investigation of the impacts that climate change will have on regional water availability. Hydrological modelling offers a means to conceptualize the interaction between climate and hydrology and quantify the impacts of climate change on water resources within a region (Leavesley, 1994; Xu, 1999a).

The Oldman River Basin is the largest watershed in southern Alberta and is a tributary to the South Saskatchewan Basin. Across the basin there is a distinct eastward transition of ecozones, from alpine and subalpine headwaters, to montane foothills and semi-arid grasslands (Byrne *et al.*, 1989). A significant portion of the runoff volume in the Oldman Basin is derived from alpine snowpack (Byrne *et al.,* 1999; Rock and Mayer, 2006), and several studies have modelled the impacts of climate change on snowpack in

the alpine headwater regions and indicated that changes in climate may have a negative impact on water resources (Byrne *et al.,* 1999; Lapp *et al.,* 2005). Downstream of the mountain headwaters, lotic systems driven by both snowmelt and rainfall events (hybrid) in the montane region are an important source of water for local livestock and wildlife, and are vital to the health of riparian areas and aquatic ecosystems (Elias, 1999). A complete understanding of the hydrological processes in the Oldman Basin is essential for determining water supply considering the unknown future supply and demand (Rock and Mayer, 2006).

Hydrological simulation, in catchments with diverse physiography, is conceptually challenging due to the variation of hydrological response with heterogeneous land cover, soils and topography (Beven and Kirkby, 1979; Beven, 1989). Physically-based, distributed hydrological models offer a mathematical conceptualization of the hydrologic cycle and provide a means to assess the impacts of climate change on the hydrological processes within a basin (Bathurst *et al.,* 2004). Physically-based models simulate the nonlinear transformation of precipitation to streamflow through mathematical representations of interception, infiltration, soil-water redistribution, evapotranspiration, snowmelt, surface, subsurface and ground water flow processes (Xu, 1999b). These models are suited to climate change impact studies because they can simulate the response of hydrology to a range of un-stationary conditions (Bitfu and Gan, 2001).

The accuracy of hydrological simulation is dependent on input data and resolution of the physical characteristics of the catchment (Daly *et al.*, 1994; Schulze, 1995; Beven, 2002). Distributed hydrological modelling captures the spatial variation of hydrological

processes and facilitates simulations in mountainous watersheds (Gurtz *et al.*, 1999). The emphasis of spatial techniques in the parameterization of model inputs has been shown to increase the accuracy of spatially distributed hydrological simulations (Nurmohamed *et al.,* 2006). Geographic Information Systems (GIS) have been used to facilitate the parameterization of distributed models in catchments with complex terrain (Kienzle *et al.,* 1997; Nurmohamed *et al.,* 2006). Spatial interpolation techniques are a common method to estimate areal precipitation from irregularly spaced rainfall gauges and provide the most important input for distributed hydrological modelling (Tabios and Salas, 1985; Dirks *et al.*, 1998).

Previous assessments of climate change impacts have integrated the catchment-scale accuracy of hydrological models with downscaled projections of future climate from large-scale, global climate models (Gleick, 1986; Loukas *et al.,* 2002; Morrison *et al.*, 2002; Schulze and Perks, 2003; Toth *et al.*, 2006; Nurmohamed *et al.*, 2007). These simulations provide a scientific means of examining the effects of changing atmospheric composition on hydrology and water resources (Gleick, 1986; Xu, 2005). The predicative ability of this technique is largely dependent on the accuracy of the hydrological model in reproducing observed streamflows (Bathurst *et al.,* 2004). A model suitable in structure and complexity is needed for the simulation of hydrology in a catchment with spatially heterogeneous physiography and hydrological processes found within the montane and grassland regions of the Oldman Basin.

The ACRU agro-hydrological model (Schulze, 1995) is applied in this study as it is capable of simulating all elements of the regional water balance with a focus on soil moisture and evapotranspiration routines. The ACRU model has been used extensively in

climate change impact studies (Schulze *et al*., 2000; Schulze *et al.*, 2004; Schulze and Perks, 2003) and hydrological assessments (Kienzle and Schulze, 1991; Kienzle *et al.*, 1997; Everson, 2001). The daily water budget implemented by the ACRU model is well suited to assessing the impacts of climate change on the hydrological processes in a hybrid, tributary catchment to the Oldman River Basin. Parameterization and verification of the ACRU model for the spatially heterogeneous hydrological processes in the catchment will provide a simulation tool for the assessment of climate change impacts on water supply.

3.2 Objectives

The first objective of this study was to parameterize the ACRU modelling system for a single catchment in the Oldman River Basin using available climate, land use and soils data. The second objective was to verify the accuracy of the simulation by comparing the simulated streamflows with historical observations. The modelling performance was evaluated to determine if the accuracy obtained was sufficient to apply this parameterization to scenarios of a perturbed climate. This was the preliminary step in establishing the foundation for a streamflow sensitivity assessment of future climate scenarios.

The following sections describe the characteristics of the study catchment, explain the key concepts of the ACRU modelling system and outline the parameterization of major contributing input variables into the ACRU model. This is followed by a description of the results and analysis of modelling performance in the study catchment over the verification period.

3.3 Methods

3.3.1 Study Area

The Beaver Creek study catchment, centered at 49° 44'N, 113° 52'W, is a tributary of the Oldman River (Figure 3.1), a major headwater to the South Saskatchewan River Basin. The creek is maintained by perennial flow with a bimodal hydrograph indicating the influence of both snowmelt and rainfall processes (Water Survey of Canada, 2007), and is classified as a hybrid stream. The Beaver Creek catchment has two ungauged, ephemeral tributaries (Five Mile Creek and Nine Mile Creek), both originate on the west-facing slopes of the catchment (Figure 3.1). The headwaters stem from the higher elevation slopes of the Porcupine Hills, east of the Front Range of the Rocky Mountains, Alberta.

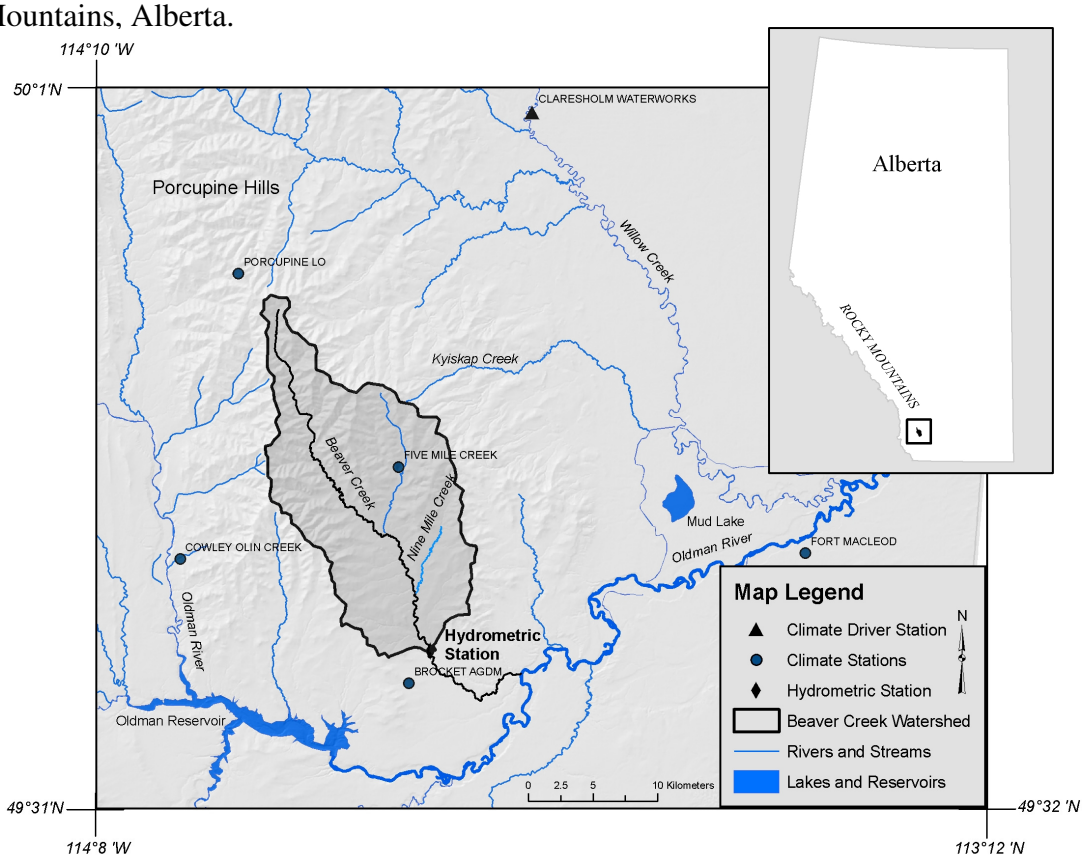

Figure 3.1: Map of Beaver Creek study catchment; climate stations, main hydrological features and gauging station.

The Beaver Creek catchment has a drainage area of 254km^2, defined by the Water Survey of Canada hydrometric station (05AB103) located near Brocket, approximately 7km northwest of its confluence with the Oldman River (Figure 3.1). Elevations in the Beaver Creek catchment range between 1500m AMSL, with the general aspect facing south, south-east with slopes ranging from flat in the lower elevation rangelands to 28° on the southwest and north east facing hillslopes.

The Porcupine Hills are characterized by the rapid spatial transition from montane forest to aspen parkland and prairie grasslands, creating a unique habitat for many plant species native to southern Alberta (Elias, 1999). The upper elevations receive adequate precipitation to sustain mixed coniferous and deciduous forests (Elias, 1999). Conifer forests consisting mainly of white spruce (*Picea glauca)*, lodgepole pine (*Pinus contorta* var. *latifolia*), balsam fir (*Abies balsamea)* with some Douglas-fir (*Pseudotsuga menziesii*) cover the upper elevation slopes and ridge-tops. Thick deciduous forests of Trembling Aspen (*Populus tremuloides)* are found on the mid-elevation slopes with grassland ecosystems located on dry lower slopes (Elias, 1999). Predominant plant species in the grasslands include rough fescue (*Festuca scabrella),* timothy (*Pheleum pretense)* and brome (*Bromus inermis)* grasses. Cultivated crops are also established on the lower plains that include canola (*Brassica napus),* barley *(Hordeum distychum)* and wheat (*Triticum aestivum).*

Soils in the forested regions of the upper elevations are of the Luvisolic soil order. The surface horizon has a sandy clay loam texture, while the subsurface horizon is dominantly clay. The mid-elevation grasslands are typical of a Chernozemic soil order that exhibits higher clay fractions in the surface horizon while the subsurface soils are a

mix of silty clay loam and sandy loam. The cultivated croplands have a sandy clay loam surface horizon and a clay loam subsurface horizon, to be expected in areas under cultivation. The grassland region is characterized by shallower surface horizons relative to the forested area while the subsurface horizon is deeper. The cultivated areas have the deepest surface horizons but shallower subsurface horizons relative to the grasslands.

Elevations in the Porcupine Hills are similar to the foothills in the eastern slopes of the Rocky Mountains, however, their geologic stratification more closely resembles the Cypress Hills and Milk River Ridge (AENV, 2000). The Porcupine Hills were not formed by the processes of mountain building, but through glacio-fluvial erosion during the last ice age. Consequently the underlying sandstone bedrock is not thrust-faulted but in the original, horizontal orientation as it was deposited (Elias, 1999).

The Claresholm Water Works climate station, located approximately 25km northeast of the Beaver Creek catchment, was chosen to drive the hydrological model. This station received an average annual precipitation (1971-2000) volume of 428.2mm, apportioned between 304.9 mm of rain and 123.4mm of snow (Environment Canada, 2007). Mean daily temperature in the summer is 16°C and –6.1°C in the winter. A complete 40-year climate record overlapping the hydrometric observations and similar physiographic characteristics to the Beaver Creek catchment made this the most representative climate station for the simulation.

In the southern Alberta region, winter precipitation events result primarily from frontal air masses while summer events are typically convective in nature (i.e. June lows). The proximity to the eastern slopes of the Rocky Mountains exposes the area to the rainshadow effect and high Chinook winds (Grace, 1987). Therefore, due to the

orographic influences on this area, it is not uncommon for a deficit in the annual moisture budget due to high evapotranspiration relative to precipitation.

3.3.2 Hydrological Model

The ACRU agro-hydrological modelling system was developed by the Department of Agricultural Engineering (now the School of Bioresources Engineering and Environmental Hydrology) at the University of KwaZulu-Natal, South Africa, in the late 1970s and has been continuously refined and updated. The ACRU model is a multi-purpose, multi-level integrated physical-conceptual model that can simulate total evaporation, soil water and reservoir storages, land cover and abstraction impacts on water resources, and streamflow at a daily time step (Schulze, 1995; Schulze and Smithers, 1995).

The most recent version of the ACRU model includes the simulation of rain and snow precipitation to broaden the application to environments where snowmelt is a major contributor to local hydrology. The structure of the ACRU model (Figure 3.2) is conceptual in that it theorizes the processes that govern the hydrological cycle, and is physical in that the physical laws of hydrology are mathematically represented within the conceptual framework (Schulze, 1995). ACRU is also capable of simulating catchments characterized as a lumped or distributed model. The version of the ACRU model applied in this thesis simulates the principal hydrological processes of rain and snow interception, infiltration, snowpack accumulation and soil water storages, unsaturated and saturated soil water redistribution, total evaporation (a daily summation of snow sublimation, plant

transpiration from rooting zone (s) and evaporation from the soil surface) and temporally discrete runoff generation.

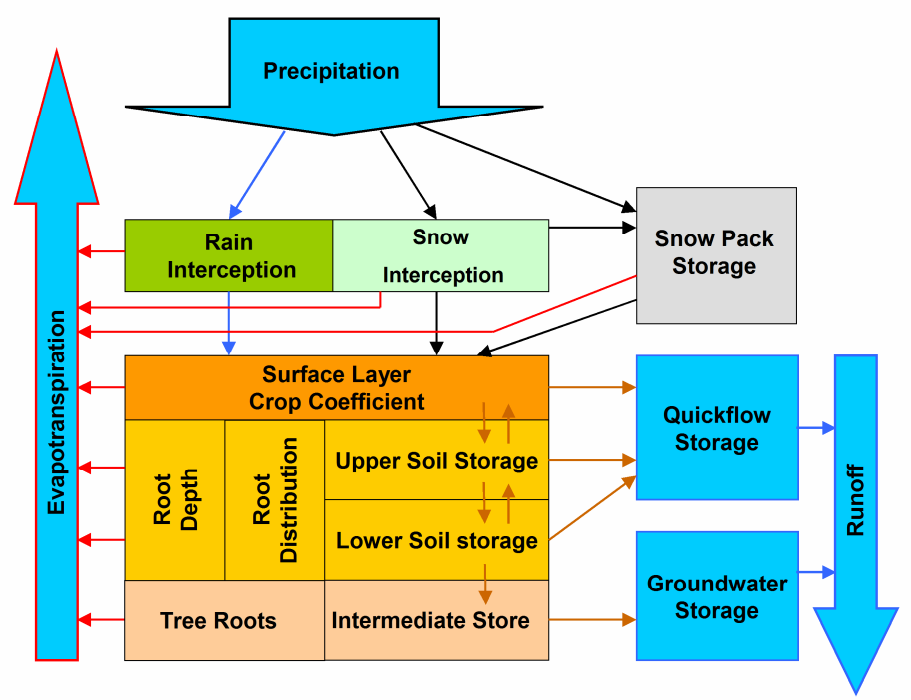

Figure 3.2: Major components of the ACRU agro-hydrological modelling system illustrating the conceptual representation of the water balance.

3.3.2.1 Conceptual Structure of ACRU

The snowmelt routine of the ACRU model is based on a water retention concept where the storage capacity of liquid water in the snowpack regulates the quantity and timing of water release from the snow storages. The snow sub-module uses a temperature-based method to quantify snow accumulation and ablation processes. The snow module considers precipitation form (i.e. discretization between rain, snow and mixed precipitation), the volumetric properties of snowpack (i.e. snow water equivalent, density, depth and liquid water retention), heat and mass balances/exchanges of the

snowpack, and the temporal changes in physical snowpack characteristics that affect storage and melt (i.e. metamorphosis and sublimation). The releases of water from the snow module are added to the net precipitation store of the ACRU structure.

The net portion of precipitation that is not intercepted is modelled in a two-layer soil profile (surface and subsurface). Soil depth and texture of both surface and subsurface horizons determine the three critical volumetric soil water retention constants of total porosity, field capacity and wilting point. Volumetric soil water in excess of the field capacity is redistributed at the saturated rate (determined by texture), while soil water less than field capacity but greater than the wilting point is redistributed at the unsaturated rate both in the upward (subsoil) and downwards directions (surface and subsoil) (Schulze, 1995).

Evapotranspiration takes place from several principal stores of water in the ACRU soil water budgeting routine including previously intercepted snow and rain, snowpack and soil storages. Daily potential evapotranspiration (maximum daily evaporation) is determined using the reference evaporation and empirically derived, monthly crop coefficients. ACRU partitions daily evaporation and transpiration relative to vegetation phenology. The apportionment of transpiration between soil horizons is controlled by the root mass distribution between the respective horizons. Soil water in excess of the permanent wilting point is considered available for transpiration by plants (Schulze, 1995).

Streamflow production by the ACRU model is comprised of simulated runoff (both same day and delayed response) and baseflow volumes. Runoff generation is based on a modified Soil Conservation Service (SCS) procedure by the United States

Department of Agriculture (1985) where runoff potential is conceptualized as a depth, and is a function of the soils relative wetness. Baseflows are generated from saturated drainage out of the rooting zone and added to the groundwater store (Schulze, 1995). The temporal response of surface runoff and baseflows are controlled by empirically derived response coefficients that are fitted to recession curves of the observed hydrographs.

The concepts and physical processes of the ACRU model make it highly responsive to changes in land use and climate (Schulze and Smithers, 1995). When accurately parameterized and verified, the ACRU model is capable of simulating all the elements of the hydrological cycle and in doing so, establishes the fundamental basis for hydrologic impact studies. ACRU has been used extensively in South Africa for water resources assessments (Kienzle *et al.*, 1997; Everson, 2001; Schulze *et al.*, 2004), and also in Chile, Germany, the USA, and New Zealand. The most recent version of the ACRU model, including the snow module, was applied in Canada for the first time in this study. The key physical equations of the ACRU modelling system used in this thesis are presented in Appendix A.

3.3.2.2 Data Requirements and Modelling Pathways

The ACRU modelling system is a multi-level application where multiple pathways or alternative methods can be invoked contingent on the availability of data (Smithers and Schulze, 1995). The model is capable of simulating the catchment processes as a lumped or distributed model. Regardless of the spatial complexity required, the compulsory data required for streamflow simulations commences with

general information that includes the area, elevation and altitude of the catchment or subcatchments.

The required climate data includes daily observations of precipitation, minimum temperature and maximum temperature. The ACRU model includes an option to correct precipitation values on a monthly basis for systematic differences between climate station and catchment (subcatchments). Temperatures can also be corrected for altitudinal differences between catchment (subcatchments) and the climate station using mean regional lapse rates.

The ACRU modelling system has multiple options for the estimation of daily reference potential evaporation that range from A-Pan observations to physically-based methods. The ACRU model uses the United States Weather Bureau Class A evaporation pan as the standard reference potential evaporation to which all other estimation methods are adjusted (Schulze, 1995). To determine daily evaporation, ACRU requires monthly crop coefficients and the proportion of roots in the surface soil horizon. Interception of precipitation by the vegetation canopy can be estimated using a variety of methods, which require either crop coefficients, leaf area index (LAI) or field observations.

The ACRU model requires soil texture and depth information for both the surface (A) and subsurface (B) horizons. From this information the porosity, wilting point, field capacity (of surface and subsurface horizons), fraction of water redistributed from surface to subsurface horizons and from subsurface to groundwater store can be derived from literature or the model documentation (Schulze, 1995; Smithers and Schulze, 1995).

The volume and temporal behaviour of streamflow is simulated using coefficients that are derived from observed hydrographs or values derived from model

documentation. Streamflow observations are also required for the verification of simulated streamflow and optimization of streamflow control variables. The ACRU model conceives of streamflow simulation through the daily soil water budget, and as such, requires daily input. With the exception of climate data, the ACRU model is designed to accommodate monthly-level input by transforming monthly values into 365 daily values internal to the model structure using Fourier Analysis.

3.3.3 Model Parameterization

3.3.3.1 Selected Model Structure for the Beaver Creek Simulations

The ACRU modelling routines selected for the Beaver Creek study were chosen based on the availability of data in this region. The heterogeneity of the catchments physical characteristics (elevation, soil and land cover) required the parameterization of ACRU as a distributed model, which required the delineation of hydrological response units. Spatial modelling techniques were also applied to increase the areal representation of point data. A GIS was used to area-weight all model variables and parameters for input into the distributed modelling system.

The physically-based Penman (1948) method for reference evaporation was selected as the reference evaporation method as it is the preferred technique by the model developers (Schulze, 1995) and has been shown to be the most regionally robust method for southern Alberta (McKenney and Rosenberg, 1993). Canopy interception was estimated using the Von Hoyningen-Huene method, which relates interception to monthly leaf area index values. The parameterization of the remaining ACRU model variables such as soils, land cover and streamflow control parameters were completed

using the available databases, estimates from literature or model documentation (Schulze, 1995; Schulze and Smithers, 1995). All input data and model parameters used in the simulations for the Beaver Creek are presented in Appendix B.

3.3.3.2 Hydrologic Response Units

Hydrologic Response Units (HRUs) are user-defined areas of homogenous hydrological response (Flugel, 1997; Beven, 2002). These are parameterized individually for input into the ACRU modelling system. Three major physiographic data types were utilized in this analysis: a 30m digital elevation model, generalized land cover from the Prairie Farm Rehabilitation Administration, and Integrated Plant Available Water (INTPAW) calculated from the Agricultural Region of Alberta Soil Inventory Database (AGRASID) (Figure 3.3). A GIS was used to delineate these variables and construct a digital file showing the boundaries of the HRU's. The parameterization of all subsequent model input parameters (i.e. soils and land cover) were area-weighted to each HRU, constructing the spatially representative input files for the ACRU modelling system.

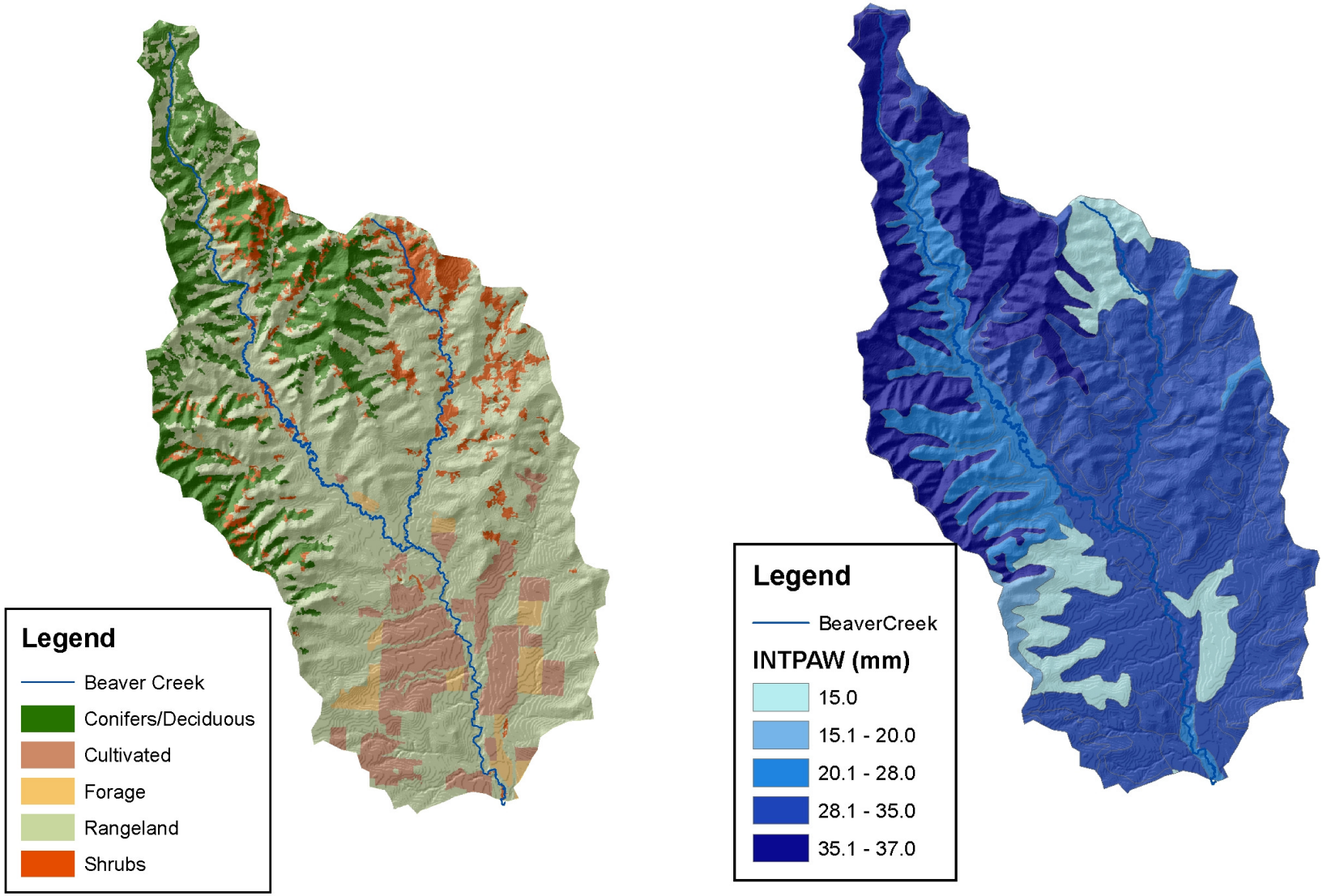

Figure 3.3: Physiographic characteristics of the Beaver Creek catchment including; generalized land use (left) and integrated plant available water (INTPAW) (right).

3.3.3.3 Precipitation

Climate stations in southern Alberta are constructed and maintained by Environment Canada Meteorological Service. There are multiple stations within proximity to the Beaver Creek catchment, with one station positioned within the bounds of the catchment (Figure 3.1). Field inspection of the in basin station revealed that the data quality was insufficient for modelling applications. Communication with the volunteer data collector revealed that measurements were not recorded in a consistent manner, specifically the rainfall gauge was not monitored on a regular basis.

Multiple attempts were made to combine and statistically correlate climate records from stations surrounding the catchment with streamflow observations at the Beaver Creek. It was concluded that the Claresholm Waterworks station, approximately 25 kilometers northeast of the center of the catchment, had the longest and most complete record with the highest association to Beaver Creek streamflows. For these reasons it was selected as the source for climate data used in this study.

Monthly correction factors were calculated to account for discrepancies between precipitation recorded at the climate station and the behaviour of precipitation at each of the HRUs in the catchment. The ANUSPLIN 4.3 interpolation software (Hutchinson, 2004) was used to create climate surfaces of monthly 30-year normals at a 100m-grid cell resolution. ANUSPLIN uses a thin plate splining technique to fit a smoothed spline curve through point climate data using elevation from a digital elevation model as a co-variate. Hutchison (2005) described the thin plate splining algorithm of ANUSPLIN as the substitution of a smoothed, non-parametric function applied to generalized, multi-variate linear regression. The application of the ANUSPLIN algorithm has been an effective

means to estimate unsampled points from multi-variate, observed climate data (Bonsal *et al.,* 2003).

The ANUSPLIN algorithm was applied to thirty-one stations within a 50km buffer of the Oldman Basin, east of the Continental Divide using a 100m-resolution elevation grid as a co-variate. Monthly surfaces of precipitation normals were interpolated with corresponding error surfaces. Using the relationships between grids overlying the individual HRUs and the grid cell that over-laid the climate station, a systematic monthly correction factor, specific to each HRU, was derived to adjust daily precipitation input for each HRU.

The problem of point-to-area rainfall conversion can be addressed using depth-area relationships. The point rainfall depths recorded at the driver station are not a realistic representation of the depth of precipitation received over the entire area of the catchment. To derive an equivalent estimate for the total catchment area, areal reduction factors are often applied (Asquith and Famiglietti, 2000; Veneziano and Langousis, 2004). A simple areal reduction factor (Equation 3.1) was used to correct daily precipitation events. Where P_{corr} is the corrected daily precipitation volume and P is the original volume recorded at the climate station:

$$P_{corr} = P * (1 - (0.005 * P)) \qquad \text{[Eq. 3.1]}$$

This method constructed a precipitation record that is adjusted for each HRU that conserved the variability of the driver station while avoiding unrealistic extremes, potentially created by using point measurements for an entire watershed.

3.3.3.4 Reference Evaporation

The Penman (1948) model was used to simulate daily reference evaporation, expressed in the ACRU model and determine the A-PAN equivalent evaporation (mm/day). The Penman (1948) equation has three major components; 1. the energy budget, 2. mass transfer and 3. the energy budget-weighting factor. The latter component places greater importance on the energy budget component in the summer season (Schulze, 1995). As daily radiation data were not available, the Penman model was applied on a monthly time step. Data requirements for the Penman (1948) equation include monthly values of incoming radiation, air temperature, relative humidity and windspeed.

Modelled solar radiation data, estimated by the publicly available System for Automated Geoscientific Analysis (SAGA, 2007) GIS lighting tool, was used in the monthly Penman equation. This tool calculated the solar radiation input of a monthly mean sun exposure. The SAGA lighting tool produces hourly solar radiation therefore, for each gridcell on the 30m DEM of the catchment, hourly data were summed for each day and monthly totals were then averaged. To account for atmospheric transmissivity, shortwave radiation observations at the Environment Canada climate station in Stavely, Alberta, approximately 35 km north of the Beaver Creek watershed, were compared with the GIS modelled radiation. Differences between modelled and observed monthly average values were between 15% and 20%, therefore the SAGA-derived values were corrected to match the regional observations.

The mass transfer component of the Penman equation describes the flux of vapor from a vegetated surface (Schulze, 1995). The three major variables involved in this

component of the Penman equation are windrun (km/day), saturated vapour pressure and mean daily relative humidity (%). Daily mean windspeed (km/h) was downloaded from the Pincher Creek climate station (Environment Canada), the nearest station with available wind speed data. These values were reduced by 10% to match the nearby to match the wind database provided by Alberta Environment over the Beaver Creek catchment, interpolated by Environment Canada. The final 12 monthly average values were converted to the ACRU format of windrun measured in km/day.

Monthly means of daily average relative humidity were taken from the Stavely climate station, the nearest data source to the study catchment. Ten years of data were averaged to produce 12 monthly values. Saturated vapour pressure is empirically related to observed temperature using Tetens' (1930) equation that is calculated internally within the model structure.

3.3.3.5 Soil Data

Soil data in the agricultural regions of Alberta have been sampled and documented in the AGRASID digital database. Soil polygons over the study area contained multiple sampling sites. These data were aggregated within the boundaries of each soil polygon for dominant texture and horizon depths. Soil polygons were area-weighted to the overlying HRU using a GIS. Soil water redistribution and retention values were all derived from empirical data available from the ACRU Theory documentation, specific to the textural and depth properties of each horizon. This information was compiled by Schulze (1995). The soil horizon depth and surface cracking was field checked at various locations within the Beaver Creek catchment.

3.3.3.6 Land Cover Information

Generalized land cover data was provided by the Prairie Farm Rehabilitation Administration (PFRA). This data is publicly available and was complied by the PFRA in October, 2001. The digital dataset was classified from 30m Landsat 7 imagery into the dominant land cover classifications. These included cultivated cropland, forage, grasslands, shrubs, trees, wetlands, water, non-agricultural lands, clouds and shadows, mud sand/saline, and unclassified areas. Land cover polygons were area-weighted to each HRU using a GIS. The PFRA land cover data was field verified to ensure accuracy across the watershed.

Non-destructive estimates of LAI were collected *in situ* using the LAI-2000 plant canopy analyzer (Li-Cor Inc., Lincoln, NE). Measurements were collected for forest, shrub, grassland and crop canopies for various periods during the growing seasons of 2006 and 2007. Field measurements considered dual-stage canopies with understory vegetation as well as row crops by taking multiple measurements. These measurements were used as field verification for a monthly LAI dataset provided Dr. Anne Smith at the Agriculture and Agri-Food Canada Lethbridge Research Centre (Lethbridge, Alberta).

Monthly crop coefficients were calculated for the dominant vegetation of each land use according to the method outlined in the FAO Irrigation and Drainage Paper No. 56 (Allen *et al.,* 1998) and were adjusted according to the guidelines provided in the ACRU User Documentation (Schulze, 1995). The ACRU model uses the A-Pan reference evaporation and therefore, short-grass reference crop coefficients (Allen *et al.,* 1998) were divided by 1.2 for application in the ACRU model according to the specifications of the model documentation (Schulze and Smithers, 1995).

3.3.3.7 Streamflow Control Variables

The monthly coefficients of initial abstraction, or the amount of water lost to interception, depression storage and infiltration, were estimated from physically applicable ranges provided in the ACRU user documentation. The runoff response depth was estimated from the dominant runoff producing mechanism within the catchment (i.e. climate, vegetation and soil characteristics). Recommended values were provided in the ACRU user documentation (Schulze, 1995). The variables, which control the temporal response of streamflow, were fitted to observed hydrographs. These coefficients are optimized in an iterative process based on graphical analysis of runoff dynamics between observed and simulated hydrographs.

3.3.4 Verification of Streamflow Simulations

The ACRU model was verified against streamflow observations obtained from the Beaver Creek hydrometric station (#05AB013). A complete record of daily observations from the years 1966-2005, for the months March-October, was obtained from the Water Survey of Canada online database (Water Survey of Canada, 2007). Observations were reported as discharge (m^3/sec) and converted to depths (mm) for comparison with the ACRU output.

The effectiveness of the ACRU modelling system at simulating observed streamflows in the Beaver Creek was determined using objective functions consisting of both conservation and regression statistics. Additionally, the verification analysis included other objective functions of modelling performance common to hydrologic modelling (Legates and McCabe, 1999; Krause *et al.,* 2005) and recommended in the

ACRU user documentation (Schulze, 1995). Visual verification of observed versus simulated hydrographs was also conducted for mean daily streamflows, and accumulated daily and monthly mean streamflow volumes.

Descriptive statistics including mean, variance and standard deviation were used in the model verification to compare the distributions of observed and simulated streamflow. A student's t-test determined if the sample means were significantly different. Finally, the discrepancies between observed and modelled streamflows were quantified with mean absolute error.

The coefficient of determination (r^2) was used to indicate the degree of co-variation between observations and simulations. The r^2 is maximized at a value of 1 and represents the proportion of variance in the observed streamflows that were explained by the simulated streamflows. The slope and base constant of the linear regression model were used to describe the nature of the unexplained data. The Nash-Sutcliffe coefficient of efficiency (E) was applied as an advanced objective function analogues to the coefficient of determination (Nash and Sutcliffe, 1970). Values for E range from $-\infty$ to a perfect fit of 1.0. A value of $E < 0$ indicates that that the mean of the observations had greater predictive power than the simulations.

3.4 Results and Discussion

3.4.1 Parameterization

3.4.1.1 Hydrologic Response Units

The final selection of HRUs is illustrated in Figure 3.4, with the general characterization of each response unit given in Table 3.1. The delineation of HRU 1 closely follows the 1500m-elevation contour, forested land use and zone of highest soil water storage potential. This HRU represented the deepest estimated surface soils with the highest precipitation and highest soil water content. A significant proportion of forest biomass was located in this response unit. Down- slope, HRU 2 encompasses the first of two rangeland response units. HRU 3 predominantly spans the headwaters of Five Mile Creek (Figure 3.1). Soil water availability in these HRUs was highest in HRU 2 and thus HRU 3 contained a higher proportion of drought tolerant, perennial shrubs and woody vegetation.

HRUs 4 and 5 represent the transition from the montane slopes and fescue grasslands of the upper reaches to the agricultural land uses further downstream. The separation of these two HRUs follows the division between natural (forage) and cultivated land, as soils and elevation are relatively homogenous for this area. Most importantly, the canopy interception of precipitation and plant physiology were different between perennial (forage) and annual (cultivated) species.

Table 3.1: Major physiographic characteristics of hydrological response units including area, percent area of total catchment, mean elevation, dominant soil type and generalized land cover.

HRU	Area (km^2)	Area %	Elevation (m)	Soil Type	Land Cover
1	60.03	23.63	1500	Clay Loam	Mixed Forest
2	55.88	21.99	1400	Loam	Rangeland
3	61.31	24.13	1400	Clay Loam	Shrub & Rangeland
4	46.42	18.27	1300	Clay Loam	Forage
5	30.43	11.98	1200	Sandy Clay Loam	Cultivations

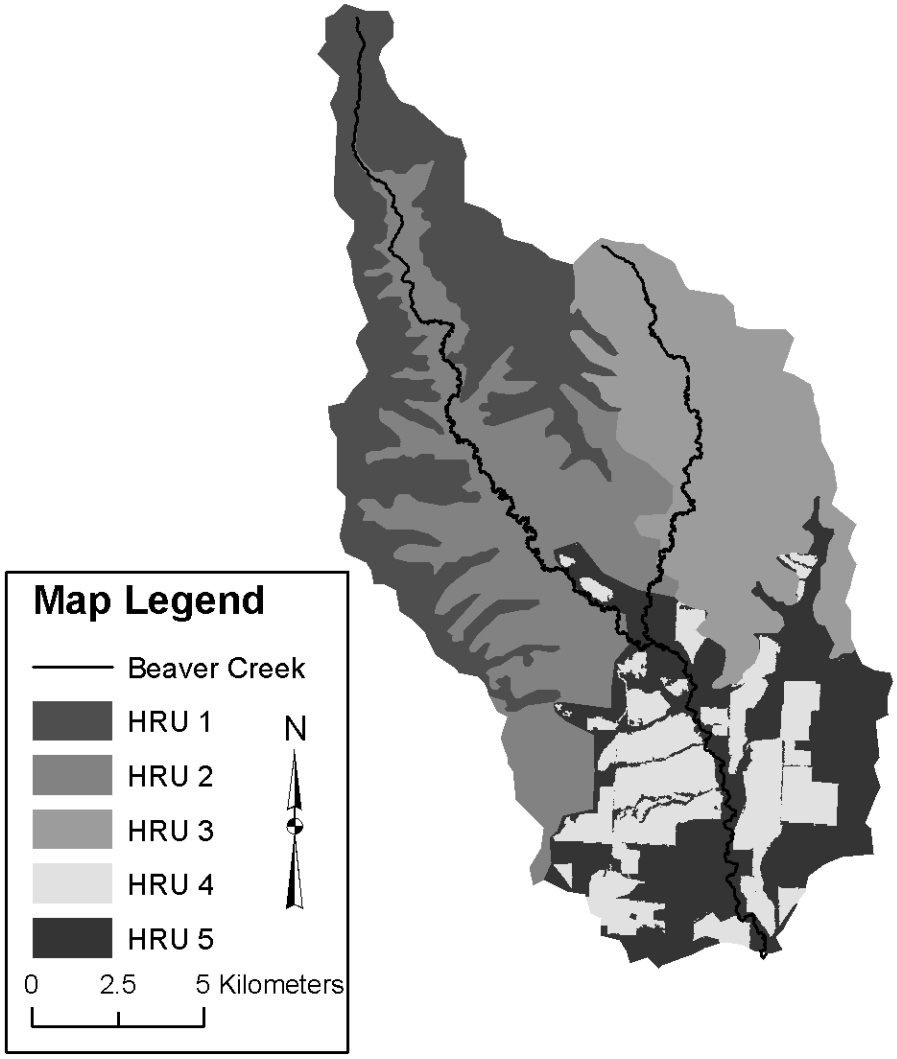

Figure 3.4: Map illustrating the hydrological response units selected for the Beaver Creek catchment.

3.4.1.2 Precipitation Correction

Monthly precipitation adjustment factors that reflected the relationship between the HRUs and climate station are listed in Table 3.2. Overall, the precipitation records of HRUs 1 and 2 received the largest adjustments as these response units were at higher elevations and thus received more precipitation relative to other HRUs. Across the catchment, the greatest monthly adjustments were increases in months of February, March and April while the only notable decreases were in the early winter period (November and December) of HRU 1 and 2. Overall, the differences in precipitation behavior between the lower elevation driver station (1008m) and the mean elevation of the catchment (1451m) were reflected in the precipitation correction values that illustrated the importance of this method in heterogeneous terrain. The ANUSPLIN interpolation algorithm was previously applied to climate data in British Columbia and Alberta by Price *et al.* (2000). They recommended ANUSPLIN as the preferred approach over regression methods, particularly when interpolating between irregularly spaced, high elevation stations.

Table 3.2: Monthly precipitation adjustment factors calculated for each HRU using monthly ANUSPLIN surfaces.

	Jan	Feb	Mar	Apr	May	Jun	Jul	Aug	Sep	Oct	Nov	Dec
HRU 1	1.24	1.39	1.27	1.54	1.24	1.12	0.96	1.09	0.96	1.21	0.97	0.77
HRU 2	1.18	1.38	1.28	1.47	1.26	1.11	1.00	1.09	1.02	1.11	1.19	0.81
HRU 3	1.22	1.40	1.25	1.34	1.23	1.08	0.99	1.04	0.98	1.09	1.17	0.86
HRU 4	1.28	1.50	1.32	1.35	1.30	1.10	1.05	1.06	1.09	1.02	1.09	0.95
HRU 5	1.28	1.50	1.32	1.28	1.29	1.08	1.05	1.02	1.08	1.01	1.24	0.99

3.4.2 Verification Analysis

The Claresholm Waterworks climate station (Figure 3.1) had the highest association between observed precipitation records and the Beaver Creek streamflow records. However, it was observed that approximately one third of the available overlapping climate records exhibited a poor correlation with the observed streamflow at the Beaver Creek. This included years with significant precipitation and associated low streamflow, and vice versa. Therefore, the objective assessment was performed twice, with the first assessment using the entire 40-year record, followed by the removal of mis-matched events and a statistical verification of the remaining representative sample. Details on the removal of outlier events are expanded upon in the proceeding sections.

Objective measures of modelling performance for monthly, accumulated volumes simulated by the ACRU model are provided in Table 3.3 (a). An under-simulation of daily observations (0.42 mm/day) resulted in an 11.19% difference in monthly sample means. The student's t-statistic (p=0.69) indicated that no significant differences were found between the sample means, however, a 7.80% difference between variances decreased the reliability of the t-statistic. The coefficient of determination (r^2=0.47, n=290) indicated that the model explained less than half of the variance in the observations. A positive y-intercept (0.86) and regression coefficient less than unity (0.66), suggested that months with low flow were over-simulated and high flows were under-simulated. The coefficient of efficiency was low (E=0.34) and approached the r^2 illustrating that no systematic errors in the simulation were apparent from this analysis.

The low association between observed and simulated samples, and lack of conservation in the distribution of the observations indicated an inaccuracy with either

the input data or parameterization. The errors in simulation were not systematic as indicated by the close association of E and r^2, and simulation bias was explained by the base constant and regression coefficient. Therefore, errors were likely not attributed to unrepresentative evapotranspiration or soil moisture storages, which would have resulted in systematic over or under-simulations. Extensive sensitivity analysis of the ACRU input parameters have indicated that precipitation is the most sensitive input variable (Schulze and Smithers, 1995). Therefore, the low association between samples was attributed to the location of the climate station, and thus the accuracy of the precipitation input.

A comparison of daily precipitation events at the Claresholm Waterworks climate station and the observed annual hydrographs at the Beaver Creek over the verification period, revealed several years where the precipitation input was not representative of the catchment streamflow behavior. These discrepancies occurred between both magnitude and timing of precipitation events and the streamflow response. It was found that considerable differences in behavior, in 13 of the 40 available years, contributed to the unrepresentative precipitation input when compared in an annual time series against observed streamflow at the catchment. The statistical integrity of the verification assessment was preserved by removing the entire year, in which the major outlying events occurred, from the analysis. The sample size of the verification period was reduced from 40 to 27 years, without selectively choosing discrete events assumed to be erroneous. The 13-year sample of outliers contained both years with above and below normal precipitation conditions.

Upon removal of outlier years, simulated flows were statistically verified for the 27- years of seasonal (March-October) daily observations that were representative. This

resulted in considerable improvement in the accuracy of the simulated streamflow volumes (Table 3.3 (b)). Mean error in simulation (mm/day) was reduced to an under-simulation of 0.086mm. This reduced the magnitude of difference between the monthly means (3.34%). The student's t statistic (p=0.13) also found no significant difference between the means and the difference in variances between each sample was reduced to 4.28%. The coefficient of determination indicated a strong correspondence between observed and modelled monthly flows (r^2 = 0.78, n=206) where the simulation explained 78% of the variance in observed streamflow. A slightly positive regression intercept (y= 0.16) indicated a minor over-simulation of low volume streamflows and the regression coefficient, greater than zero but less than unity (0.90), indicated an under-simulation of high volume streamflows. The coefficient of efficiency (E=0.77) is near optimal as it is 0.01 from the r^2 value. This supports the degree of association determined by the r^2 and indicated that an insignificant amount of systematic error in simulation was calculated.

Table 3.3: Objective measures of modelling performance for (a) 40-year verification, including years with mismatching precipitation – streamflow records, and (b) a 27-year verifications, including only years with matching precipitation – streamflow records.

Monthly Totals of Daily Streamflow		**(a) 40-year**	**(b) 27-year**
Sample Size (months)		290	**206**
Average Error in Flow (mm/day)		-0.42	**-0.09**
Means	Observed (mm)	3.77	**2.59**
	Simulated (mm)	3.35	**2.50**
	% Difference	-11.19%	**-3.34%**
t-statistic		0.69	**0.13**
Standard Deviation	Observed	7.50	**6.48**
	Simulated	7.20	**6.62**
	% Difference	3.98%	**2.12%**
Variance	Observed	56.29	**42.00**
	Simulated	51.90	**43.80**
	% Difference	7.80%	**4.28%**
RMSE		5.85	**3.16**
Coefficient of Determination (r^2)		0.47	**0.78**
Regression Coefficient (Slope)		0.66	**0.90**
Regression Intercept		0.86	**0.16**
Coefficient of Efficiency (E)		0.34	**0.77**

Overall, the ACRU model simulated the behaviour of the Beaver Creek with a reasonable level of accuracy. The mean daily observed and simulated hydrographs showed a close association in the annual volume, timing of peak flow and baseflow period (Figure 3.5 (a)). Small events occurring before Julian day 91 and 122 were under-simulated. While there is an over-simulation of streamflow volume in the rising limb occurring between Julian days 122 and 160, the peak flow date is simulated well in both timing and magnitude as illustrated in the subset (b) of Figure 3.5.

Beyond the peak flow date, the recession limb of the simulated mean hydrograph is under-simulated. Of particular importance, however, the simulated baseflow period in the fall has a close association with the observations. The accumulated daily streamflows illustrate that both years with high and low annual streamflow volumes were simulated accurately (Figure 3.6). Finally, the comparison of mean monthly volumes illustrated that, with the exception of June, the summer and fall streamflow volumes (July, August, September and October) showed a good association between observed and simulated volumes.

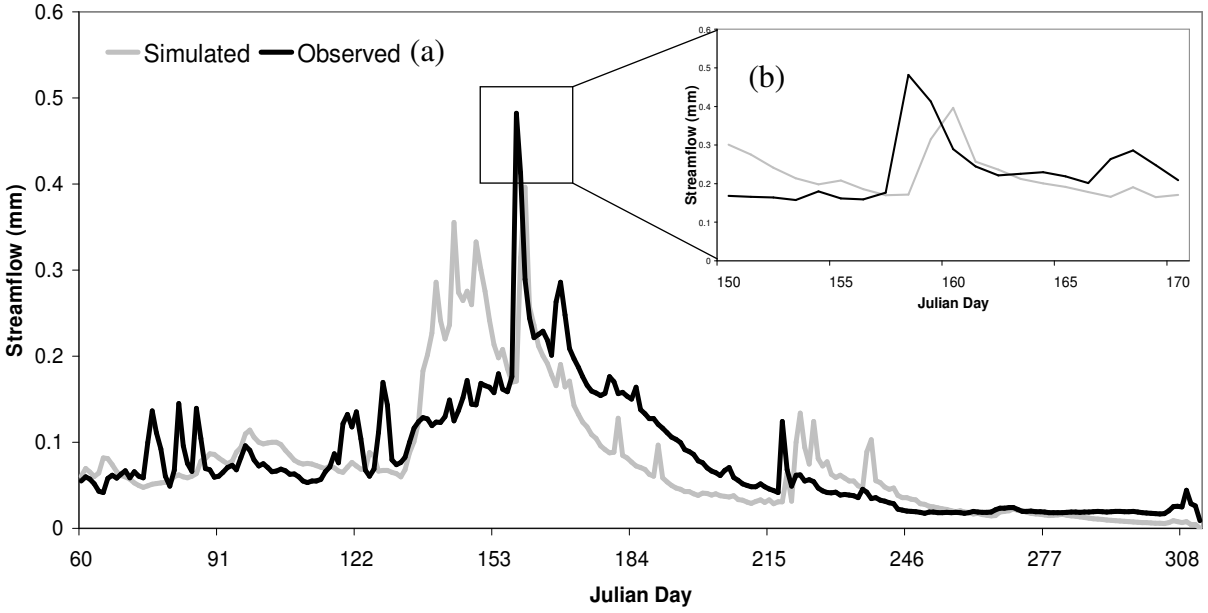

Figure 3.5: Simulated and observed mean daily hydrographs for 27-year sample (a). Subset figure (b) illustrates the behaviour of simulated and observed peak response between Julian days 155 and 165.

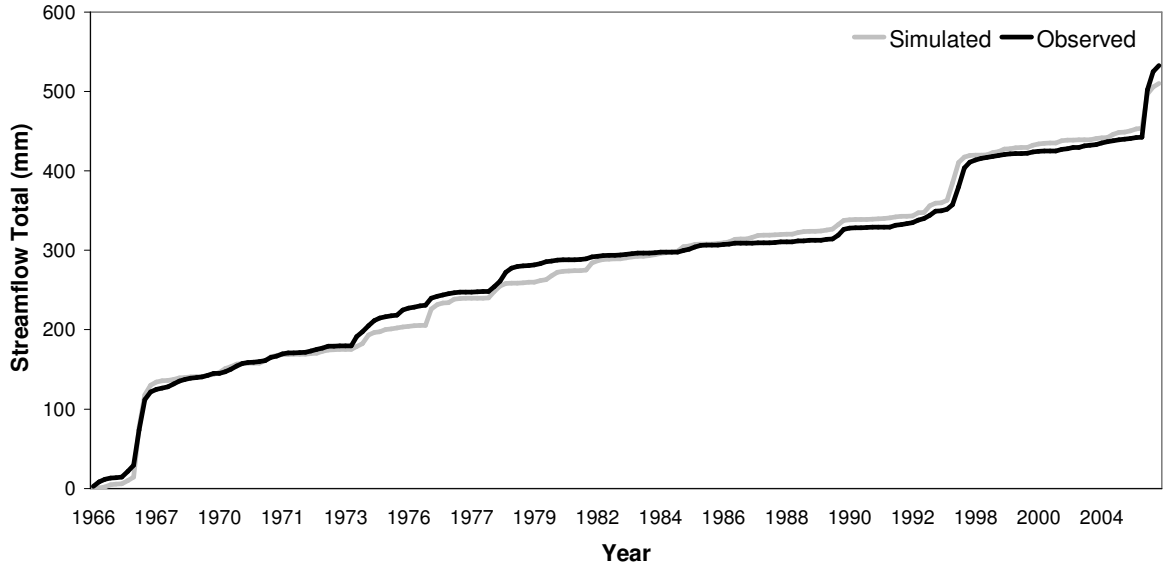

Figure 3.6: Simulated and observed accumulated daily hydrograph, 27-year sample.

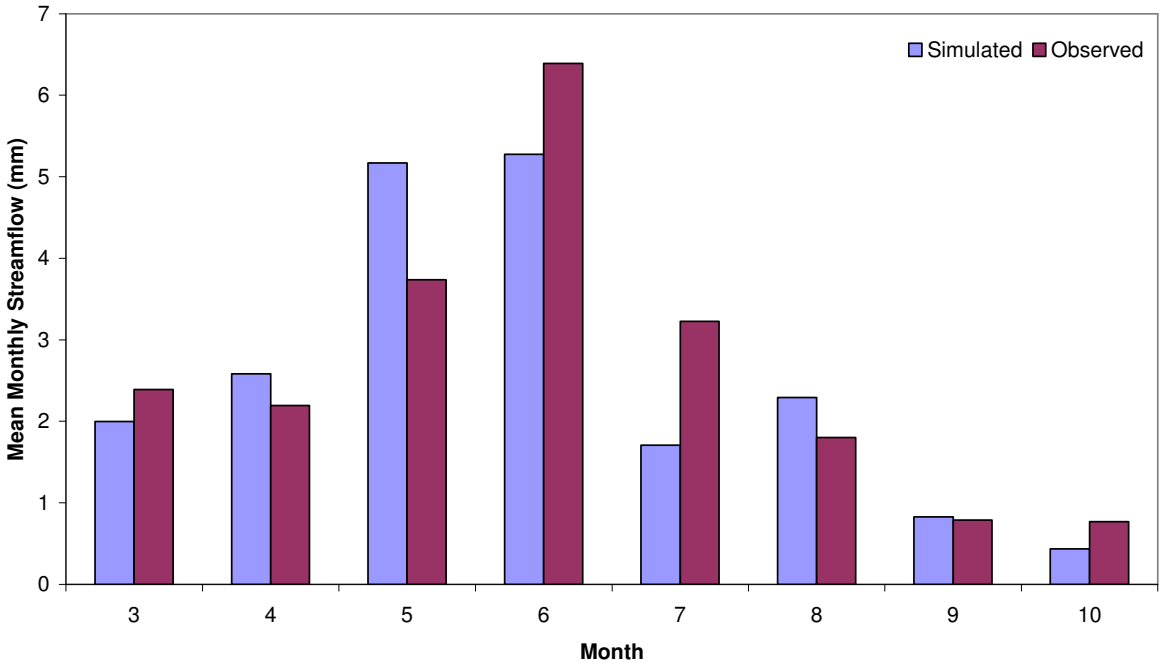

Figure 3.7: Simulated and observed mean monthly streamflow totals, 27-year sample.

The coefficient of efficiency and coefficient of determination have been criticized in their effectiveness as objective measures of simulation accuracy (Legates and McCabe, 1999; Krause *et al.*, 2005). Both of these objective functions square the error term which allows for an over-estimation of error due to larger absolute error in high flows. It follows that the parameterization of the ACRU model for the Beaver Creek was intended for water resources assessments focusing on overall water availability and in particular, availability in periods of baseflow. The strength of the coefficients of determination and efficiency were compromised due to low simulation accuracy, and thus larger squared error in months of highest flow magnitudes.

3.5 Conclusion

The application of the ACRU model to a medium sized catchment dominated by a hybrid of hydrological processes was investigated. Spatial techniques for interpolation of precipitation have expanded the capabilities of hydrological modelling in catchments where data are limited. Furthermore, the spatial delineation of land cover, soils and climate data using the HRU approach facilitated higher resolution, distributed modelling in catchments of diverse physiography, as was found in the Beaver Creek.

The verification of the ACRU modelling system for the Beaver Creek revealed the challenges of modelling endeavors in areas with low-density instrumentation and thus limited historical data records. Whilst significant efforts were made to construct be best possible precipitation record, it became evident that the quality of the record used was the principal limiting factor in this simulation. After the removal of outlier years, the linear regression model explained 78% of the variance of the observations and the coefficient of

efficiency improved to 0.77. The ACRU model simulated the mean annual hydrograph with reasonable accuracy, in particular, the timing of the peak flow and baseflow periods showed a good association with observations. The conservation of the annual water balance was illustrated in the association of simulated and observed accumulated annual volumes. Simulated mean monthly volumes showed a conservation of the observed volumes in most months with the exception of July and October that were under-simulated.

The results of the verification analysis illustrated that the ACRU model is well suited to simulating the annual water balance, while only marginal at simulating the overall behaviour of the hydrograph (i.e. mean monthly volumes). The errors in mean monthly simulation illustrated the complexities of modelling multiple hydrological processes in hybrid catchments. The accuracy of the current parameterization of the ACRU model was achieved with the optimization of only the required parameters. These results confirm that the current parameterization of the ACRU model is suitable for simulating the mean response to climate change scenarios.

CHAPTER 4

An analysis of GCM derived climate scenarios on the future hydrology of a tributary catchment in the Oldman River Basin, Alberta, Canada

4.1 Introduction

4.1.1 Background

In response to increased atmospheric concentrations of greenhouse gasses, global mean surface warming is expected to intensify of the global hydrological cycle (Loaiciga *et al.*, 1996; Douville *et al.*, 2002; Huntington, 2006). It is anticipated that this intensification will disrupt global precipitation patterns (Frederick and Major, 1997; Dore, 2005), resulting in a regionally disparate distribution of precipitation (IPCC, 1996; Douville *et al.,* 2002). Projected warming is expected to be the highest over the mid- and high-latitude regions (IPCC, 2001; Christensen *et al.,* 2007). Since many of these regions depends on winter snow accumulation and spring melt, the change in temperature may be problematic for water supply and availability (Barnett *et al.,* 2005). A common method of investigating the impacts of climate change on water resources is to use output from a general circulation model (GCM) to drive a hydrological model (Leavesley, 1994; Xu, 1999b; Merritt *et al.,* 2006).

In North America, climate change and the associated increases in temperature are expected to affect evaporation, soil moisture and the timing, form and volume of precipitation (IPCC, 2001; Christensen *et al.,* 2007). Simulations of future climate and hydrology in snowmelt dominated regions indicate a greater percentage of precipitation events in the form of rain, which will affect the volume and melt-rate of the snowpack and lead to increased winter and reduced summer runoff volumes (Lettenmaier and Gan,

1990; Loukas and Quick, 1996; Lapp *et al.,* 2005). Accordingly, a significant volume of water supply in the Canadian Prairie region depends on snowmelt runoff from the eastern slopes of the Rocky Mountains and is expected to be vulnerable to the projected changes in climate (IPCC, 1997).

Trends in climatic records indicate that, over the 20th century, the Canadian Prairies experienced a warmer and, to a lesser extent, drier climate (Gan, 1998). In southern Alberta, observations over the period 1970-2003 show a mean temperature increase of 1.4°C (Schindler and Donahue, 2006). Modelled projections of the future climate in the Canadian Prairie Provinces indicate that mean annual temperature may increase between 4°C and 5°C by 2050, relative to 1961-1990 conditions (Wheaton, 2001). For Alberta, mean annual temperature is projected to increase between 3 and 5°C by the 2050s (Barrow and Yu, 2005).

The lack of consensus in historical precipitation trends in the Prairie Provinces does not provide strong evidence to indicate whether or not the Prairie behavior is similar to annual increases observed in Canada over the 20th century (Mekis and Hogg, 1999; Zhang *et al.,* 2001). Akinremi *et al.* (1999) found increasing trends of annual precipitation (volume) in the Prairies between the years 1921 and 1995. However, Schindler and Donahue (2006) found no increases in annual precipitation in an examination of western Prairie records, most of which predate the year 1900. Projections for future precipitation in the Prairie region are also variable, synonymous with global projections (IPCC, 2001). Mean annual changes in future precipitation are expected to be between -10% and +15% in Alberta (Barrow and Yu, 2005). Based on the observed trends and modelled future projections for both temperature and precipitation, Schindler

and Donahue (2006) predict that, in the near future, forecast warming may contribute to water scarcity issues in the western Prairies.

This study was focused on quantifying the impacts of climate change on the hydrology of a single catchment in southern Alberta. The Oldman River Basin is southern Alberta's largest watershed (25,100 km^2) spanning over 200km of Rocky Mountain cordillera extending south into northwestern Montana. The watershed is separated into two distinct climatic zones; the eastern slopes of the Rocky Mountains where an annual moisture surplus in the mountain headwaters supplies water demands, largely from irrigation, in the downstream, semi-arid prairie zone. The transition from mountain to prairie physiography is followed by changes in the climate, soils, vegetation and hydrology.

Watersheds dominated by pluvial, nival and hybrid hydrological processes have elicited different responses to scenarios of future climate (Loukas and Quick, 1996; Whitfield *et al.*, 2003). Examining the effects of climate change on the hydrology in snowmelt dominated-catchments has been the subject of much research (Singh and Kumar, 1997; Hamlet and Lettenmaier, 1999; Christensen *et al.*, 2004; Barnett *et al.*, 2005; Lapp *et al.,* 2005; Merritt *et al.*, 2006). However, snowmelt dominated regions, explicitly the Western Cordillera of Canada, make up only part of the total landmass and thus are reflective of only some of the major hydrological processes. Understanding the effects of climate change on hydrology in watersheds driven by other dominant precipitation forms (e.g. pluvial or hybrid) should not be understated (Loukas and Quick, 1996; Loukas *et al.*, 2002). The hydrology of the semi-arid, montane and grassland regions in the Oldman Basin are governed by both forms (snow and rain) of precipitation.

This study investigated the impacts of climate change on a hybrid catchment in the Oldman Basin.

4.1.2 Modelling the Impacts of Climate Change on Regional Hydrology

4.1.2.1 Hydrological Modelling

The hydrological response to climate change has been studied through the application of catchment-scale hydrological models driven by GCM-derived scenarios of future climate (Loukas *et al.*, 2002; Morrison *et al.*, 2002; Schulze and Perks, 2003; Toth *et al.*, 2006; Nurmohamed *et al.*, 2007). The selection of the hydrological model requires that the model structure and conceptualization of catchment processes are well-suited to the catchment under investigation (Xu, 1999a). Physically-based hydrological models provide the accuracy required for the simulation of nonlinear hydrological processes in semi-arid catchments (Schulze, 1995).

The Agricultural Catchments Research Unit (ACRU) (Schulze 1995; Smithers and Schulze, 1995) is a physical-conceptual, distributed hydrological modelling system designed to be highly responsive to changes in land use and climate (Schulze and Smithers, 1995). The ACRU model has been used extensively in climate change impact studies (Lowe, 1997; Schulze, 1997; Schulze, 1998; Schulze and Perks 2003; Schulze *et al.*, 2004) and hydrological assessments (Kienzle and Schulze, 1991; Kienzle *et al.*, 1997; Everson, 2001).

Physically-based, spatially distributed hydrological models are an effective means to assess the impacts of climate change on hydrological response (Bathurst *et al.,* 2004). The simulation of future hydrological response to climate change is limited to the

accuracy of simulating observed conditions (Jewitt and Schulze, 2003; Bathurst *et al.,* 2004). The quality of the future hydrological simulation is constrained by the validity and accuracy of the parameters and inputs to the model (Bathurst *et al.,* 2004). The hydrological model must reproduce the characteristics of interest, in the hydrograph or component(s) of the water balance, within an acceptable range of uncertainty (Schulze, 1995; Bathurst *et al.,* 2004).

4.1.2.2 Climate Scenarios

Climate scenarios are often derived using output from general circulation model (GCM) experiments (Xu, 1999a; Xu, 1999b; Loukas *et al.*, 2004; Xu, 2005). GCMs offer a physically plausible, three-dimensional, mathematical representation of the atmosphere, ocean, ice cap and land surface (MacFarlane *et al*., 1992; Smith and Hulme, 1998). These models are important in addressing the impacts of climate change as they provide the most sophisticated simulation of the climatic response to changing concentrations of greenhouse gasses and aerosols (IPCC, 2001; Laprise *et al.,* 2003). The Special Report on Emissions Scenarios (SRES) (Nakicenovic *et al.,* 2000), recommended the use of six illustrative emissions scenarios for climate change impacts research based on calculated changes in future population, economic growth and energy consumption (IPCC, 2001).

General circulation models are, by design, proficient at estimating the effects of changes in greenhouse gas concentrations on atmospheric circulation (Smith and Hulme, 1998). The large spatial scale of GCMs (~300km x 300km) inhibits the use of these models for representing regional-scale processes (Cohen, 1990 Carter *et al.,* 1994; IPCC, 1996; Schulze, 1997). Thus the outputs from the GCMs are not appropriate for direct

application to hydrological studies at finer spatial resolutions (Xu, 1999b). This is especially true for climate variables in topographically complex regions (Loukas *et al.,* 2004) such as the eastern slopes of the Canadian Rockies.

Methods for resolving the effect of scale have been developed to facilitate the use of GCM outputs in hydrological models, and are outlined by the IPCC Task Group on Scenarios for Climate Impact Assessment (TGCIA) (1999). Downscaling refers to the process of refining coarse resolution GCM output to the sub-grid scale (Mearns *et al.,* 2001), which is then appropriate for regional scale hydrological modelling. In a comparison of two common downscaling approaches including the delta method and statistical downscaling, Hay *et al.,* (2000) concluded that while seasonal trending of future climate variables is similar, the magnitude of changes are variable between techniques. They conclude that while both approaches are to be used with caution, the delta technique resulted in more conservative simulations of runoff.

4.1.2.3 Uncertainty

The accuracy of regional-scale hydrological impact studies are challenged by several sources of uncertainty. First, the SRES emissions scenarios are based on a combination of projections of future population, economic development and technological advancement. It is well established that these scenarios are considered equally plausible representations of future concentrations of greenhouse gasses, aerosols and sulphates (IPCC, 2001) and complicates the selection of experiments that drive the impact model (Hulme and Brown, 1998).

Another source of uncertainly stems from the accuracy of the GCMs in replicating regional, observed climate (Mearns *et al.,* 1997). Bonsal *et al.* (2003) examined the performance of the publicly available GCMs in simulating regional observations of temperature and precipitation over the Western Cordillera of Canada. In a verification of the 1961-1990 baseline period, they found considerable agreement amongst the models for temperature however, considerable over-estimations, and less agreement between models for precipitation.

Additional uncertainties arise due to inconsistencies in the projections of key climate variables (i.e. temperature and precipitation) between different GCMs (IPCC, 2001; Bonsal *et al.,* 2003). Modelling uncertainty is inherent as both hydrological models and GCMs are forced with hypothetical future scenarios and simulating outside of a verifiable range (Morrison *et al.,* 2002). While there is indefinite uncertainty in the data and methods of projecting the impacts of future climate, the design of impact assessments can reduce the modelling errors (Morrison *et al.,* 2002). In recognition of the complexities of constructing GCM-based climate change scenarios for impacts analysis, Smith and Hulme (1998) quantified four major criteria for scenario development:

1. The most recent GCM simulations are the most accurate as they benefit from the most advanced knowledge.

2. GCMs with the highest spatial resolution provide increased accuracy at the regional scale.

3. GCMs with the most accurate simulation of the historical climate will, theoretically, have the most regionally representative future projections.

4. Since the estimates of climate variables (i.e. precipitation) are inconsistent between GCMs, it is preferred to utilize a range of future projections.

The current body of research in western North America indicates that water resources in the Oldman Basin may be vulnerable to the impacts of climate change. In keeping with the recommendations of Smith and Hulme (1998), this research examined the sensitivity of a hybrid catchment, in the Oldman Basin, to a range of plausible future climates. Climate change impacts were assessed using a hydrological model forced by a range of GCM-derived scenarios. Future hydrological regimes were compared to the 1961-1990 baseline conditions to determine the net effect of climate change at each of the three time periods. The evaluation of catchment response to a range of future climates is necessary to determine the potential effects of climate change on water resources in this presently, vulnerable region. Furthermore, this research contributed to the greater provincial initiative of developing a *"watershed approach"* (AENV, 2003).

4.2 Objectives

The primary research objective of this chapter was to investigate the impacts of climate change on the hydrology of a single catchment in the Oldman Basin that is governed by both snowmelt and rainfall processes. The primary objective was achieved through the selection and development of GCM-derived climate scenarios that represented the projected range of plausible future climates in this region. These scenarios were used to force the ACRU hydrological modelling system and simulated 5 scenarios of future hydrology over the recommended time periods of 2020, 2050 and 2080.

To determine the range of potential impacts on water availability, the analysis of future hydrological scenarios included an examination of the changes in annual flow volume and water balance components, shift in the seasonal contribution of streamflow and timing and magnitude of the peak flow event.

4.3 Methods

4.3.1 Study Area

The Beaver Creek study catchment, centered at 49° 44'N, 113° 52'W, is a tributary of the Oldman River (Figure 4.1), a major headwater to the South Saskatchewan River Basin. The creek is maintained by perennial flow with a bimodal hydrograph indicating the influence of both snowmelt and rainfall processes (Water Survey of Canada, 2007), and is classified as a hybrid stream (Figure 4.3). Beaver Creek has two ungauged, ephemeral tributaries (Five Mile Creek and Nine Mile Creek), both originate on the west-facing slopes of the catchment (Figure 4.1). The headwaters stem from the higher elevation slopes of the Porcupine Hills, east of the Front Range of the Rocky Mountains, Alberta.

The Beaver Creek catchment has a drainage area of 254km^2, defined by the Water Survey of Canada hydrometric station (05AB103) located near Brocket, approximately 7km northwest of its confluence with the Oldman River (Figure 4.1). Elevations in the Beaver Creek catchment range between 1100m and 1500m AMSL, with the general aspect facing south, south-east with slopes ranging from flat in the lower elevation rangelands to 28° on the southwest and north east facing hillslopes.

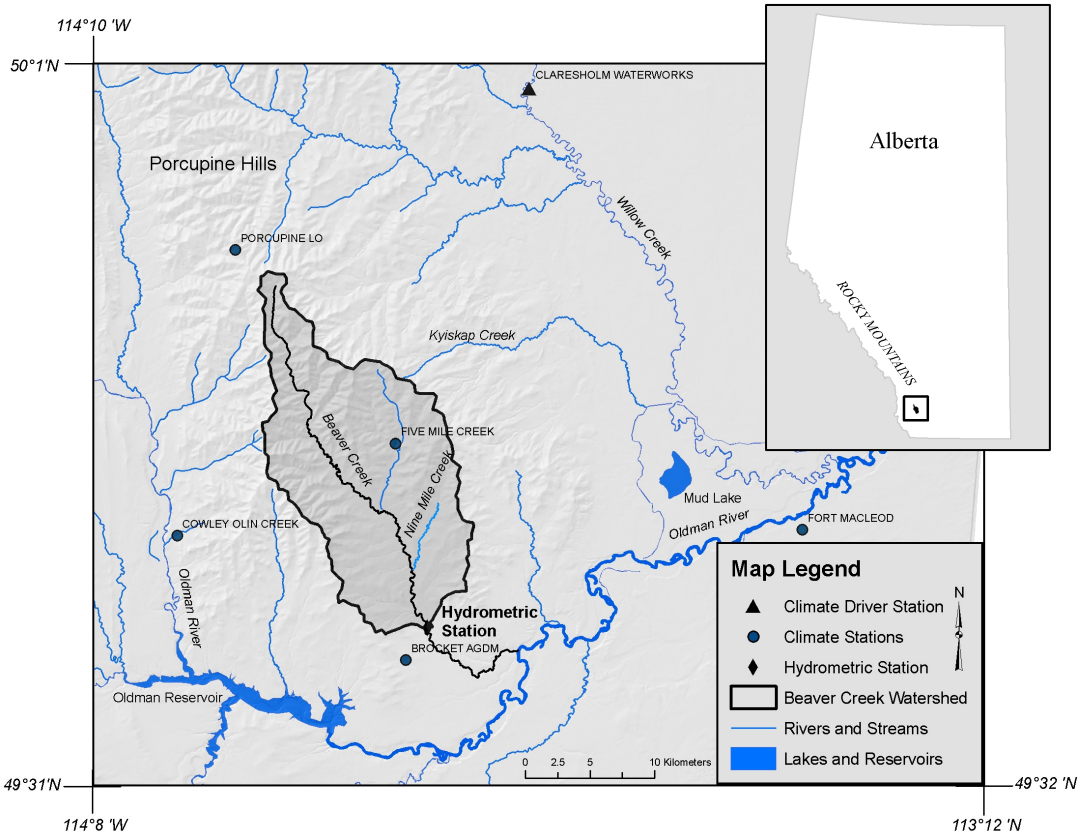

Figure 4.1: Reference map of the Beaver Creek study catchment including climate stations, main hydrological features and gauging station.

The Porcupine Hills are characterized by the rapid spatial transition from montane forest to aspen parkland and prairie grasslands, creating a unique habitat for many plant species native to southern Alberta (Elias, 1999). The upper elevations receive adequate precipitation to sustain mixed coniferous and deciduous forests (Elias, 1999). Conifer forests consisting mainly of white spruce (*Picea glauca)*, lodgepole pine (*Pinus contorta* var. *latifolia*), balsam fir (*Abies balsamea)* with some Douglas-fir (*Pseudotsuga menziesii*) cover the upper elevation slopes and ridge-tops. Thick deciduous forests of Trembling Aspen (*Populus tremuloides)* are found on the mid-elevation slopes with grassland ecosystems located on dry lower slopes (Elias, 1999). Predominant plant

species in the grasslands include rough fescue (*Festuca scabrella),* timothy (*Pheleum pretense)* and brome (*Bromus inermis)* grasses. Cultivated crops are also established on the lower plains that include canola (*Brassica napus),* barley *(Hordeum distychum)* and wheat (*Triticum aestivum).*

Soils in the upper elevation, forested regions are of the Luvisolic soil order. The surface horizon is predominantly sandy clay loam, while the subsurface horizon is dominantly clay, a distinctive characteristic of acid leaching in forested areas. The mid-elevation grasslands are typical of a Chernozemic soil order that exhibits higher clay fractions in the surface horizon while the subsurface soils are a mix of silty clay loam and sandy loam. The cultivated croplands have a sandy clay loam surface horizon and a clay loam subsurface horizon, to be expected in areas of high tillage. The grassland region is characterized by shallower surface horizons relative to the forested area while the subsurface horizon is deeper. The cultivated areas have the deepest surface horizons but shallower subsurface horizons relative to the grasslands.

Elevations in the Porcupine Hills are similar to the foothills in the eastern slopes of the Rocky Mountains, however, their geologic stratification more closely resembles the Cypress Hills and Milk River Ridge (AENV, 2000). The Porcupine Hills were not formed by the processes of mountain building, but through glacio-fluvial erosion during the last ice age. Consequently the underlying sandstone bedrock is not thrust-faulted but in the original, horizontal orientation as it was deposited (Elias, 1999).

The Claresholm Water Works climate station, located approximately 25km northeast of the Beaver Creek catchment, was chosen to drive the hydrological model. This station received an average annual precipitation (1971-2000) volume of 428.2mm,

apportioned between 304.9 mm of rain and 123.4mm of snow (Environment Canada, 2007). Mean daily temperature in the summer is 16°C and –6.1°C in the winter. A complete 40-year climate record overlapping the hydrometric observations and similar physiographic characteristics to the Beaver Creek catchment made this the most representative climate station for the simulation.

In the southern Alberta region, winter precipitation events result primarily from frontal air masses while summer events are typically convective in nature (i.e. June lows). The proximity to the eastern slopes of the Rocky Mountains exposes the area to the rainshadow effect and high Chinook winds (Grace, 1987). Therefore, due to the orographic influences on this area, it is not uncommon for a deficit in the annual moisture budget due to high evapotranspiration relative to precipitation.

4.3.2 Hydrological Modelling

4.3.2.1 The ACRU Modelling System

The ACRU agro-hydrological modelling system was parameterized for a climate change impact assessment on the hydrology of the Beaver Creek. The ACRU model is a multi-purpose, multi-level, physical-conceptual model that can simulate total evaporation, soil water, snow storages and streamflow at a daily time step. The ACRU model is conceptual in that it theorizes the processes that govern the hydrological cycle, and is physical in that the physical laws of hydrology are mathematically represented within the conceptual framework (Schulze, 1995).

The multi-layer soil water budgeting routine is the central focus of the models structure. ACRU has been developed as a total evaporation model simulating

hydrological processes within the atmosphere-plant-soil water interfaces (Figure 4.2). The total evaporation routine of the ACRU model is partitioned between growth-stage specific transpiration and soil water evaporation making it sensitive to changes in temperature (Schulze and Smithers, 1995). The concepts and structure of the ACRU model make it well suited to climate change impacts studies (Schulze, 1995; Schulze and Smithers, 1995).

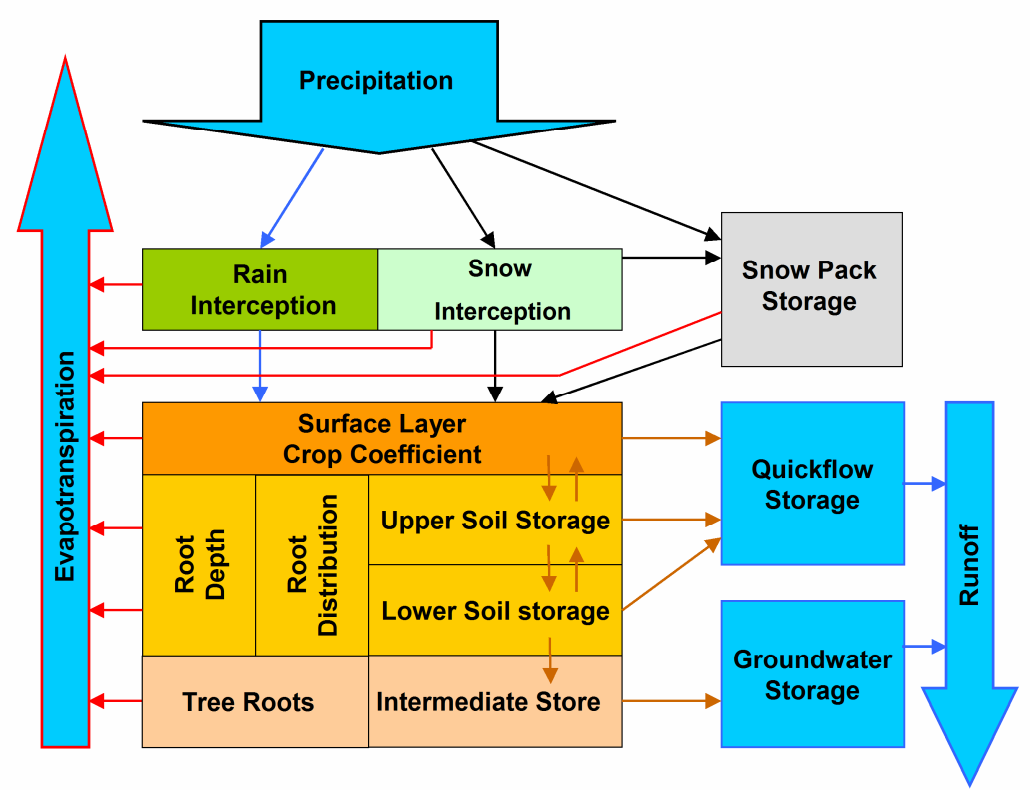

Figure 4.2: Major components of the ACRU agro-hydrological modelling system illustrating the distribution of precipitation within the atmosphere-plant-soil continuum and runoff generation processes.

4.3.2.2 Verification of the ACRU Modelling System

The ACRU modelling system was verified against seasonal daily streamflow observations (Water Survey of Canada, 2007) for a 27- year period between the years 1966-2005 in the Beaver Creek catchment. Verification accuracy was determined using objective functions of modelling performance including the coefficient of efficiency, coefficient of determination and mean error. The coefficient of efficiency and coefficient of determination are both maximized at a value of 1.0 (Schulze, 1995; Merritt *et al.,* 2006). The coefficient of efficiency measures the degree of association between observed and simulated streamflow volume and timing while the coefficient of determination describes the closeness of shape between observed and simulated hydrographs. The maximization of the coefficient of determination depends solely on the accuracy of the timing of the simulation relative to the observations (Merritt *et al.,* 2006). The mean error is utilized to quantify the differences in volume between observed and simulated streamflows at daily, monthly and annual time steps.

4.3.3 Deriving Scenarios of Future Climate

4.3.3.1 General Circulation Model Data

The Pacific Climate Impacts Consortium (http://pacificclimate.org/) has made available monthly GCM output from all publicly available SRES model experiments. The GCMs in Table 4.1 correspond to the selection of models recommended by the IPCC Data Distribution Center Task Group on Data and Scenario Support for Impact and Climate Analysis (IPCC-TGICA, 1999). Each of the experiments used in this sensitivity analysis were driven by one of six, marker emissions scenarios that resulted from the

Special Report on Emissions Scenarios (SRES) (Nakicenovic *et al.,* 2000). Thus, the model experiments used for this study were the most recent, advanced, highest resolution, publicly available data for impacts research. The nearest four GCM gridcells to the study catchment were averaged to reduce the influence imposed by using the single, overlying gridcell (von Storch *et al.,* 1993).

Table 4.1: Models and experiments currently available from the PCIC (after Barrow and Yu, 2005).

Modelling Center	Country	Model	SRES simulations
Canadian Center for Climate Modelling and Analysis	CAN	CGCM2	A2, B2
Hadley Centre for Climate Modelling and Research	UK	HadCM3	A1F1, A2, B1, B2
Max Planck Institute for Meteorology	GER	ECHAM4	A2, B2
Commonwealth Scientific and Industrial Research Organization	AUS	CSIRO-Mk2	A1, A2, B1, B2
Geophysical Fluid Dynamics Laboratory	USA	GFDL-R30	A2, B2
National Centre for Atmospheric Research	USA	NCAR-PCM	A2, B2, A1B
Centre for Climate Research Studies	JPN	CCSR/NIES	A1F1, A1T, A1B, A2, B1, B2

4.3.3.2 Climate Change Scenario Selection

A method consisting of a combination of the hypothetical technique (e.g. Nemec and Schaake, 1982; Xu, 2000) with projections from all available GCMs, facilitated a less-biased sensitivity analysis to the full range of projected regional climates. Five GCM experiments were selected based on their representation of the range of possible future

climates of warmer-wetter, warmer-drier, median, hotter-[1]wetter and hotter-drier. Where the selection was complicated by similarities between the experiment results, selection was based on the greatest change in precipitation.

The proposed method satisfied the final recommendation of Smith and Hulme (1998) by applying a range of GCM- based scenarios. This resulted in a hypothetical *"envelope"* of the projected alternatives of future climate and constructed an appropriate stimulus for the analysis of future hydrology in Beaver Creek. This method of climate scenario selection was adapted from Barrow and Yu (2005) who constructed climate scenarios for the province of Alberta.

4.3.3.3 Regional Downscaling

The "delta" method (Arnell, 1996; Hay *et al.,* 2000) has been used to downscale GCM output in several regional hydrological impacts studies (Morrison *et al.,* 2002; Schulze and Perks, 2003; Andreasson *et al.,* 2004; Loukas *et al.,* 2004; Cohen *et al.,* 2006; Merritt *et al.,* 2006). This method calculates the relative change, of a GCM-derived climate variable, between the baseline period (1961-1990) and a future time period. Observed climate records are assumed to be more accurate at capturing local behavior of climate variables than raw GCM output. Therefore, monthly change fields calculated by the delta method were utilized to perturb the locally representative observed climate record. Future temporal scales assessed in this study followed the IPCC-TGICA (1999) recommended periods of 2020s (2010-2039), 2050s (2040-2069) and the 2080s (2070-2099). Thirty-year periods are believed to capture the normal range of inter-annual

[1] "hotter" designates those scenarios which have higher projected temperature increases than the "warmer" designation as the models unanimously predict warmer temperatures in all scenarios at all timesteps.

variability while preserving the longer multi-decadal climate change signal (IPCC-TGICA, 1999).

This hydrological assessment of Beaver Creek required monthly changes to be calculated for minimum temperature, maximum temperature and precipitation. Changes in both temperature variables were calculated as the absolute change and changes in precipitation were calculated as a ratio change in the mean of the monthly precipitation. The 12 monthly mean changes were smoothed by a Fourier transformation (Epstein 1991; Schulze, 1995; Morrison *et al.,* 2002) that constructed continuous daily adjustments for minimum and maximum temperature and precipitation. This procedure reduces the discontinuities between monthly values, producing a more natural intra-annual signal. The delta method applies the climate change signal to the mean of the observed data, however, it does not account for the anticipated changes to the variability of future climate (Wood *et al.*, 1997; Hay *et al.*, 2000).

For the purposes of this study, the thirty-year record of observations (1961-1990) was assumed to reflect the regional variability imposed by large-scale indices such as the Pacific Decadal Oscillation and the El Nino Southern Oscillation. While the behavior of these indices and climate variability as a whole are anticipated to change in the future, this method assumed no change from the 1961-1990 baseline period.

Application of the above method resulted in a complete 30-year, daily climate record that reflected the spatial and temporal behavior of the climate station, while representing the monthly changes projected by a GCM for this region. The delta method eliminated the error between surface climate and the GCM by taking the mean monthly relative change between the GCM modelled baseline (1961-1990) and future climates

(i.e. 2020, 2050, 2080). This provided a relatively simple method to test the sensitivity of a particular variable (i.e. streamflow) to a range of future climates. The transformed monthly changes were applied to the observed climate for five scenarios, each with three time periods. The original station observations were used as the baseline scenario to compare the 15 model runs, and determine the hypothetical change in future hydrological conditions.

4.3.4 Analysis of Future Hydrological Conditions

The analysis of the scenarios was primarily focused on how the changes in temperature and precipitation affect the hydrological regime of Beaver Creek. The results were focused on how the scenario-derived future projections in temperature and precipitation affected the major water balance components, annual flow volume, seasonality of the hydrologic regime, date of peak flow and magnitude of the peak flow event. The date and magnitude of peak flow were determined using the average Julian day where peak flow occurred over the 30-year simulation period. The results were compared over the three recommended time periods, and were analyzed relative to the baseline simulation.

4.4 Results

4.4.1 Verification of the Hydrological Modelling System

The ACRU model simulated the observed streamflow record in the Beaver Creek with reasonable accuracy over the 27-year verification period. Figure 4.3 illustrates the simulated and observed mean daily hydrographs. The coefficient of efficiency (0.77),

coefficient of determination (r^2 =0.78) and an average monthly over- simulation of 3.5% indicate a reasonable fit between observed and modelled monthly flows, taking into the consideration the accuracy of both the timing and volume of simulated flows. Visual inspection of the simulated mean annual hydrograph (Figure 4.3) shows that the timing and magnitude peak flow event and baseflow period were simulated with accuracy. The ACRU model had greater success in simulating the monthly and seasonal streamflow volumes in the Beaver Creek. It was determined that the accuracy of the ACRU model achieved over the verification period was sufficient for simulating the mean response to climate change scenarios.

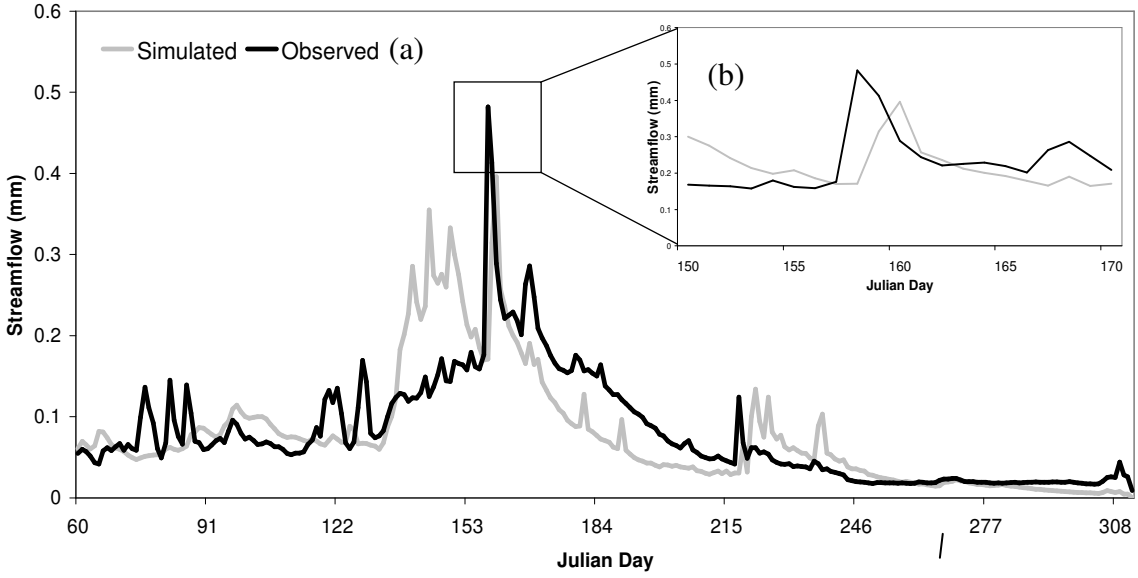

Figure 4.3: Simulated and observed mean daily hydrographs, 27-year verification sample of the Beaver Creek. The subset (b) illustrates the timing of peak flow.

4.4.2 Climate scenario selection

The climate scenario selection consisted of 27 experiments output from GCM runs of the SRES emission scenarios, over the three recommended time periods. Only the experiments with outputs for monthly precipitation and minimum and maximum temperature were included in the analysis, as these variables were required by the ACRU modelling system. Climate scenarios were selected based on the distribution of mean annual temperature and precipitation over the 2020s. The 2020 period was used, as the projections for the nearest time periods are believed to have the least uncertainty (Barrow and Yu, 2005).

The distribution in Figure 4.4 illustrates that the models were not in uniform agreement as to the direction or magnitude of changes for the 2020s. The distribution of model experiments in Figure 4.4 illustrates the agreement amongst the models of an increase in mean annual temperature. The magnitude of change ranged between 0.36°C and 2.14°C increase from the 1961-1990 mean. Model predictions for the change in precipitation (percent) were considerably more variable, ranging from an annual increase of 9.42% to a decrease of 5.01% relative to baseline conditions. The medians indicated that while the experiments were quite well distributed in both increasing and decreasing precipitation, a higher number of experiments projected an increase of annual precipitation.

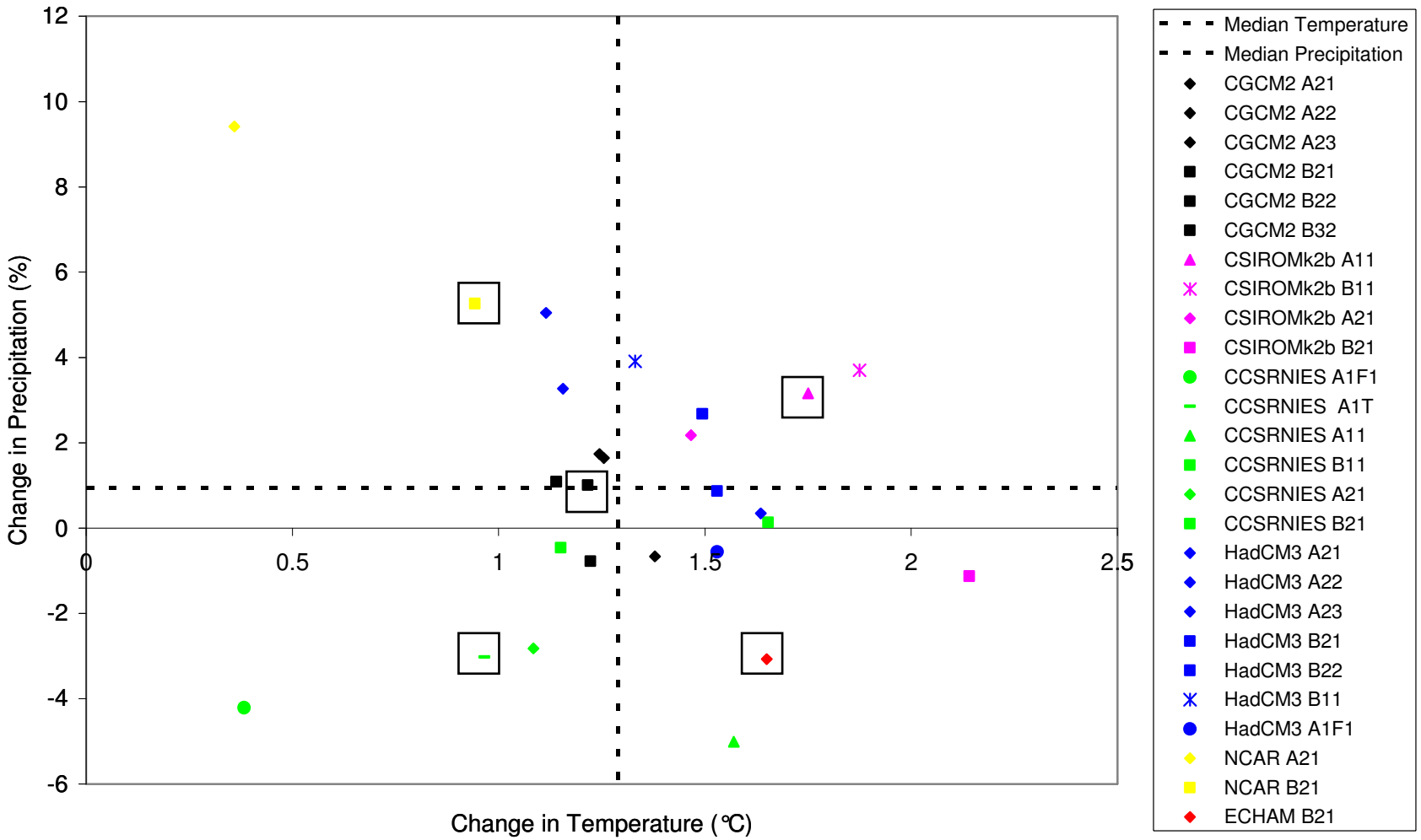

Figure 4.4: Mean annual projections of all publicly available GCM experiments for change in mean annual temperature (°C) and the mean annual change in precipitation (%) for the period 2010-2039 over the Beaver Creek catchment. Colors denote different models while symbols reflect different SRES emissions scenarios. Dashed black lines represent the median of all available scenarios and boxed scenarios represent the selected scenarios (After Barrow and Yu, 2005).

Five scenarios of future climate were selected based on their predictions for annual temperature and precipitation changes for the 2020 period of warmer wetter (WW), warmer drier (WD), median (MD), hotter wetter (HW) and hotter drier (HD) climates. The resulting five scenarios consisted of a range of GCMs and SRES emissions scenarios (Table 4.2). The monthly changes of minimum, maximum temperature and precipitation from each of the five scenarios were used to perturb the 1961-1990 baseline observed climate at the Claresholm Waterworks station. This provided the input to the ACRU hydrological modelling system for future hydrological scenarios.

Table 4.2: Models and experiments used in this study (after Barrow and Yu, 2005).

Scenario	GCM	Emissions Scenario	Resolution (°)
HD	ECHAM4	B2 (1)	2.8 x 2.8
HW	CSIRO-Mk2	A1 (1)	5.6 x 3.2
MD	CGCM2	B2 (1)	3.75 x 3.75
WD	CCSR	A1T	5.62 x 5.62
WW	NCAR-PCM	B2 (1)	2.8 x 2.8

The mean annual changes in temperature and precipitation as well as the mean seasonal changes in temperature and precipitation for the five representative scenarios are presented in Table 4.3. It is important to note that since the selection of the representative scenarios were based on the relative performance of the GCMs over the 2020 period, the five representative scenarios in the 2050 and 2080 periods do not necessarily reflect the same relative distribution. Thus, the interpretation of the results herein must be directly related to the individual scenario changes in temperature and precipitation as illustrated in Table 4.3. The scenarios in which this occurs are denoted by an * in Table 4.3.

Table 4.3: Mean annual and seasonal GCM projections of temperature and precipitation for 2020, 2050 and 2080 periods. Temperature is expressed as mean change in degrees Celsius relative to the 1961-1990 baseline and precipitation is expressed as the percentage change in mean precipitation relative to the 1961-1990 baseline. The seasonal periods are defined as Winter (DJF), Spring (MAM), Summer (JJA) and Fall (SON).

		Mean Annual GCM Projections		Mean Seasonal GCM Projections							
Scenario	**Period**	**Temp**	**Precip**	**Winter**		**Spring**		**Summer**		**Fall**	
		(°C)	(%)	T(°C)	P(%)	T(°C)	P(%)	T(°C)	P(%)	T(°C)	P(%)
HD	2020	1.7	-3.1	1.4	4.9	1.0	-2.8	2.5	-15.5	1.8	1.1
HW	2020	1.8	3.2	2.6	16.5	1.3	4.3	1.6	-5.3	1.6	-2.9
MD	2020	1.2	1.0	1.6	10.0	1.6	2.8	1.6	-5.6	0.7	-3.2
WD	2020	0.9	-3.0	-0.2	-5.5	1.8	1.7	1.2	-3.5	0.9	-4.8
WW	2020	0.9	5.3	1.7	0	0.7	12.4	1.1	10.2	1.2	-1.5
HD*	2050	2.8	1.6	1.8	9.1	1.8	6.7	1.9	-10.4	1.8	0.8
HW	2050	3.5	2.6	3.9	19.4	2.8	19.0	3.5	-15.5	3.8	-12.4
MD*	2050	2.4	2.3	2.6	8.9	3.2	4.4	2.2	-5.7	1.6	1.4
WD*	2050	4.3	2.5	4.5	9.4	4.4	9.9	4.3	-3.5	4.1	-5.8
WW	2050	1.5	6.0	1.3	1.3	1.3	7.4	2.0	5.2	1.6	10.2
HD*	2080	4.0	-0.2	3.7	12.3	2.8	7.2	5.2	-17.9	4.1	-2.4
HW	2080	5.1	9.3	6.4	33.0	3.8	27.4	5.0	-15.2	5.2	-7.8
MD*	2080	3.2	3.7	3.5	8.1	4.5	13.1	2.9	-9.7	2	3.4
WD*	2080	6.4	8.4	6.9	13.8	6.4	19.8	6.3	-2.1	5.8	2.1
WW	2080	2.0	15.3	2.2	11.2	1.6	20.5	2.3	17.1	2	12.5

4.4.3 Simulated Mean Annual Water Balance Components

The simulated changes in the mean annual water balance components are listed in Table 4.4. A current limitation of the ACRU modelling system is that it does not consider the initial catchment conditions (i.e. 'warming up' period), such as the average groundwater storage. Therefore, a small percentage of the annual input (<1%) is not allocated to the major water balance components (< 4mm).

Table 4.4: Mean annual water balance components simulated by the ACRU model for the baseline, 2020, 2050 and 2080 time periods. Total precipitation (summation of rain, snow and mixed precipitation), APAN (Potential evapotranspiration), AET (Actual evapotranspiration from all storages, including interception) and Q (Total streamflow) are expressed in millimeters. The WB (water balance) reflects the residual water not allocated due to 'warming up' period.

	Period	Rain (mm)	Snow (mm)	Mixed (mm)	Total P (mm)	APAN (mm)	AET (mm)	Q (mm)	WB (mm)
Baseline	**61-90**	**218**	**209**	**33**	**460**	**959**	**431**	**25**	**4**
HD	2020	228	176	30	435	1111	411	20	3
HW	2020	245	186	36	466	1106	435	28	3
MD	2020	250	181	30	462	1089	433	25	3
WD	2020	245	171	32	448	1089	422	22	3
WW	2020	282	179	33	494	1085	461	29	3
HD	2050	252	179	29	459	1156	430	26	3
HW	2050	242	179	39	460	1180	423	34	3
MD	2050	266	169	33	468	1141	440	25	3
WD	2050	269	162	35	467	1216	436	28	2
WW	2050	281	177	32	490	1106	460	27	3
HD	2080	240	173	30	443	1208	415	26	3
HW	2080	267	182	38	487	1245	444	40	2
MD	2080	280	161	34	475	1179	445	28	3
WD	2080	310	148	40	497	1302	463	32	2
WW	2080	303	194	37	534	1116	493	38	3

4.4.3.1 Precipitation

Annual precipitation volume increased in the majority of scenarios (Table 4.4). Reductions of annual precipitation below the baseline volume (460mm/year) occurred in the HD (435mm/year) and WD (448mm/year) scenarios over the 2020 period. Beyond the 2020 period, marginal reductions in annual precipitation occurred in the HD scenario over the 2050 period, while the largest reduction of annual precipitation occurred in the HD 2080 scenario (443mm/year). All scenarios resulted in a greater volume of the precipitation as rainfall and reduction in the volume of precipitation as snowfall.

Over all time periods the largest reductions in snow below the baseline conditions occurred in the WD scenario, which was the only scenario to experience a reduction of winter precipitation over the 2020 period and also had the largest increases in winter temperatures in the later time periods (Table 4.3). The smallest reductions over the 2020 and 2050 periods occurred in the HW scenario, which also had the largest increases in winter precipitation. The smallest reduction over the 2080 period occurred in the WW scenario, which experienced the least increase in winter temperature.

4.4.3.2 Potential Evapotranspiration

Potential evapotranspiration was estimated using the Penman (1948) method but is expressed in the standardized ACRU format as the equivalent APAN evaporation (Table 4.4). The simulated baseline (’61-‘90) mean annual APAN (959mm/year) was verified for accuracy against lake evaporation in the Beaver Creek region. Modelled lake evaporation of 756mm/year (AENV, 2005) converted to a Pan-equivalent of 995mm/year using a 30% conversion according to Linacre (1993).

APAN equivalent potential evapotranspiration increased beyond the baseline simulation in all scenarios. The greatest increases occurred in the scenarios with the greatest increase in temperature (Table 4.3), and each scenario increased throughout the time periods with the greatest increases of APAN potential evapotranspiration projected for the 2080 period.

4.4.3.3 Actual Evapotranspiration

The simulated changes in actual evapotranspiration (AET) reflected the changes in available moisture (i.e. free water) throughout the scenarios. Over the 2020 period, both dry scenarios exhibited a decrease in AET. The WW scenario, which also experienced the highest increase in annual precipitation, had the largest increase relative to baseline conditions (Table 4.3). The largest decrease in AET over the 2050 period occurred in the HW scenario, while in the 2080 period, the greatest decrease occurred in the HD scenario. In all scenarios, the changes in AET are related to the changes in precipitation (Table 4.3).

4.4.3.4 Streamflow

The simulated changes in mean annual streamflow (Q), relative to the baseline, reflected the changes to the simulated water balance components (Table 4.4). Over the 2020 period, two scenarios exhibited reductions of mean annual flow with the greatest reduction occurring in the HD scenario. By the 2050 and 2080 periods, all scenarios simulated no change or an increase in annual flow volume. While the majority of these scenarios exhibited minor increases in annual flow volume, the HW and WW scenarios

exhibited a significant increase in annual volume in the 2080 period. Overall, the simulated changes in mean annual streamflow in the 2020 2050 and 2080 periods were negligible with respect to the uncertainty in the model parameterization and water balance accounting.

4.4.4 Mean Seasonal Flow Volumes

The seasonal contributions to mean annual streamflow were calculated for the baseline and each scenario over the three time periods (Table 4.5). The baseline period received the greatest contribution to annual streamflow from the spring (March, April and May), followed by summer (June, July, August), winter (December, January, February) and fall (September, October, November) seasons respectively. This inter-annual behaviour was maintained by all scenarios in the 2020 simulations. However, in the 2050 time period the HW and WD scenarios simulated a seasonal shift where the winter volume became the second largest contributing season to annual streamflow. Similarly in the 2080 period, this shift also occurred in the HD, HW and WD scenarios.

Table 4.5: Mean changes in seasonal streamflow for 2020, 2050 and 2080 periods in millimeters of streamflow from 1961-1990 baseline.

	Winter (mm)	Spring (mm)	Summer (mm)	Fall (mm)
Baseline	**2.3**	**13.8**	**6.9**	**1.8**
HD2020	3.1	12.1	4.0	1.1
HW2020	4.4	17.6	5.0	1.3
MD2020	3.8	14.5	5.8	1.1
WD2020	2.1	13.5	5.3	1.3
WW2020	3.0	14.9	9.1	1.9
Baseline	**2.3**	**13.8**	**6.9**	**1.8**
HD2050	3.9	16.1	4.7	1.6
HW2050	5.9	22.1	5.6	0.4
MD2050	4.1	14.4	5.6	1.4
WD2050	5.1	16.9	4.9	1.1
WW2050	3.1	14.1	8.1	2.1
Baseline	**2.3**	**13.8**	**6.9**	**1.8**
HD2080	4.6	16.4	4.0	0.7
HW2080	8.6	25.9	5.3	0.6
MD2080	4.7	16.2	5.4	1.4
WD2080	6.4	18.8	5.5	1.7
WW2080	4.6	19.2	11.4	2.6

The seasonal streamflow response to the climate change scenarios in the 2020 period exhibited a range of seasonal variations between the five scenarios. The WW scenario resulted in an increase of streamflow in all seasons, while the WD scenario resulted in a reduction across all seasons. Seasonal streamflow was reduced below the baseline scenario in all seasons except winter in the HD scenario. There was also an increase in winter and spring and decrease of summer and fall streamflow volumes in the HW and MD scenarios. The increased winter and spring volumes simulated over the 2020 period were consistent in the majority of scenarios (4 of 5) in the 2050 and 2080 time periods. The outlying response occurred in the WW scenario, which consistently projected an increase in the volume of streamflow in every season, over all time periods.

The simulated seasonal streamflow volumes for the baseline period were 2.3mm, 13.8mm, 6.9mm and 1.8mm for winter, spring, summer and fall seasons respectively. Over the 2020 period the range of simulations (i.e. minimum and maximum scenarios) were between 2.1mm - 4.4mm for winter, 12.1mm – 14.9mm for spring, 4.0mm – 9.1mm for summer and between 1.1mm – 1.9mm for the fall season. By the 2050 period, the range of changes expanded in most seasons between 3.1mm – 5.9mm, 14.1mm – 22.1mm, 4.7mm – 8.1mm and 0.4mm – 2.1mm for the winter, spring, summer and fall seasons respectively. And finally, for the 2080 time period, an even greater range of changes is projected where seasonal streamflow volume is projected to be between 4.6mm – 8.6mm, 16.4mm – 25.9mm, 4.0mm -11.4mm and 0.6mm – 2.6mm for the winter, spring, summer and fall seasons respectively.

4.4.5 Peak Streamflow

4.4.5.1 Date of Peak Streamflow

The date of peak streamflow historically occurred in the rainfall driven portion of the Beaver Creek hydrograph (second maxima) as illustrated in Figure 4.3. This date signifies the central tendency of the hydrograph and provides an indication of the seasonal distribution of streamflow production. Over the 2020 period, the greatest advancement in peak flow date occurred in the HD scenario (38 days earlier), the smallest advancement occurred in the WD scenario (10 days earlier) and the WW scenario projected a delay of peak flow by 12 days (Table 4.5). A similar range of simulations occurred in the 2050 and 2080 periods with the HD scenario projecting the largest advancement and the WW projecting a later peak flow date.

4.4.5.2 Magnitude of Peak Streamflow

Over the 2020 and 2050 periods, the magnitude of peak flow (Table 4.5) increases in both wet and MD scenarios and decreases in both dry scenarios, relative to the baseline peak flow volume. The MD scenario projected an increase in peak flow magnitude in the 2020 period however by the 2050 period, peak flow magnitude is reduced (-1.9%) from baseline conditions. By the 2080 period, all scenarios projected an increase in peak flow magnitude with the exception of the HD scenario, which projected a 13.8% decrease from the baseline values. Over the three simulated future time periods, HD was the only scenario to consistently project decreases in the peak flow magnitude while both wet scenarios projected increases throughout all three future time periods.

Table 4.6: Mean change in peak flow date (days) and peak flow magnitude (% relative to baseline) for all scenarios at the over the three time periods.

Scenario	Period	Δ Days	Magnitude (%)
HD	2020	-38.0	-30.3
HW	2020	-28.0	14.1
MD	2020	-22.0	1.9
WD	2020	-10.0	-12.7
WW	2020	12.0	19.4
HD	2050	-41.0	-2.8
HW	2050	-36.0	45.0
MD	2050	-8.0	-1.9
WD	2050	-18.0	-2.2
WW	2050	11.0	17.5
HD	2080	-35.0	-13.8
HW	2080	-18.0	67.0
MD	2080	-18.0	7.0
WD	2080	-13.0	13.3
WW	2080	14.0	43.7

4.5 Discussion

4.5.1 Projected Climate Change

The selection of scenarios from the 2020 period reflected the range of uncertainty in future regional climate projections. Through all time periods and across all scenarios, there was a projected increase in mean annual temperature from the baseline, and greater increase of mean annual temperature in more distant decades. For the 2020 selection period, wet and dry scenarios projected increases and decreases in annual precipitation from the baseline period. However, in the future time periods (2050 and 2080), annual precipitation was projected to increase in all scenarios, with the exception of the HD scenario in the 2080 period. Therefore, in some cases, the drier scenarios in later time periods reflected an increase in annual precipitation.

All scenarios, with the exception of HD 2020, HD 2080, and WD 2020, projected an increase in annual temperature and precipitation similar to the most recent summary of regional climate projections in North America (Christensen *et al.,* 2007). The range of annual mean temperature and precipitation projections over the 2020 period was similar to the projections for the province of Alberta by Barrow and Yu (2005). They projected a range of increases in mean temperatures between 0°C to 2°C and a range between decrease of 10% and an increase of 10% change in mean annual precipitation over the 2020 period. The trend in seasonal projections which indicated increased winter and spring precipitation and decreased summer precipitation over the 2020 period (MD, HW, HD), was comparable to the projections in southern regions of Canada concluded by the IPCC (Christensen *et al.,* 2007).

The application of a sensitivity analysis to the full range of plausible future regional climates was complicated by the variability between the GCM projections for this region, common to areas with strong orographic forcing (Christensen *et al.,* 2007). The selection of the five representative scenarios was based on the mean annual projection for both temperature and precipitation over the 2020 period. However, at later time periods, the seasonal and monthly projected changes did not result in a consistent representation of the range of the original five scenarios. An example of this was illustrated in the 2050 and 2080 periods when the HD scenarios did not project as large a warming as the WD scenarios, which complicated the interpretation of the results.

4.5.2 Sensitivity of the ACRU Modelling System to Climate Scenarios

The sensitivity of the ACRU modelling system to the projected changes in temperature and precipitation were reflected in the changes in the major annual water balance components (Table 4.4). The sensitivity of the ACRU modelling system to changes in winter temperature was seen in reduction of snow, relative to the baseline, at every time period and across all five scenarios. The ACRU snowmelt module is based on a threshold of temperature, which determines the form of precipitation and thus the changes in snow storage. The changes in the simulated precipitation were consistent with other research that investigated the impacts of climate change in mountainous catchments (Hamlet and Lettenmaier, 1999; Loukas *et al.,* 2002). The reduction of snow accumulation due to increased winter temperatures has been illustrated in several studies in western Canada (Loukas and Quick, 1996; Loukas *et al.,* 2004; Lapp *et al.,* 2005). The simulated change in the form of precipitation in the Beaver Creek was also consistent

with the findings of Whitfield *et al.* (2002) who projected an increase in rain on snow events in hybrid catchments in southern British Columbia.

The changes in the peak flow date were also impacted by the effect that increased winter temperatures have on the precipitation form and snowmelt behavior. In the drier future scenarios, the smaller volume of snowpack melted quicker under higher temperatures, and resulted in earlier peak flow dates relative to scenarios with the highest increase in temperature. The volume of snowpack also influenced the changes in the magnitude of the peak streamflow event.

The simulated changes in annual actual evapotranspiration confirmed that the ACRU modelling system was sensitive in the soil moisture budgeting and total evaporation routines, as the annual changes appear to be consistent with changes in available moisture (i.e. precipitation). Annual potential evapotranspiration increased from the baseline in every scenario while annual actual evapotranspiration was limited by available moisture in the dry scenarios over the 2020 period. Additional reductions of actual evapotranspiration occurred in the HD and HW scenarios over the 2050 period, which incurred the largest reductions of summer and fall precipitation (Table 4.3). A similar response of actual evapotranspiration was observed in the HD 2080 scenario where an annual reduction of precipitation (-0.2%) was projected. This illustrated the resilience of actual evapotranspiration to warmer temperatures (i.e. potential evapotranspiration) in a semi-arid climate. The HD 2080 scenario did not result in a decrease of annual streamflow, however, relative to the other scenarios over this period, the increase in this scenario was negligible (2.8%) (Table 4.4).

Changes in annual precipitation volume had a discernible impact on simulated streamflow volume. The two scenarios with the largest decreases in annual precipitation (HD 2020 and WD 2020) resulted in the only reductions in annual streamflow volumes out of the 15 simulations. Beyond the 2020 period, all five scenarios were in agreement on the increasing mean annual volume of streamflow in the Beaver Creek streamflow. While they were not exclusively related to the projected changes in precipitation, they were substantially influenced by increases in mean annual precipitation. The annual results indicated that with future warming, it is probable that wet years may result in higher annual volumes while dry years may have an opposing effect on the total annual streamflow volume.

4.5.3 Seasonal Shifts in Hydrology

The simulations of streamflow in the Beaver Creek revealed a shift in the seasonal streamflow distribution beyond the 2020 time period. In each season, the majority of scenarios were in agreement on the direction of change, which projected higher winter and spring flow volumes, and reduced summer and fall flow volumes relative to the baseline simulation. Byrne *et al.* (1999) estimated that spring runoff volumes in the Oldman Basin would increase in a 2 X CO_2 climate. Leith and Whitfield (1998) also found that warmer temperatures resulted in higher winter flows and reductions in summer and fall streamflow volumes in south-central British Columbia. In the semi-arid Okanagan Basin, Cohen *et al.* (2006) and Merritt *et al.* (2006) found that future scenarios projected reductions of summer flow volumes. In the future, while the annual volumes may increase due to warmer and wetter winter and spring seasons, the ACRU model has

simulated an overall drying and concomitant lower streamflows in the majority of summer and fall seasons beyond the 2020 period.

4.5.4 Impact of Climate Scenarios on Late Season Flows

The seasonal results have indicated that water supply will be dramatically reduced in the summer and fall seasons. To gain a better perspective on the maintenance of baseflow volumes in the Beaver Creek, the relationship between seasonal precipitation and late season streamflow was investigated based on available climate and hydrological observations. A number of predictors such as seasonal precipitation, rain and snow were tested for their ability to establish a linear relationship with mean volumes of streamflow in the late summer/early fall period. Of all possible combinations of months, seasons and forms of precipitation, the only significant relationship that emerged in a stepwise multiple linear regression was predicted by spring (MAM) rainfall (R^2= 0.37, n=39). Seasonal snow volume and summer rainfall made no contribution to the linear regression model.

These results have indicated that it is plausible that groundwater recharge in the spring melt period may have the greatest effect on baseflow production in the summer and fall months. Similarly, Rock and Mayer (2006) concluded through isotope analysis that groundwater is a principal contributor to peak streamflow in the Oldman Basin. The Beaver Creek is a perennial stream, yet the majority of precipitation is received in the months of May, June and July. Therefore, a significant portion of perennial flow is likely maintained by groundwater. Understanding how the projected changes in annual temperature and precipitation will manifest in groundwater recharge and thus baseflow

volumes is essential to estimating the full range of impacts on the hydrological regime of the Beaver Creek.

The climate change projections for the Beaver Creek (WD 2020 excluded) would suggest that a higher volume of liquid water would be available in the winter season (more precipitation as rainfall) for infiltration and contribution to the groundwater store. However, despite the presence of warmer and wetter winters, four of the five scenarios projected decreases in the fall streamflow volume. A closer examination of the 2050 simulations illustrated the impact of the changes in temperature and precipitation on the simulated storages, and thus water available for baseflows in the fall season.

Soil moisture storages are shown to be increasing above baseline conditions beginning in the early winter and continuing through early spring (Figure 4.5). Beyond the Julian day 106 (April), this storage falls below the baseline condition until Julian day 320 (November). Figure 4.6 shows that actual evapotranspiration, simulated by the ACRU model, responded to the higher potential evapotranspiration and exceeded the baseline in the winter months (Julian dates 350-46). This response proceeded until Julian day 75 (April), when several of the scenarios fell below baseline evapotranspiration, which indicated that moisture was limited at this point. Actual evaporation was below the baseline level in the majority of scenarios after Julian day 197 (July).

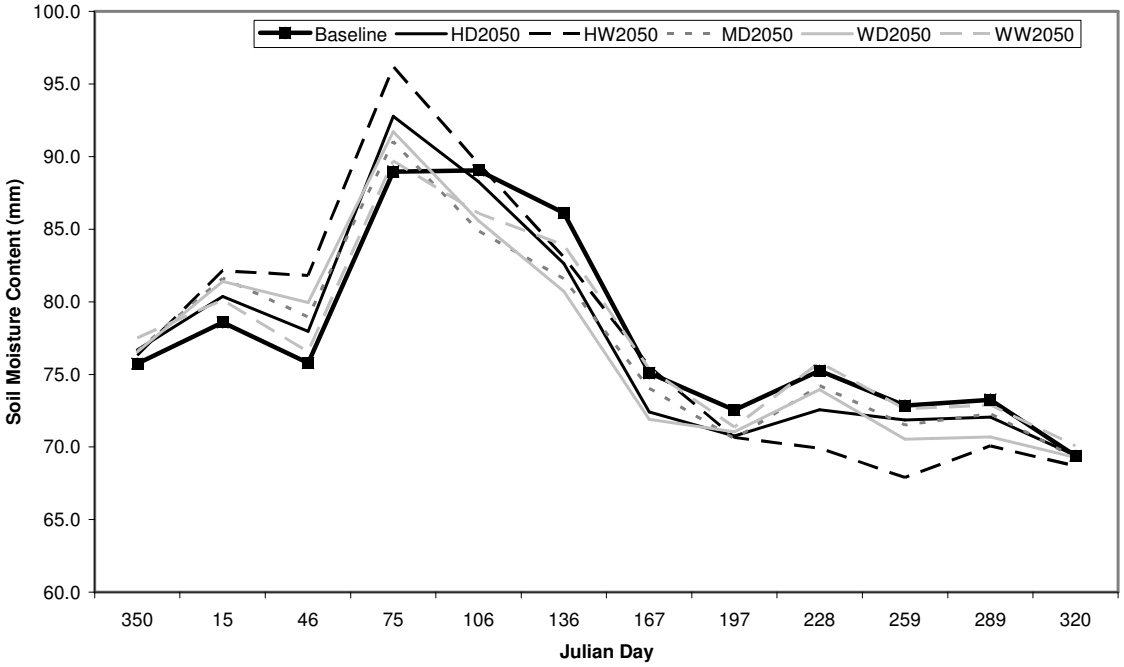

Figure 4.5: Mean monthly change in soil moisture content of surface and subsurface horizons over the 2050 period.

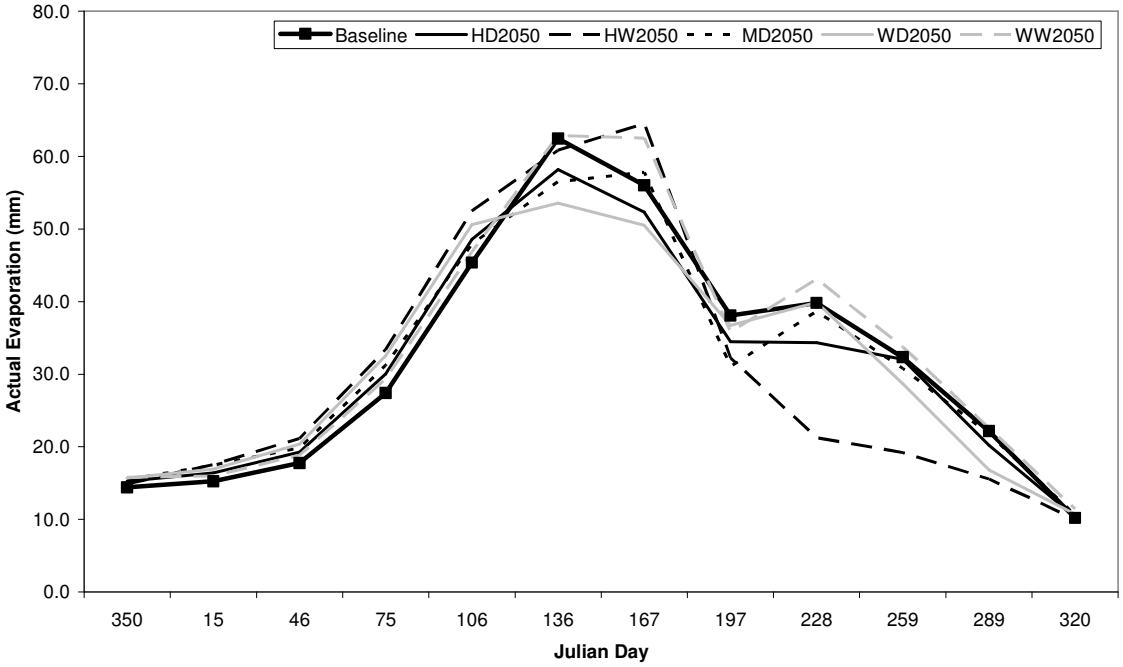

Figure 4.6: Mean monthly change in actual evapotranspiration for the 2050 period.

In the ACRU model, groundwater storages are recharged when soil moisture levels exceed the field capacity of the subsurface soil horizon, and water is redistributed to the groundwater storage. Therefore, a reduction of soil moisture below baseline conditions resulted in a reduced number of events when soil moisture exceeded the field capacity. Consequently, this resulted in a reduction of the total volume of groundwater recharge and thus baseflow storage (Figure 4.7). The warmer and drier summer conditions resulted in an earlier recession of the baseflow store relative to the baseline period. Near Julian day 320, the baseflow storage did not contain the volume required to sustain baseflow contributions of the baseline period. In addition to the reductions of precipitation, reduced groundwater contribution may have contributed to the declining flows simulated by four of the five scenarios in this period.

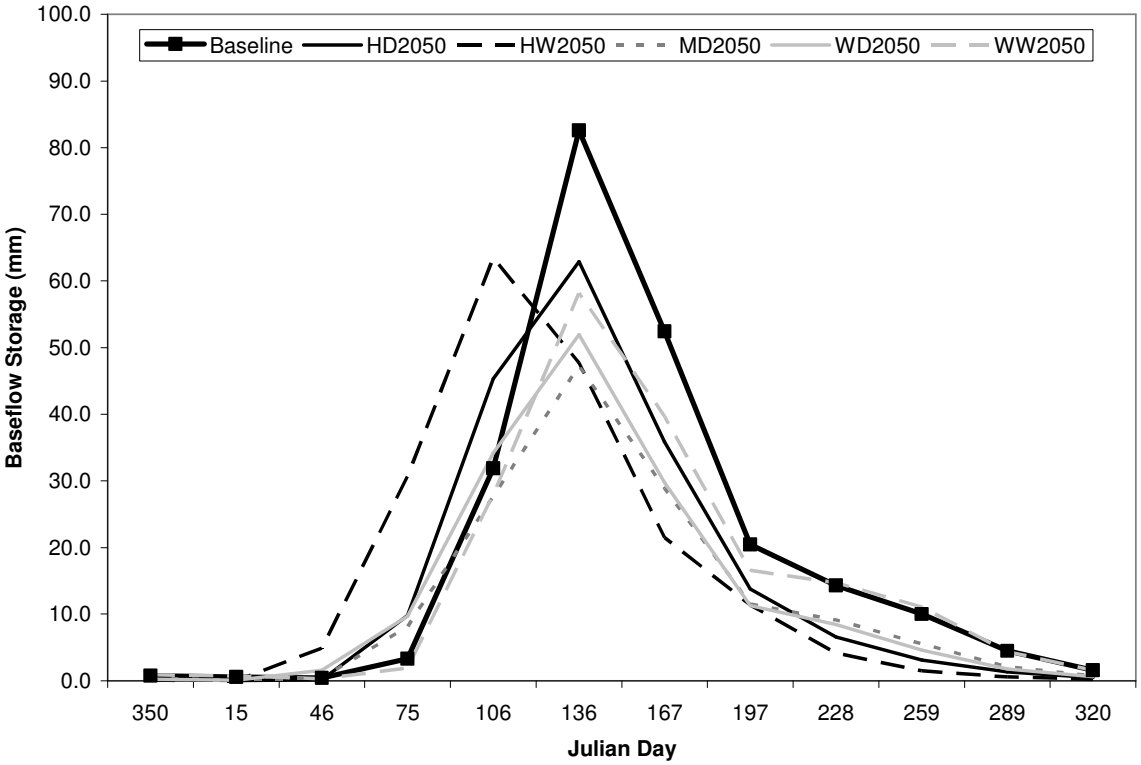

Figure 4.7: Mean monthly change in baseflow storage for the 2050 period.

4.5.5 Uncertainty

The interpretation of the simulations presented here is limited due to the assumptions and uncertainties in both data and methods. The validity of the hydrological model over the verification period has a significant influence on the bias of the results as the best parameterization resulted in a 3.5% mean monthly under-simulation. The simulations of future hydrological response also assume that the parameterization for the 1965-2005 period will be accurate in future climates. Further, the Beaver Creek catchment was assumed to have no groundwater exchange with neighboring watersheds. The assumption was that the catchment received no groundwater contribution from outside the watershed, and released all groundwater upstream of the catchment outlet (i.e. the gauging station).

The results simulated for the Beaver Creek catchment illustrated that the choice of downscaling method likely impacted the outcome of results. Akinremi *et al.* (1999) found that, while annual precipitation in the Prairies increased in recent decades, the total precipitation volume was attributed to a higher frequency of low-intensity events. Applying the mean monthly change between the baseline climate and future climates (delta method) assumed that the variability observed in the baseline period would persist in the future. This method does not account for changes in the behaviour of future meteorological variables, particularly important for projections of precipitation. The importance of groundwater recharge in the Beaver Creek suggests that both the frequency and intensity of future precipitation may impact infiltration and depression storages. Methods such as statistical downscaling, which use daily GCM output rather than the mean change, may prove to be beneficial in addressing these research questions.

4.6 Conclusion

This study examined the impact of climate change on the hydrological regime of the Beaver Creek catchment. This research was focused on examining the effects of the range of projected regional climate changes on the hydrological response. Previous work in the Oldman Basin had not explicitly focused on climate change impacts in a hybrid catchment, nor had a study focused on modelling hydrological response in the Porcupine Hills. The simulations of the potential future hydrology in the Beaver Creek have illustrated the sensitivity of hydrological processes to changes in temperature and precipitation. This has provided important information on the future of water availability in the Beaver Creek based on changes in climate presently forecast by GCMs for this region.

The projections for future regional climate are within the range reported for North America and the province of Alberta. All scenarios were in agreement on the increase of mean annual temperature in the future. Projections of future regional precipitation were less certain in the direction of change, however, the majority of models projected increased annual volumes, particularly in later time periods.

Hydrological simulations of these projections have shown that, while the majority of scenarios projected an increase in annual precipitation, the seasonal availability of streamflow, particularly in the summer and fall months, was affected by the seasonal projections of temperature and precipitation. The majority of scenarios projected increased winter and spring precipitation while summer and fall precipitation was projected to decrease below the baseline volume. As a result, the majority of

hydrological simulations (i.e. 4 of 5 scenarios) indicated an increase in winter and spring streamflows and a decrease of summer and fall (late) season streamflow volumes.

The 1961 – 1990 baseline simulations for summer and fall streamflow volumes were 6.9mm and 1.8mm respectively. Of the scenarios that projected a reduction in these volumes (4 of 5), the range of reductions for the 2020 time period projected streamflow to decline between 4.0mm - 5.8mm and between 1.1mm - 1.3mm for summer and fall seasons respectively. By the 2050 period, this range was simulated between 4.7mm – 5.6mm for summer and between 0.4mm and 1.6mm for the fall season. Finally, by the 2080 period, the range was simulated between 4.0mm – 5.5mm and between 0.6mm – 1.7mm for the summer and fall seasons.

The shift in seasonal streamflow volume was also observed in the earlier occurrence of the peak flow event in the majority of the scenarios. The simulated soil water storages have also illustrated the importance of groundwater in the hydrology of the Beaver Creek and its potential vulnerability to climate change, despite projections of warmer and wetter winters in the future.

This research provided an initial indication of the impacts of climate change on hydrological processes in a southern Alberta catchment. Future work needs to compare these results to simulations driven by other methods of downscaling, particularly those which incorporate changes in precipitation variability such as statistical downscaling. Recognizing that only changes to precipitation and temperature were made in these simulations, future work should also include changes in other meteorological variables as well as land cover to improve the overall simulation of the effects of climate change on the Beaver Creek catchment.

CHAPTER 5

Summary and Recommendations

5.1 Summary

This thesis applied the ACRU hydrological modelling system to a catchment in the Beaver Creek catchment in southern Alberta, and examined the potential impacts of climate change on hydrology. The first objective was to determine if the ACRU hydrological model could successfully simulate the observed hydrology of the Beaver Creek catchment. Once verified, the second objective of this thesis was to use the ACRU model to investigate the impacts of potential climate change on the Beaver Creek catchment. The completion of both objectives provided the initial investigation of climate change impacts on the hydrology of a hybrid catchment in the Porcupine Hills of southern Alberta.

For the completion of the first objective, the ACRU hydrological modelling system was parameterized and verified against monthly streamflow observations in a 27-year verification analysis. The parameterization focused on achieving the highest simulation accuracy of observed monthly volumes while ensuring that all parameters input to the modelling system were physically meaningful.

The ACRU simulation explained 78% of the variation in the monthly streamflow observations, while under-simulating the monthly volume by an average of 3.34% per month. The visual verification of the simulated and observed hydrographs indicated a reasonable simulation, particularly in the timing of peak streamflow and, rising and recession limbs. The mean monthly volumes were well simulated, particularly in the late summer and fall baseflow periods. The parameterization and verification of the ACRU

model for the Beaver Creek catchment provided the fundamental basis for a climate change impacts study.

Climate change scenarios were downscaled from GCM output for five scenarios representing warmer-wetter, warmer-drier, hotter-wetter, hotter-drier and median projected mean annual changes in temperature and precipitation for the southern Alberta region, relative to current conditions. These scenarios were downscaled using the delta method (Xu, 1999a), where monthly changes, determined by the GCM, were applied to a climate baseline of daily observations (1961-1990) in the study area. The perturbed climate records for the five scenarios were used to drive the parameterized ACRU model and simulate the hydrological response in the Beaver Creek catchment.

The projections of potential future climates indicated a consistent warming in all scenarios for the three future time periods of 2020, 2050 and 2080. Although in all scenarios, annual precipitation was projected to increase in all scenarios beyond the 2020 period, the majority of scenarios indicated increased winter and spring precipitation and decreased summer and fall precipitation. The ACRU model simulated a similar response in mean seasonal streamflow volumes for the three time periods in the Beaver Creek catchment.

The majority of ACRU simulations (i.e. 4 of 5 scenarios) indicated that future summer and fall (late) season streamflow volumes would be reduced below the 1961-1990 mean conditions. Across the five simulated scenarios, the WW scenario consistently projected the only wetter conditions, which resulted in increased streamflow volume over the late seasons, throughout all time periods. However, the majority of the scenarios (4 of 5) projected decreased streamflow in the late season.

The 1961 – 1990 baseline simulations for summer and fall streamflow volumes were 6.9mm and 1.8mm respectively. Of the scenarios that projected a reduction in these volumes (4 of 5), the range of reductions for the 2020 time period projected streamflow to decline between 4.0mm - 5.8mm and between 1.1mm - 1.3mm for summer and fall seasons respectively. For the 2050 period, this range was simulated between 4.7mm – 5.6mm for summer and between 0.4mm and 1.6mm for the fall season. Finally, for the 2080 period, the range was simulated between 4.0mm – 5.5mm and between 0.6mm – 1.7mm for the summer and fall seasons.

The reductions in seasonal water volumes in the Beaver Creek catchment were due to changes in the components of the regional water balance. Despite projected increases in winter and spring precipitation, higher potential and actual evapotranspiration, relative to the baseline, resulted in a reduction of soil moisture storages below baseline levels (Figure 4.5). This resulted in a reduction of groundwater recharge and a concomitant reduction in baseflow contribution to streamflows in the summer and fall seasons in the Beaver Creek catchment. Annual baseflow storage volumes simulated for the 2050 period were reduced by as much as 36% (MD) relative to the baseline conditions (Figure 4.7).

The ACRU simulations highlighted the sensitivity of hydrological processes to the projected changes in monthly temperature and precipitation in this region. Despite increases in potential evapotranspiration, actual evapotranspiration was reduced in response to limited soil moisture. Additionally, the simulated redistributions of soil moisture, specifically groundwater recharge, have illustrated that the interactions of the water balance components in this region should be investigated as a system. Process-

based hydrological modelling in this region, specifically the ACRU modelling system, has provided valuable insight into how projected future changes may affect water availability.

The results of the Beaver Creek catchment were similar to those concluded in previous research that have investigated the impacts of climate change on the hydrological systems and processes in western Canada. Whitfield *et al.* (2002) concluded that hybrid streams in southwestern British Columbia would experience increased winter flows under scenarios of future climate, similar to the projections for the Beaver Creek catchment. Seasonal departures from present conditions in the late season were also concluded by Merritt *et al.* (2006), who projected reductions of summer streamflow volumes between 50% and 80% by the 2080 time period in subwatersheds of the semi-arid Okanagan Basin. They also simulated reduced seasonal flow volumes despite increased winter precipitation, and found variable responses of annual flow volumes under different climate change scenarios in the Okanagan subwatersheds, similar to the results in the Beaver Creek catchment. The mountain headwater areas of the Oldman Basin were investigated by Lapp *et al.* (2005) who projected that winter snowpack would decline over the period 2021 through 2050, which would lead to potential issues for water resources. Similarly, the Beaver Creek simulations have illustrated the potential reduction of available water resources in the semi-arid, Porcupine Hills area of the Oldman Basin beginning as early as the 2010-2039 time period.

The simulations of potential future hydrological responses presented in this research have illustrated that climate change could seriously reduce the availability of water resources in the Beaver Creek catchment. The quantification of climate change

impacts on a tributary catchment of the Oldman Basin provided an initial indication of the potential impacts of climate change in this region. The information presented in this thesis may be beneficial for many sectors, including agriculture, water resources and human and ecosystem health.

5.2 Recommendations

Further research opportunities exist to enhance our understanding of the simulation accuracy of the ACRU model in this region, and the projected future regional changes in climate. The initial parameterization and verifications of the ACRU model in Beaver Creek were challenged by the limitations of the available data and the scale of simulation required to verify the model. It would be beneficial for future research to continue the development of areal data sets for this region, in particular for precipitation as monitoring is less prevalent in remote and high elevation regions, which constitute many headwater watersheds. The incorporation of remote sensing would offer additional benefits for land cover classification, vegetation biomass and phenology, in particular the response of vegetation to drought stress. More extensive field validation of modelled data sets would improve the confidence in model simulations and quantify the hydrological and meteorological processes specific to this region.

Given the potential changes projected for winter climate in the region, collection of streamflow data throughout the winter months would improve the verification of the winter snow modelling. The acquisition of higher resolution land cover data would also improve the land phase of the simulation and allow further research into “hydrologically relevant” parameters. The hydrological behavior of soils and vegetation in this region

should be studied at a local-scale to improve on the existing information. The collection, verification and refinement of all data would benefit the parameterization of ACRU in southern Alberta as well as other physically-based modelling endeavors in semi-arid climates in the future.

As with all projections of future climate change, the uncertainty of future greenhouse gas and aerosol emissions and their associated radiative forcing complicate the simulation of future global climate. However, improved regionalization of current GCM output in this region would be of great benefit to the validity of future research. The limitations of the delta method illustrated that future simulations be driven with scenarios that include the projected changes in precipitation variability. This could be achieved through the application of the statistical downscaling regionalization technique. The incorporation of future variability in precipitation projections would facilitate research focusing on the dynamics of snow, canopy and soil storage and improve the overall simulation of future hydrological processes in this region.

As a result of the semi-arid climate in southern Alberta, crop irrigation is a common agricultural practice. In light of the findings of this research, it would be beneficial to examine the impacts of climate change on catchments that have irrigated crops. Additional research could examine the frequency and intensity of irrigation applications and their impact on soil moisture volumes and soil water redistribution. Furthermore, the future changes in climate will presumably alter the current distribution and productivity of vegetation. Future simulations in Beaver Creek could examine the impacts of changing land use or crop water consumption on streamflow volumes.

This thesis has presented the initial simulations of climate change impacts on the Beaver Creek catchment. The results have indicated that despite projections for wetter years in the future, water availability in the summer and fall seasons may be compromised due to the projected changes in temperature and precipitation for the southern Alberta region. However, in the future, the investigation of the impacts of climate change on the entire hydrological system in southern Alberta will be necessary to obtain the most realistic projection of future conditions. The simulation of changes in both demand and supply on water resources is required if future climate change adaptation strategies are to be successful.

REFERENCES CITED

Abbott, M.B., Bathurst, J.C., Cunge, J.A., O'Connell, P.E., Rasmussen, J., 1986. An introduction to the European Hydrological System- Systeme Hydrologique Europeen, "SHE", 1: History and philosophy of physically-based, distributed modeling system. *Journal of Hydrology,* 87, 45-59.

Alberta Environment (AENV), 2003. *Water For Life. Alberta's Strategy for Sustainability.* Government of Alberta.

Alberta Environment (AENV), 2000. Alberta Topography. The University of Alberta.

Akinremi, O.O., McGinn, S.M., 1999. Precipitation Trends on the Canadian Prairies. *Journal of Climate,* 12 (10), 2996-3003.

Akinremi, O.O., McGinn, S.M., Cutforth, H.W., 2001. Seasonal and Spatial Patterns of Rainfall Trends on the Canadian Prairies. *Journal of Climate,* 14 (9), 2177-2182.

Andreasson, J., Lindstrom, G., Grahn, G., Johansson, B., 2004. Runoff in Sweden-Mapping of Climate Change Impacts on Hydrology. *Nordic Hydrological Programme,* NHP Report, 48 (2), 625-632.

Arnell, N.W., 1999. Climate change and global water resources. *Global Environmental Change,* 9, 31-49.

Arnold, J.G., Srinivasan, R., Muttiah, R.S., Williams, J.F., 1998. Large area hydrologic modeling and assessment Part I: Model development. *Journal of the American Water Resources Association,* 34 (1), 73-89.

Arora, V.K., Boer, G.J., 2001. The effects of simulated climate change on the hydrology of major river basins. *Journal of Geophysical Research,* 106 (D4), 3335-3348.

Barnett, T.P., Adam, J.C., Lettenmaier, D.P., 2005. Potential impacts of warming on water availability in snow dominated regions. *Nature,* 438, 303-309.

Barrow, E., Yu, G., *Climate Scenarios for Alberta* A Report Prepared for the Prairie Adaptation Research Collaborative (PARC) in co-operation with Alberta Environment. Alberta Environment, Regina, Saskatchewan.

Bathurst, J.C., Ewen, J., Parkin, G., O'Connell, P.E., Cooper, J.D., 2004. Validation of catchment models for predicting land-use and climate change impacts. 3. Blind validation for internal and outlet responses. *Journal of Hydrology,* 287 (1-4), 74-94.

Belatos, S., Prowse, T., Bonsal, B., MacKay, R., Romolo, L., Pietroniro, A., Toth, B., 2006. Climatic effects on ice-jam flooding of the Peace-Athabasca Delta. *Hydrological Processes,* 20, 4031-4050.

Betts, R.A., Cox, P.M., Woodward, F.I., 2000. Simulated responses of potential vegetation to doubled –CO_2 climate change and feedbacks on near-surface temperature. *Global Ecology and Biogeography,* 9, 171-180.

Beven, K.J., 2002. *Rainfall-Runoff Modelling: The Primer.* John Wiley and Sons, Ltd. Chichester, New York, Weinheim, Brisbane, Singapore, Toronto.

Beven, K., 2001. How far can we go in distributed hydrological modelling? *Hydrology and Earth System Sciences,* 5 (1), 1-12.

Beven, K., Binley, A., 1992. The future of distributed models: model calibration and uncertainty prediction. *Hydrological Processes,* 6 (3), 279-298.

Beven, K., 1989. Changing Ideas in Hydrology-The Case of Physically-Based Models. *Journal of Hydrology,* 105, 157-172.

Beven, K.J., Kirkby, M.J. 1979. A Physically-Based, Variable Contributing Area Model of Basin Hydrology. *Hydrological Sciences Bulletin,* 24(1), 43-69.

Betts, R.A., Boucher, O., Collins, M., Cox, P.M., Falloon, P.D., Gedney, N., Hemming, D.L., Huntingford, C., Jones, C.D., Sexton, D.M.H., Webb, M.J., 2007. Projected increase in continental runoff due to plant responses to increasing carbon dioxide. *Nature,* 448, 1037-1042.

Betts, R.A., Cox, P.M., Woodward, F.I., 2000. Simulated responses of potential vegetation to doubled-CO_2 climate change and feedbacks on near-surface temperature. *Global Ecology and Biogeography*, 9, 171-190.

Biftu, G.F., Gan, T.Y., 2001. Semi-distributed, physically based, hydrologic modeling of the Paddle River Basin, Alberta, using remotely sensed data. *Journal of Hydrology,* 244, 137-156.

Boer, G.J., Flato, G., Ramsden, D., 2000. A transient climate change simulation with greenhouse gas and aerosol forcing: projected climate to the twenty-first century. *Climate Dynamics,* 16, 427-450.

Bonsal, B.R., Wheaton, E.E., 2005. Atmospheric Circulation Comparisons between the 2001 and 2002 and the 1961 and 1988 Canadian Prairie Droughts. *Atmosphere-Ocean*, 43(2), 163-172.

Bonsal, B.R., Prowse, T.D., Pietroniro, A., 2003. An assessment of global climate model-simulated climate for the western cordillera of Canada (1961 – 90). *Hydrological Processes,* 17, 3703-3716.

Bonsal, B.R., Lawford, R.G., 1999. Teleconnections between El Nino and La Nina event and summer extended dry spells on the Canadian Prairies. *International Journal of Climatology,* 19(13), 1445-1458.

Bonsal, B.R., Zhang, X., Hogg, W.D., 1999. Canadian Prairie growing season precipitation variability and associated atmospheric circulation. *Climate Research,* 11, 191-208.

Bronstert, A., Niehoff D., Gurger, G., 2002. Effects of climate and land-use change on storm runoff generation: present knowledge and modelling capabilities. *Hydrological Processes,* 16, 509-529.

Brown, R.D., Goodison, B.E., 1996. Interannual Variability in Reconstructed Canadian Snow Cover, 1915-1992. *Journal of Climate,* 9, 1299-1318.

Boyle, D.P., Gupta, H.V., Sorooshian, S., Kornen, V., Zhang, Z., Smith, M., 2001. Toward improved streamflow forecasts: Value of semidistributed modeling. *Water Resources Research,* 37(11), 2749-2759.

Burn, D.H., Hesch, N.M., 2007. Trends in evaporation for the Canadian Prairies. *Journal of Hydrology,* 336, 61-73.

Burn, D.H., Abdul Aziz, O.I., Pietroniro, A., 2004. A Comparison of Trends in Hydrological Variables for Two Watersheds in the Mackenzie River Basin. *Canadian Water Resources Journal*, 29 (4), 284-298.

Burn, D.H., Hag Elnur, M.H., 2002. Detection of hydrologic trends and variability. *Journal of Hydrology,* 255, 107-122.

Burn, D.H., 1994. Hydrologic effects of climatic change in west-central Canada. *Journal of Hydrology,* 160*, 53-70.*

Byrne, J.M., Berg, A., Townshend, I., 1999. Linking observed and general circulation model upper air circulation patterns to current and future snow runoff for the Rocky Mountains. *Water Resources Research.* 35, 3793–3802.

Byrne, J.M., Berg, A.A., 1998. Spatial Analysis of Temperature and Precipitation Anomalies on the Canadian Prairies During Two Strong El Nino Events. *Canadian Water Resources Journal,* 23 (3), 231-243.

Byrne, J.M., Barendregt, R., Schaffer, D., 1989. Assessing Potential Climate Change Impacts on Water Supply and Demand in Southern Alberta. *Canadian Water Resources Journal,* 14 (4), 5-10.

Carter, T.R, Parry, M.L., Harasawa, H., Nishioka, S., 1994. *IPCC Technical Guidelines for Assessing Climate Change Impacts and Adaptations.* London: Department of Geography, University College London.

Case, R.A., MacDonald, G.M., 1995. A Dendroclimatic Reconstruction of Annual Precipitation on the Western Canadian Prairies since A.D. 1505 from *Pinus flexilis* James. *Quaternary Research,* 44, 267-275.

Changnon, D., T., McKee,B., Doesken, M.J.,1993. Annual snowpack patterns across the Rockies: Long-term trends and associated 500-mb synoptic patterns. *Monthly Weather Review,* 121**,** 633–647.

Chetty, K., Smither, J., 2005, Continuous simulation modelling for design flood estimation in South Africa: Preliminary investigations in the Thukela catchment. *Physics and Chemistry of the Earth,* 30, 634-638.

Christensen, J.H., B. Hewitson, A. Buisuioc, A. Chen, X. Gao, I. Held, R. Jones, R.K. Kolli, W.-T. Kwon, R. Laprise, V. Magana Rueda, L. Mearns, C.G. Menendez, J. Ralsanen, A. Rinke, A. Sarr , P. Whetton, 2007. Regional Climate Projections. In: Climate Change 2007: The Physical Science Basis, Contribution of Working Group 1 to the Fourth Assessment Report of the Intergovernmental Panel on Climate Change [Solomon, S., D. Quin, M.Manning, Z. Chen, M. Marquis, K.B. Averyt, M.Tignor, H.L. Miller (eds.)]. Cambridge University Press, United Kingdom and New York, NY, USA.

Christensen, N.S., Wood, A.W., Voisin, N., Lettenmaier, D.P., Palmer, R.N., 2004. The Effects of Climate Change on the Hydrology and Water Resources of the Colorado River Basin. *Climatic Change,* 62, 337-363.

Cohen, S.J., Neilsen, D., Smith, S., Neale, T., Taylor, B., Barton, M., Merritt, W., Alila, Y., Shepherd, P., McNeill, R., Tansey, J., Carmichael, J., Langsdale, S., 2006. Learning with Local Help: Expanding the Dialogue on Climate Change and Water Management in the Okanagan Region, British Columbia, Canada. *Climatic Change*, 75, 331-358.

Cohen, S.J., 1991. Possible Impacts of Climatic Warming Scenarios on Water Resources in the Saskatchewan River Sub-Basin, Canada. *Climatic Change,* 19, 291-317.

Cohen, S.J., 1990. Bringing the global warming issue closer to home. The challenge of regional impact studies. *Bulletin of the American Meteorological Society,* 71, 520-526.

Coulibaly, P., Burn, D.H., 2005. Spatial and Temporal Variability of Canadian Seasonal Streamflows. *Journal of Climate,* 18 (1), 191-210.

Cramer, W., Bondeau, A., Woodward, R.I., Prentice, I.C., Betts, R.A., Brovkin, V., Cox, P.M., Fisher, V., Foley, J.A., Friend, A.D., Kucharik, C., Lomas, M.R., Ramankuty, N., Sitch, S., Smith, B., White, A., Young-Molling, C., 2001. Global response of terrestrial

ecosystem structure and function to CO_2 and climate change: results from six dynamic global vegetation models. *Global Change Biology,* 7, 357-373.

Daly, C., Neilson, R.P, Phillips, D.L., 1994. A Statistical-Topographic Model for Mapping Climatological Precipitation over Mountainous Terrain. *Journal of Applied Meteorology,* 33, 140-158.

Dent, M.C. 1988. Estimating crop water requirements for irrigation planning in southern Africa. *Agricultural Engineering in South Africa*, 20, 7-19.

Dettinger, M. D., Cayan,D.R., 1995. Large-scale atmospheric forcing of recent trends toward early snowmelt runoff in California. *Journal of Climate,* 8**,** 606–623.

Diaz, H.F., 2004. *Regional Changes and Global Connections: Monitoring Climate Variability and Change in the Western United States*. USDA Forest Service.

Dingman, S.L., 2002. *Physical Hydrology*, 2nd edn. Prentice-Hall: Upper Saddle River, NJ, USA.

Dirks, K.N., Hay, J.E., Stow, C.D., Harris, D., 1998. High-Resolution Studies of Rainfall on Norfolk Island Part II: Interpolation of Rainfall Data. *Journal of Hydrology,* 208 (3), 187-193.

Dooge, J.C.I., 1992. Hydrologic models and climate change. *Journal of Geophysical Research,* 97 (D3), 2677-2686.

Doorenbos, J., Pruitt, W.O., 1977. Guidelines for predicting crop-water requirements. FAO *irrigation and drainage paper 24.* FAO, Rome, pp 1-107.

Dore, M.H.I., 2005. Climate Change and changes in global precipitation patterns: What do we know? *Environment International,* 31, 1167-1181.

Douville, H., Chauvin, F., Planton, S., Royer, J.F., Salas-Melia, D., Tyteca, S., 2002. Sensitivity of the hydrological cycle to increasing amounts of greenhouse gases and aerosols. *Climate Dynamics*, 20, 45-68.

Drake, B.G., Gonzalez-Meler, M.A., 1997. More Efficient Plants: A Consequence of Rising Atmospheric CO_2? *Annual Review of Plant Physiology and Plant Molecular Biology,* 48, 609-639.

Elias, P.D.E., 1999. *From Grassland to Rockland. An Explorer's guide to the Ecosystem of Southernmost Alberta.* Rocky Mountain Books, Calgary, Alberta, Canada.

Epstein, D., Ramirez, J.A., 1994. Spatial Disaggregation for Studies of Climatic Hydrologic Sensitivity. *Journal of Hydraulic Engineering,* 120 (12), 1449-1467.

Everson, C.S., 2001. The water balance of a first order catchment in the montane grasslands of South Africa. *Journal of Hydrology,* 241, 110-123.

Feenstra, J.F., Burton, I. Smith, J., Tol, R.S.J. (eds.), 1998. *Handbook on Methods for Climate Change Impact Assessment and Adaptation Strategies,* UNEP/Vrije Universiteit Institute for Environmental Studies, Amsterdam.

Field, C.B., Mortsch, L.D., Brklacich, M., Forbes, D.L., Kovacs, P., Patz, J.A., Running, S.W., Scott, M.J., 2007. North America. *Climate Change 2007: Impacts, Adaptation and Vulnerability. Contribution of Working Group II to the Fourth Assessment Report of the Intergovernmental Panel on Climate Change,* Parry, M.L., Canziani, O.F., Palutikof, van der Linden, J.P., Hanson, C.E. (eds.). Cambridge University Press, Cambridge, UK, 717-652.

Flato, G.M., Boer, G.J., Lee, W.G., McFarlane, N.A., Ramsden, D., Reader, M.C., Weaver, A.J., 2000. The Canadian Centre for Climate Modelling and Analysis global coupled model and its climate. *Climate Dynamics*, 16, 451-467.

Flato, G.M., Boer, G.J., 2001. Warming Asymmetry in Climate Change Simulations. *Geophysical Research Letters,* 28 (1), 195-198.

Flugel, W.A., 1995. Delineating Hydrological Response Units by Geographical Information System Analysis for Regional Hydrological Modelling Using PRMS/MMS in the Drainage Basin of the River Brol, Germany. *Hydrological Processes,* 9, 423-436.

Flugel, W.A., 1997. Combining GIS with regional hydrological modelling using hydrological response units (HRUs): An application from Germany. *Mathematics and Computers in Simulation,* 43, 297-304.

Forster, P., Ramaswamy, V., Artaxo, P., Bernsten, T., Betts, R., Fahey, D.W., Haywood, J., Lean, J., Lowe, D.C., Myhre, G., Nganga, J., Prinn, R., Raga, G., Schulz, M., Van Dorland, R, 2007. Changes in Atmospheric Constituents and in Radiative Forcing. *In: Climate Change 2007: The Physical Science Basis. Contribution of Working Group I to the Fourth Assessment Report of the Intergovernmental Panel on Climate Change* [Solomon, S., Qin, D., Manning, M., Chen, Z., Marquis, M., Averyt, K.B., Tignor, M., Miller, H.L. (eds.)]. Cambridge University Press, Cambridge, United Kingdom and New York, NY, USA.

Frederick, K.D., Major, D.C., 1997. Climate change and water resources. *Climatic Change,* 37(1), 1573-1480.

Fyfe, J.C., Flato, G.M., 1999. Enhanced Climate Change and Its Detection over the Rocky Mountains. *Journal of Climate,* 12 (1), 230.243.

Gan. T.Y., 2000. Reducing Vulnerability of Water Resources of Canadian Prairies to Potential Droughts and Possible Climatic Warming. *Water Resources Management,*14, 111-135.

Gan, T.Y., 1998. Hydroclimatic trends and possible climatic warming in the Canadian Prairies. *Water Resources Research,* 34 (11), 3009-3015.

Gan, T.Y., 1995. Trends in air temperature and precipitation for Canada and Northeastern United States. *International Journal of Climatology* (Royal Meteorological Society), 15, 1115–1134.

Gan, T.Y., Dlamini, E.M., Biftu, G.F., 1997. Effects of model complexity and structure, data quality, and objective functions on hydrologic modeling. *Journal of Hydrology,* 192, 81-103.

Garnett, E.R., Khandekar, M.L., Babb, J.C., 1998. On the Utility of ENSO and PNA Indices for Long-Lead Forecasting of Summer Weather over the Crop-Growing Region of the Canadian Prairies. *Theoretical and Applied Climatology.* 60, 37-45.

Giorgi, F., Whetton, P.H., Jones, R.G., Christensen, J.H., Mearns, L.O., Hewitson, B., von Storch, H., Francisco, R., Jack, C., 2001. Emerging patterns of simulated regional climatic changes for the 21st century due to anthropogenic forcings. *Geophysical Research Letters,* 48 (17), 3317-3320.

Giorgi, F., Mearns, L.O., 1991. Approaches to the simulation of regional climate change : A review. *Reviews of Geophysics,* 29 (2), 191-216.

Gleick, P.H., 1993. Water and Conflict: Fresh Water Resources and International Security. *International Security*, 18 (1), 79-112.

Gleick, P.H., 1986. Methods for Evaluating the Regional Hydrologic Impacts of Global Climatic Changes. *Journal of Hydrology,* 99, 97-116.

Grace, B.W., 1987. Chinooks. *Chinook,* 9, 52-56.

Groisman, P.Y., Legates, D.R., 1995. Documenting and Detecting Long-Term Precipitation Trends: Where We Are and What Should be Done. *Climatic Change,* 31, 601-622.

Groisman, P.Y., Knight, R.W., Easterling, D.R., Karl, T.R., Hegerl, G.C., Razuvaev, V.N., 2005. Trends in Intense Precipitation in the Climate Record. *Journal of Climate,* 18 (9), 1326-1350.

Groisman, P.Y., Knight, R.W., Karl, T.R., Easterling, D.R., Sun, B., Lawrimore, J.H., 2004. Contemporary Changes of the Hydrological Cycle over the Contiguous United States: Trends Derived from In Situ Observations. *Journal of Hydrometeorology,* 5, 64-85.

Gullet, D.W., Skinner, W.R.,1992. The state of Canada's climate: temperature change in Canada 1895–1991. Environment Canada SOE Report 92-2. Department of Supply and Services, Ottawa, Canada.

Gurtz, J., Baltensweiler, A., Lang, H., 1999. Spatially distributed hydrotope-based modelling of evapotranspiration and runoff in mountainous basins. *Hydrological Processes,* 13, 2751-2768.

Hamlet, A.F., Lettenmaier, D.P., 1999. Effects of Climate Change on Hydrology and Water Resources in the Columbia Basin. *Journal of the American Water Resources Association.* 35(6), 1597-1623.

Hauer, F.R., Baron, J.S., Campbell, D.H., Fausch, K.D., Hostetler, S.W., Leavesley, G.H., Leavitt, P.R., McKnight, D.M., Stanford, J.A., 1997. Assessment of Climate Change and Freshwater Ecosystems of the Rocky Mountains, USA and Canada. *Hydrological Processes,* 11, 903-924.

Hay, L.E., Clark, M.P., 2003. Use of statistically and dynamically downscaled atmospheric model output for hydrologic simulations in three mountainous basins in the western United States. *Journal of Hydrology,* 282, 56-75.

Hay, L.E., Wilby, R.L., Leavesley, G.H., 2000. A Comparison of Delta Change and Downscaled GCM Scenarios for Three Mountainous Basins in the United States. *Journal of the American Water Resources Association,* 36(2), 387-397.

Held, I.M., Soden, B.J., 2006. Robust Responses of the Hydrological Cycle to Global Warming. *Journal of Climate,* 19, 5686-5699.

Hengeveld, H.G., 1990. Global Climate Change: Implications for Air Temperature and Water Supply in Canada. *Transactions of the American Fisheries Society,* 119, 176-182.

Herpertz, D., 2001.Schneehydrologische Modellierung im Mettelgebirgsraum. Unpublished PhD Thesis. Universität Jena, pp 253.

Herrington, R., Johnson, B., Hunter, F., 1997. *Responding to global climate change in the prairies* Volume III of the Canada country study: climate impacts and adaptation. Environment Canada, Regina, Saskatchewan.

Hogg, E.H., Hurdle, P.A., 1995. The Aspen Parkland in Western Canada: A Dry-Climate Analogue for the Future Boreal Forest? *Water, Air and Soil Pollution,* 82, 391-400.

Hood, J.L., Roy, J.W., Hayashi, M., 2006. Importance of groundwater in the water balance of an alpine headwater lake. *Geophysical Research Letters,* 33, 1-5.

Hulme, M., Mitchell, J., Ingram, W., Lowe, J., Johns, T., New, M., Viner, D., 1999. Climate change scenarios fro global impacts studies. *Global Environmental Change,* 9, S3-S19.

Huntington, T.G., 2006. Evidence for intensification of the global water cycle: Review and synthesis. *Journal of Hydrology,* 319, 83-95.

IPCC, 2007: *Climate Change 2007: The Physical Science Basis. Contribution of Working Group I to the Fourth Assessment Report of the Intergovernmental Panel on Climate Change* [Solomon, S., Qin, D., Manning, M., Chen, Z., Marquis, M., Averyt, K.B., Tignor, M., Miller, H.L. (eds.)]. Cambridge University Press, Cambridge, United Kingdom and New York, NY, USA, 996pp.

IPCC, 2001. Climate Change 2001: Impacts, Adaptation, and Vulnerability. Summary for Policymakers. A Report of Working Group II of the Intergovernmental Panel on Climate Change. Available at http://www.ipcc.ch/pub/wg2SPMfinal.pdf

IPCC, 2001. *Climate Change 2001: The Scientific Basis. Contributions of Working Group I to the Third Assessment Report of the Intergovernmental Panel on Climate Change,* J.T. Houghton et al., Cambridge University Press, Cambridge, 881pp.

IPCC-TGCIA, 1999. *Guidelines on the Use of Scenario Data for Climate Impact and Adaptation Assessment.* Version 1. Prepared by Carter, T.R., M. Hulme, M. Lal, Intergovernmental Panel on Climate Change, Task Group on Scenarios for Climate Impact Assessment, 69pp.

IPCC, 1997. The Regional Impacts of Climate Change: An Assessment of Vulnerability, Summary for Policy Makers. A Special Report of Working Group II. Watson, R.T., Zinyowera, M.C., Moss, R.H., [eds.]. Cambridge University Press, Cambridge, UK, 517pp.

IPCC, 1995. Scientific Assessments of Climate Change. The Policymaker's Summary of Working Group 1 to the Intergovernmental Panel on Climate Change, WMO/UNEP.

Jackson, R. B., Sala, O.E., Field, C.B., Mooney, H.A., 1994. CO_2 alters water use, carbon gain, and yield for the dominant species in a natural grassland. *Occologia,* 98, 257-262.

Jewitt, G.P.W., Garratt, J.A., Calder, I.R., Fuller, L., 2004. Water resources planning and modelling tools for the assessment of land use change in the Luvuvhu Catchment, South Africa. *Physics and Chemistry of the Earth,* 29, 1233-1241.

Jewitt, G.P.W., Shulze, R.E., 1999. Verification of the ACRU model for forest hydrology applications. *Water SA,* 25(4), 483-490.

Kaleris,V., Papanastasopolous, D., Lagas, G., 2001. Case study on impact of atmospheric circulation changes on river basin hydrology: uncertain aspects. *Journal of Hydrology*, 245, 137-152.

Kienzle, S.W., 2006. The use of the recession index as an indicator for streamflow recovery after a multi-year drought. *Water Resources Management,* 20, 991-1006.

Kienzle, S.W., Lorenz, S.A., Schulze, R.E., 1997. Hydrology and Water Quality of the Mgeni Catchment. *Water Research Commission,* Pretoria, Report TT87/97, 1-88.

Kienzle, S.W., Schulze, R.E. 1991. The simulation of the effect of afforestation on shallow ground water in deep sandy soils. *Water SA,* 18 (4), 265-272.

King, G.A., Neilson, R.P., 1992. The Transient Response of Vegetation to Climate Change: A Potential Source of the CO_2 to the Atmosphere. *Water, Air and Soil Pollution,* 64, 365-383.

Kite, G.W., 1993. Application of a Land Class Hydrological Model to Climatic Change. *Water Resources Research,* 29 (7), 2377-2384.

Kite, G.W., Dalton, A., Dion, K., 1994a. Simulation of streamflow in a macroscale watershed using general circulation model data. *Water Resources Research,* 30 (5), 1547-1559.

Kite, G.W., Kouwen, N., 1992. Watershed Modeling Using Land Classifications. *Water Resources Research,* 28 (12), 3193-3200.

Knapp, A.K., Fay, P.A., Blair, J.M., Collins, S.L., Smith, M.D., Carlisle, J.D., Harper, C.W., Danner, B.T., Lett, M.S., McCarron, J.K., 2002. *Science,* 298 (5601), 2202-2206.

Krause, P., Boyle, D.P, Base, F., 2005. Comparison of different efficiency criteria for hydrological model assessment. *Advances in Geosciences,* 5, 89-97.

Kundezewicz Z.W., Somlyody, L., 1997. Climate Change Impact on Water Resources in a Systems Perspective. *Water Resources Management*, 11, 407-435.

Kunkel, K.E., 2003. North American Trends in Extreme Precipitation. *Natural Hazards,* 29, 291-305.

Lapp, S., Byrne, J., Townshend, I., Kienzle, S., 2005. Climate warming impacts on snowpack accumulation in an alpine watershed. *International Journal of Climatology*, 25, 521-36.

Lapp, S., Byrne, J., Kienzle, S., Townshend, I., 2002.Linking Global Circulation Model Synoptics and Precipitation for Western North America. *International Journal of Climatology*, 22, 1807-1817.

Leavesley, G.H., 1994. Modelling the Effects of Climate Change on Water Resources – A Review. *Climatic Change,* 28, 159-179.

Legates, D.R., McCabe Jr., G.J., 1999. Evaluation the use of "goodness-of-fit" measures in hydrologic and hydroclimatic model validation. *Water Resources Research,* 35(1), 233-241.

Leung, L.R., Ghan, S.J., 1999. Pacific Northwest Climate Sensitivity Simulated by a Regional Climate Model Driven by a GCM. Part II: 2 x CO_2 Simulations. *Journal of Climate,* 12 (7), 2031-2053.

Limaye, A., Kluzek, E.B., Bingham, G.E., Riley, J.P., 1996. Linking Atmospheric and Hydrologic Models at the Basin Scale. *Physics and Chemistry of the Earth,* 21 (3), 311-318.

Linacre, E.T., 1993. Estimating U.S. Class A Pan evaporation from few climate data. *Water International,*19, 5-14.

Liu, Z., Todini, E., 2002. Towards a comprehensive physically-based rainfall-runoff model. *Hydrology and Earth System Sciences,* 6(5), 859-881.

Loaiciga, H.A., Valdes, J.B., Vogel, R., Garvey, J., Schwartz, H. 1996. Global Warming and the Hydrological Cycle. *Journal of Hydrology,* 174 (1/2), 83-127.

Loukas, A., Vasiliades, L., Dalezios, N.R., 2004. Climate Change Implications on Flood Response of a Mountainous Watershed. *Water, Air and Soil Pollution: Focus*, 4, 331-347.

Loukas, A., Vasiliades, L., Dalezios, N.R., 2002. Potential climate change impacts on flood producing mechanisms in southern British Columbia, Canada using the CGCMA1 simulation results. *Journal of Hydrology,* 259, 163-188.

Loukas, A., Quick, M.C., 1996. Effect of Climate Change on Hydrologic Regime of Two Climatically Different Watersheds. *Journal of Hydrologic Engineering,* 1 (2), 77-87.

Manabe, S., Wetherald, R.T., 1980. On the Distribution of Climate Change Resulting from an Increase in CO_2 Content of the Atmosphere. *Journal of the Atmospheric Sciences,* 37, 99-118.

McGinn, S.M., Shepherd, A., Akinremi, O.O., 2001. *Assessment of climate change and impacts on soil moisture and drought on the Prairies.* Final Report for the Climate

Change Action Fund (CCAF) Science, Impacts and Adaptation. Agriculture and Agri-Food Canada, Lethbridge, AB.

McKenney, M.S., Rosenberg, N.J., 1993. Sensitivity of some potential evapotranspiration estimation methods to climate change. *Agricultural and Forest Meteorology,* 64, 81-110.

Mearns, L.O., Rosenzweig, C., Goldberg, R., 1997. Mean and Variance Change in Climate Scenarios: Methods, Agricultural Applications, and Measures of Uncertainty. *Climatic Change*, 35, 367-396.

Meehl, G.A., Stocker, T.F., Collins, W.D., Friedlingstein, P., Gaye, A.T., Gregory, J.M., Kitoh, A., Knutti, R., Murphy, J.M., Noda, A., Rapter, S.C.B., Watterson, I.G., Weaver, A.J., Zhao, Z.C., 2007. Global Climate Projections. In: *Climate Change 2007: The Physical Science Basis. Contribution of Working Group I to the Fourth Assessment Report of the Intergovernmental Panel on Climate Change* [Solomon, S., Qin, D., Manning, M., Chen, Z., Marquis, M., Averyt, K.B., Tignor, M, Miller, H.L. (eds.)]. Cambridge University Press, Cambridge, United Kingdom and New York, NY, USA.

Meehl, G.A., Zwiers, F., Evans, J., Kuntson, T., Mearns, L., Whetton, P., 2000. Trends in Extreme Weather and Climate Events: Issues Related to Modeling Extremes in Projections of Future Climate Change. *Bulletin of the American Meteorological Society,* 81(3), 427-436.

Mekis, E., Hogg, W.D., 1999. Rehabilitation and Analysis of Canadian Daily Precipitation Time Series. *Atmosphere-Ocean*, 37 (1), 53-85.

Merritt, W.S., Alila, Y., Barton, M., Taylor, B., Cohen, S., Neilsen, D., 2006. Hydrological response to scenarios of climate change in sub watersheds of the Okanagan basin, British Columbia. *Journal of Hydrology*, 326, 79-108.

Middelkoop, H., Daamen, K., Gellens, D, Grabs, W., Kwadijk, J.C.J., Lang, H., Parmet, B.W.A.H., Schadler, B., Schulla, J., Wilke, K., 2001. Impact of Climate Change on Hydrological Regimes and Water Resources Management in the Rhine Basin. *Climatic Change,* 49, 105-128.

Miller, N.L., Bashford, K.E., Strem, E., 2003. Potential Impacts of Climate Change on California Hydrology. *Journal of the American Water Resources Association (JAWRA),* 39(4), 771-784.

Mtetwa, S., Kusangaya, S., Schutte, C.F. 2003. The application of geographic information systems (GIS) in the analysis of nutrient loadings from an agro-rural catchment. *Water SA*, 29(2), 189-193.

Morrison, J., Quick, M.C., Foreman, M.G.G., 2002. Climate change in the Fraser River watershed: flow and temperature projections. *Journal of Hydrology,* 263, 230-244.

Mote, P.W., 2003. Trends in snow water equivalent in the Pacific Northwest and their climatic causes. *Geophysical Research Letters,* 30 (12), 1-4.

Muzik, I., 2002, A first-order analysis of the climate change effect on flood frequencies in a subalpine watershed by means of a hydrological rainfall-runoff model. *Journal of Hydrology,* 267, 65-73.

Myneni, R.B., Keeling, C.D., Tucker, C.J., Asrar, G., Nemani, R.R., 1997. Increased plant growth in the northern high latitudes from 1981-1991. *Nature,* 386, 698-702.

Nakicenovic, N., Alcamo, J., Davis, G., de Vries, B., Fenhann, J., Gaffin, S., Gregory, K., Grubler, A, Jung, T.Y., Kram, T., La Rovere, E.L., Michaelis, L., Mori, S., Morita, T., Pepper, W., Pitcher, H., Price, L. Raihi, K., Roehrl, A., Rogner, H-H., Sankovski, A., Schlesinger, M., Shukla, Pl, Smith, S, Swart, R, van Rooijen, S., Victor, N., Dadi, Z., 2000. *Emissions Scenarios. A Special Report of Working Group III of the Intergovernmental Panel on Climate Change.* Cambridge University Press, Cambridge, U.K., and New York, N.Y., U.S.A., 599pp.

Neilson, R.P., Marks, D., 1994. A global perspective of regional vegetation and hydrologic sensitivities from climatic change. *Journal of Vegetative Sciences,* 5, 715-730.

Nemec, J., Schakke, J., 1982. Sensitivity of Water Resource Systems to Climate Variation, *Hydrological Sciences Journal,* 27(3), 327-343.

Nurmohamed, R., Naipal, S., De Smedt, F., 2007. Modeling hydrological response of the Upper Suiname river basin to climate change. *Journal of Spatial Hydrology,* 7(1), 1-22.

Nurmohamed, R., Naipal, S., De Smedt, F., 2006. Hydrologic modeling of the Upper Suriname River basin using WetSpa and ArcView GIS. *Journal of Spatial Hydrology,* 6 (1), 1-17.

Parry, M.L., Rosenzweig, C., Iglesias, A., Livermore, M., Fischer, G., 2004. Effects of climate change on global food production under SRES emissions and socio-economic scenarios. *Global Environmental Change,* 14, 53-67.

Parry, M., and Carter, T. 1998. *Climate Impact and Adaptation Assessment: A Guide to the IPCC Approach.* London: Earthscan.

Penman, H.L., 1948. Natural evaporation from open water, bare soil and grass. *Proceedings of the Royal Society of London. Series A, Mathematical and Physical Sciences,* 193 (1032), 120-145.

Ragab, R., Prudhomme, C. (2002) Climate Change and Water Resources Management in Arid and Semi-arid regions: Prospective and Challenges for the 21st Century. Keynote Paper. Biosystems Engineering. 81(1), 3-34. Silsoe Research Institute.

Refsgaard, J.C., Henriksen, H.J., 2004, Modelling guidelines – terminology and guiding principles. *Advances in Water Resources,* 27, 71-82.

Refsgaard, J.C., Knudsen, J., 1996. Operational validation and intercomparison of different types of hydrological models. *Water Resources Research,* 32 (7), 2189-2202.

Regonda, S.K., Rajagobpalan, B., Clark, M., Pitlick, J., 2005. Seasonal cycle shifts in hydroclimatology in western United States. *Journal of Climate,* 18, 372-284.

Romero, D. Madramootoo, C.A., Enright, P., 2002. Modelling the hydrology of an agricultural watershed in Quebec using SLURP. *Canadian Biosystems Engineering,* 44, 1.11-1.20.

Rood, S.B., Samuelson, G.M., Weber, J.K., Wywrot, K.A., 2005. Twentieth-century decline in streamflows from the hydrographic apex of North America. *Journal of Hydrology,* 306, 215-233.

Rock, L., Mayer, B., 2006. Isotope hydrology of the Oldman River basin, southern Alberta, Canada. *Hydrological Processes,* 21(24), 3301-3315.

Rosenzweig, C., Iglesias, A., Yang, X.B., Epstein, P.R., Chivian, E., 2001. Climate change and extreme weather events: Implications for food production, plant diseases, and pests. *Global Change and Human Health,* 2(2), 90-104.

Rosenzwieg, C., Parry, M.L., 1994. Potential impact of climate change on world food supply. *Nature,* 367, 133-138.

Sabin, A.L., Pisias, N.G., 1996. Sea Surface Temperature Changes in the Northeastern Pacific Ocean during the Past 20, 000 Years and Their Relationship to Climate Change in Northwestern North America. *Quaternary Research,* 46, 48-61.

Saunders, I.R., Byrne, J.M., 1996. Generating regional precipitation from observed and GCM synoptic-scale pressure fields, southern Alberta, Canada. *Climate Research,* 6, 237-249.

Saunders, I.R., Byrne, J.M., 1994. Annual and Seasonal Climate and Climatic Changes in the Canadian Prairies Simulated by the CCC GCM. *Atmosphere – Ocean,* 32 (3), 621-642.

Sauchyn, D.J., Stroich, J., Beriault, A., 2003. A paleoclimatic context for the drought of 1999-2001 in the northern Great Plains of North America. *The Geographical Journal,* 169 (2), 158-167.

Sauchyn, D.J., Barrow, E.M., Hopkinson, R.F., Leavitt, P.R., 2000. Aridity on the Canadian Plains. *Geographie physique et Quaternaire,* 56 (2-3).

Sauchyn, D.J., Beaudoin, A.B., 1998. Recent Environmental Change in the Southwestern Canadian Plains. *The Canadian Geographer,* 42 (4), 337-353.

Schindler, D.W., Donahue, W.F., 2006. An impending water crisis in Canada's western prairie provinces. *PNAS*, 103 (19), 7210-7216.

Schindler, D.W., 1997. Widespread Effects of Climatic Warming on Freshwater Ecosystems in North America. *Hydrological Processes,* 11, 1043-1067.

Schulze, R.E., Lorentz, S., Kienzle, S.W., Perks, L. 2004: Modelling the impacts of land-use and climate change on hydrological responses in the mixed underdeveloped / developed Mgeni catchment, South Africa. In: Kabat, P. *et al.* (Eds.): Vegetation, Water, Humans and the Climate A New Perspective on an Interactive System. BAHC-IGBP Publication, Springer, 17pp, with 14 Figures and 2 tables.

Schulze, R.E., Perks, L.A., 2003. The Potential Threat of Significant Changes to Hydrological Responses in Southern Africa as a Result of Climate Change: A Threshold Analysis on When These Could Occur, and Where the Vulnerable Areas are. *In:* Schulze, R.E. (Ed.) *Modelling as a Tool in Integrated Water Resources Management: Conceptual Issues and Case Study Applications.* Water Research Commission, Pretoria, RSA, WRC Report 749/1/02. Chapter 14, 250-258.

Schulze, R.E., 2000. Modelling Hydrological Responses to Land Use and Climate Change: A Southern African Perspective. *Royal Swedish Academy of Sciences,* 29 (1), 12-22.

Schulze, R.E., 1995. *Hydrology and Agrohydrology: a text to accompany the ACRU 3.00 agrohydrological modelling system.* Report TT69/95. Water Research Commission, Pretoria, RSA.

Schulze, R.E., Smithers, J.C., Lynch, S.D., Lecler, N.L., 1995. Obtaining and interpreting output from ACRU. *In:* Smithers, J.C. and Schulze, R.E. *ACRU Agrohydrological Modelling System: User Manual Version 3.00.* Water Research Commission, Pretoria, Report TT70/95. pp AM7-1 to AM7-21.

Shabbar, A., Skinner, W., 2004. Summer Drought Patterns in Canada and the Relationship to Global Sea Surface Temperatures. *Journal of Climate,* 17 (14), 2866-2880.

Shepherd, A., McGinn, S.M., 2003. Assessment of Climate Change on the Canadian Prairies from Downscaled GCM Data. *Atmosphere – Ocean,* 41 (4), 301-316.

Solomon, S., Qin, D, Manning, M., Alley, R.B., Berntsen, T., Bindoff, N.L., Chen, Z., Chidthaisong, A., Gregory, J.M., Hegerl, G.C., Heimann, M., Hewitson, B., Hoskins, B.M., Joos, F., Jouzel, J., Kattsov, V., Lohmann, U., Matsuno, T., Molina, M., Nicholls, N., Overpeck, J., Raga, G., Ramaswamy, V., Ren, J., Rusticucci, M., Somerville, R.,

Stockler, T.F., Whetton, P., Wood, R.A., Wratt, D., 2007. Technical Summary. In: *Climate Change 2007: The Physical Science Basis. Contribution of Working Group I to the Fourth Assessment Report of the Intergovernmental Panel on Climate Change* [Solomon, S., Qin, D., Manning, M., Chen, Z., Marquis, M., Averyt, K.B., Tignor, M., Miller, H.L. (eds.)]. Cambridge University Press, Cambridge, United Kingdom and New York, NY, USA.

Stephenson, N.L.,1990, Climatic Control of Vegetation Distribution: The role of the Water Balance. *The American Naturalist,*135 (5), 649-667.

Stewart, I.T., Cayan, D.R., Dettinger, M.D., 2005. Changes toward Earlier Streamflow Timing across western North America. *Journal of Climate,* 18, 1136-1155.

Su, M., Stolte, W.J., van der Kamp, G., 2000. Modelling Canadian prairie wetland hydrology using a semi-distributed streamflow model. *Hydrological Processes,* 14, 2405-2422.

Tabios, G.Q., Salas, J.D., 1985. A Comparative Analysis of Techniques for Spatial Interpolation of Precipitation. *Journal of the American Water Resources Association,* 21 (3), 365-380.

Tarboton, K.C., Schulze, R.E. 1993. Hydrological consequences of development scenarios for the Mgeni catchment. Proceedings of the Sixth South African National Hydrological Symposium, University of Natal, Pietermaritzburg, Department of Agricultural Engineering, pp. 297–304.

Todini, E., 1988. Rainfall-Runoff Modeling-Past, Present and Future. *Journal of Hydrology,* 100, 341-352.

Toth, B., Pietroniro, A., Malcom Conly, F., Kouwen, N., 2006. Modelling climate change impacts in the Peace and Athabasca catchment and delta: I-hydrological model application. *Hydrological Processes,* 20, 4197-4214.

Toyra, J., Pietroniro, A., Bonsal, B., 2005. Evaluation of GCM Simulated Climate over the Canadian Prairie Provinces. *Canadian Water Resources Journal,* 30 (3), 245-262.

Trenberth, K. E., 1999. Conceptual framework for changes of extremes of the hydrological cycle with climate change. *Climatic Change*, 42, 327–339.

Viessman Jr. W., Lewis G.L., Knapp J.W. Introduction to hydrology. New York: Harper & Row, 1989:780.

Von Storch, H., Zorita, E., Cubasch, U., 1993. Downscaling of global climate change estimates to regions scales: an application to Iberian winter rainfall. *Journal of Climate,* 6, 1161-1171.

Westmacott J.R., Burn D.H., 1997. Climate change effects on the hydrologic regime within the Churchill-Nelson River Basin. *Journal of Hydrology*, 202, 263-279.

Wheaton, E., 2001. Limited Report. *Changing Climates: Exploring Possible Future Climates of the Canadian Prairie Provinces*, SRC Publication No. 11341-3E01, Government of Canada.

Whitfield, P.H., Fraser, D., Cohen, S., 2003a. Climate Change Impacts on Water in Georgia Basin / Puget Sound – Special Issue. *Canadian Water Resources Journal,* 28(4), 523-529.

Whitfield, P.H., Wang, J.Y., Cannon, A.J., 2003b. Modelling Future Streamflow Extremes- Floods and Low Flows in Georgia Basin, British Columbia. *Canadian Water Resources Journal,* 28(4), 633-656.

Whitfield, P.H., Bodtker, K., Cannon, A.J., 2002. Recent Variation in Seasonality of Temperature and Precipitation in Canada, 1976-95. *International Journal of Climatology,* 22, 1617-1644.

Whitfield, P.H., Cannon, A.J., 2000. Recent Variations in Climate and Hydrology in Canada. *Canadian Water Resources Journal,* 25 (1), 19-65.

Wigley, T.M.L., Jones, P.D., 1985. Influences of precipitation changes and direct CO_2 effects on streamflow. *Nature,* 314, 149-152.

Wilby, R.L., Hay, L.E., Leavesley, G.H., A comparison of downscaled and raw GCM output: implications for climate change scenarios in the San Juan River basin, Colorado. *Journal of Hydrology,* 225, 67-91.

Wild, M., Ohmura, A., Gilgen, H., 2004. On the consistency of trends in radiation and temperature records and implications for the global hydrological cycle. *Geophysical Research Letters,* 31, 1-4.

Wood, A.W., Lettenmaier, D.P., Palmer, R.N., 1997. Assessing Climate Change Implications for Water Resources Planning. *Climatic Change,*37, 203-228.

Xu, C.Y., 2005. Modelling Hydrological Consequences of Climate Change – Progress and Challenges. *Advances in Atmospheric Sciences*, 22(6), 789-797.

Xu, C.Y., 2000. Modelling the Effects of Climate Change on Water Resources in Central Sweden. *Water Resources Management*, 14, 177-189.

Xu, C.Y., 1999a. Climate Change and Hydrologic Models: A Review of Existing Gaps and Recent Research Developments. *Water Resources Management*, 13, 369-382.

Xu, C.Y., 1999b. From GCMs to river flow: a review of downscaling methods and hydrologic modelling approaches. *Progress in Physical Geography*, 23(2), 229-249.

Xu, C.Y., 1999c. Operational testing of a water balance model for predicting climate change impacts. *Agricultural and Forest Meteorology,* 98-99, 295-304.

Yue, S., Pilon, P., Phinney, B., Cavadias, G., 2001. Patterns of Trend in Canadian Streamflow. 58th Eastern Snow Conference, Environment Canada.

Yulianti, J.S., Burn, D.H., 1998. Investigating Links Between Climatic Warming and Low Streamflow in the Prairies Region of Canada. *Canadian Water Resources Journal,* 23 (1), 45-60.

Zhang, X., Harvey, K.D., Hogg, W.D., Yuzyk, T.R., 2001a. Trends in Canadian Streamflow. *Water Resources Research,* 37 (4), 987-998.

Zhang, X., Hogg, W.D., Mekis, E., 2001b. Spatial and Temporal Characteristics of Heavy Precipitation Events over Canada. *Journal of Climate*, 14, 1923-1936.

Zwiers, F.W., Weaver, A.J., 2000. The causes of 20th century warming. *Science,* 290 (5499), 2080-2083.

Zwiers ,F.W., Kharin V.V., 1998. Changes in the extremes of the climate simulated by CCC GCM2 under CO2 doubling. *Journal of Climate*,11, 2200–2222.

Nonperiodical Internet Links

Environment Canada (n.d.) Retrieved October, 2005 from:
http://climate.weatheroffice.ec.gc.ca/climateData/canada_e.html

System for an Automated Geographical Analysis (SAGA), Retrieved April, 2007 from:
http://www.saga-gis.uni-goettingen.de/html/index.php

Water Survey of Canada (n.d.) Retrieved November, 2005 from:
http://www.wsc.ec.gc.ca/hydat/H2O/index_e.cfm?cname=HydromatD.cfm

Alberta Environment (n.d.) Retrieved October, 2007 from:
http://www3.gov.ab.ca/env/water/GWSW/quantity/learn/what/CLM_climate/CLM1_metdata.html

APPENDIX A

Major Components of the ACRU Model

A.1: Modified SCS Equation for Stormflow Depth:

$$Q = \frac{(P_g - cS)^2}{P_g + S(1-c)}$$

Where:

Q = Stormflow depth (mm)
P_g= gross daily precipitation amount (mm)
S= Potential maximum retention (mm), which is equated to a soil water deficit
$_C$ = coefficient of initial abstraction.

A.2: Baseflow

$Q_b = St_b * B_{coeff}$

Where:

Q_b = baseflow [mm]
St_b = baseflow storage [mm]
B_{coeff} = outflow coefficient [dimensionless].

A.3 Interception: Von Hoyningen-Huene (1983)

$I = 0.30 + 0.27\ P_g + 0.13LAI - 0.013LAI^2 + 0.0285P_g.LAI - 0.007\ LAI^2$

Where:

I = Interception (mm)
Pg = Gross precipitation (mm)
LAI = Leaf Area Index.

A.4 Reference Potential Evapotranspiration: Penman (1948) Equation

Generalized Penman:

$$E_r = \frac{\Delta/\gamma R_n + E_a}{\Delta/\gamma + 1}$$

Where:

E_r = Reference potential evapotranspiration (mm)
Δ = Slope of the saturation vapour pressure curve
R_n = Net radiation (i.e. the energy budget component)
γ = Psychrometric "constant"
E_a = Mass transfer component for a vegetated surface.

A.4.1 Mass Transfer Component (E_a):

$E_a = 3.985 \times 10^{-7} (160.9 + u_{2kd})(100 - RH)\, e_a$

Where:

E_a = Mass transfer component of the Penman evaporation equation ($MJ.m^{-2}.day^{-1}$)
u_{2kd}= Windrun at 2m ($km.day^{-1}$)
RH= Mean daily relative humidity (%)
e_a = Saturate vapour pressure at air temperature (Pa).

Saturated Vapour Pressure (e_a):

$e_a = 610.78\ _{EXP}[17.2694\ T_a / (273.3 + T_a)]$

Where:

e_a = Saturated vapour pressure at air temperature (Pa)
T_a = Mean air temperature (°C).

Energy Budget Weighting Factor, (Δ/γ):

Psychrometric constant (γ):
$\gamma = (c_p P_a) / (L_v M_r)$

Where:

γ = Psychrometric constant ($Pa.°C^{-1}$)
c_p= Specific heat of dry air (1004 $J.kg^{-1}.°C^{-1}$)
P_a= Atmospheric pressure (Pa) = Po - ρ.g.z
M_r= Ratio of the molecular mass of dry air to that of water (0.62198)
L_v = Latent heat of vapourisation $(2.50177-0.00241T_a) \times 10^6$ $J.kg^{-1}$

Po = Atmospheric pressure (P_a) at sea-level (97400Pa)
ρ_a = Density of air (1.292[273.2 / (273.2 + Ta)] $kg.m^{-3}$)
g = Gravitational acceleration (9.80665 $m.s^{-2}$)
z = altitude (m)
T_a = Mean air temperature (°C).

Slope of the e_a vs. T_a curve (Δ):

$$\Delta = 4098e_a /(273.2 + T_a)$$

A.4.2 The Energy Budget Component: Net Radiation

$$R_s = R_a (1- \alpha) (a_r + b_r n_s /N)$$

Where:

R_s = Net shortwave radiation component of the Penman equation
R_a = Extra-terrestrial radiation i.e. radiation received on a horizontal plane at the top of the atmosphere
α = Mean daily albedo (reflectivity) value of the evaporating surface (0.25 for short grass, 0.14 for forests)
a_r, b_r = Regression constants for estimation of shortwave radiation from sunshine duration. Default values are 0.24 and 0.53 for a_r, b_r respectively.
n_s = Actual sunshine duration (hours)
N = Maximum possible sunshine duration (hours), which varies with latitude and time of year.

Estimating extraterrestrial radiation (R_a):

$$R_a = 14.9158 (h.\sin\Phi.\sin\delta + \cos\Phi.\cos\delta.\sin h)/r_v^2$$

Where:

R_a= Extra-terrestrial solar radiation (mm equivalent.day^{-1})
r_v = Sun's radius vector (1 + 0.017 cos [0.017 (186 – D_j)] radians)
Φ = Latitude north or south of the Equator (radians)
δ = Declination (0.409 cos [0.017 (173 - D_j) radians)
h = Sunrise hour angle (arcos (-tanΦ.tanδ).

Estimating maximum possible sunshine duration (N):

$$N = 24 \; x \; h/\pi + 0.22$$

Where:

h = arcos (-tanδ.tanΦ)
δ = 0.409 cos [0.017(173 –D_j)].

Estimation of net longwave radiation (R_l):

$$R_l = [\sigma_{sb} T_k^4][0.56 - c_{ea} (e_a . RH)^{0.5}][f_{bs} + (1-f_{bs}) n_s/N]$$

Where:

T_k= Mean air temperature (273.2 + Ta °C)
σ_{sb}= Stefan-Boltzmann constant (2.03×10^{-9} mm.day^{-1})
RH =Mean daily relative humidity (%)
c_{ea} = 0.0008 if e_a in Pa
f_{bs}= Coefficient to account for back scattering by cloud cover (default = 0.1).

A.5 Estimation of Maximum Evaporation

$$E_m = E_r \times K_{cm}$$

Where:

E_m =Maximum evaporation (mm)
E_r = Reference potential evaporation (mm)
K_{cm} = Crop coefficient

A.6 Apportionment of Maximum Evapotranspiration to Maximum Soil Water Evaporation and Maximum Transpiration

A.6.1 Maximum Transpiration:

For $2.7 < LAI_D > 0.1$

$$F_t = 0.7\ LAI_D^{0.5} - 0.21$$

Where:

LAI_D = Daily value of leaf area index
F_t = Fraction of evaporative energy available for transpiration (cannot exceed 95% of E_m).

A.6.2 Maximum Evaporation:

$$E_{sm} = (1-F_t)\ E_r$$

Where:

E_{sm}= Maximum soil water evaporation (mm).

A.7 Calculation of Actual Evapotranspiration

A.7.1 Actual evaporation from the soil surface:

Stage 1: $E_s = E_{sm}$
When: $Es > U_I$

Where:

$U_I = 9(\alpha_s - 3)^{0.42}$

U_I = Stage 1 upper limit (mm)

α_s = soil water transmission parameter (relational to texture class, hard coded in ACRU).

Stage 2:

$E_s = \alpha_s t_d^{0.5} - (t_d - 1)^{0.5}$

Where:

t_d = number of days since Stage 2 soil evaporation began.

A.7.2 Actual Transpiration:

$E_t = E_{tm}$

$E_t < E_{tm}$ when soil water is (a) deficient or (b) in excess.

Actual Transpiration Under Conditions of Water Deficiency:

A-horizon:

$E_{tA} = E_{tmA} (\theta_A - \theta_{PWPA}) / (f_s . PAW_A)$

B-horizon:

$E_{tB} = E_{tmB} (\theta_B - \theta_{PWPB}) / (f_s . PAW_B)$

Where:

$E_{tA/B}$ = Actual transpiration for A-horizon/B-horizon

$E_{tmA/B}$= Maximum transpiration for A-horizon/B-horizon

$PAW_{A/B}$= Plant available water (mm) (PWP < PAW > DUL)

f_s = Fraction of maximum available soil water to the plant:

$$f_s = 0.94 + 0.0026 \Psi^{cr} / E_r$$

Where:

Ψ^{cr}= Critical leaf water potential of a plant (kPa), with the value being negative because of suction.

Actual Transpiration Under Condition of Soil Water Excess:

A-horizon:

$E_{tA} = E_{tmA} [0.7 (\theta_{POA} - \theta_A) / (\theta_{POA} - \theta_{DULA}) + 0.3]$

B-horizon:

$$E_{tB} = E_{tmB} [0.7 (\theta_{POB} - \theta_B) / (\theta_{POB} - \theta_{DULB}) + 0.3]$$

A.8 Unsaturated Soil Water Rate of Redistribution

A.8.1 Downwards:

When $\theta_A > \theta_B$;

$R_{\theta AB} = 0.02[(\theta_A / \theta_{DULA}) - \theta_B / \theta_{DULB})]$

Where:

R_{AB}= Redistribution rate from A to B horizon
θ_A = Soil water content of the A-horizon
θ_B = Soil water content of the B-horizon
θ_{DULA}= Drained upper limit of the A-horizon
θ_{DULB} = Drained upper limit of the B-horizon.

A.8.2 Upwards:

When $\theta_B > \theta_A$;

$R_{\theta BA} = 0.01[(\theta_B / \theta_{DULB}) - \theta_A / \theta_{DULA})]$

Where:

R_{BA}= Redistribution rate from B to A horizon
θ_A = Soil water content of the A-horizon
θ_B = Soil water content of the B-horizon
θ_{DULA}= Drained upper limit of the A-horizon
θ_{DULB} = Drained upper limit of the B-horizon.

A.9 Saturated Soil Water Drainage

A.9.1 Surface:

When $\theta_A > \theta_{DULA}$;

$SR_{\theta AB} = (\theta_A - \theta_{DULA}) * ABRESP$

Where:

$S_{\theta AB}$= Volume of soil water redistributed through saturated drainage from A to B-horizons (mm)
K_{AB} = Saturated redistribution rate (mm day^{-1}).

A.9.2 Subsurface:

When $\theta_B > \theta_{DULB}$;

$SR_{\theta BF} = (\theta_B - \theta_{DULB}) * BFRESP$

Where:

$S_{\theta BF}$= Volume of soil water redistributed through saturated drainage from B to groundwater store (mm)
K_{BF} = Saturated redistribution rate (mm day^{-1}).

A.10 Snow Subroutines (Herpertz, 2001)

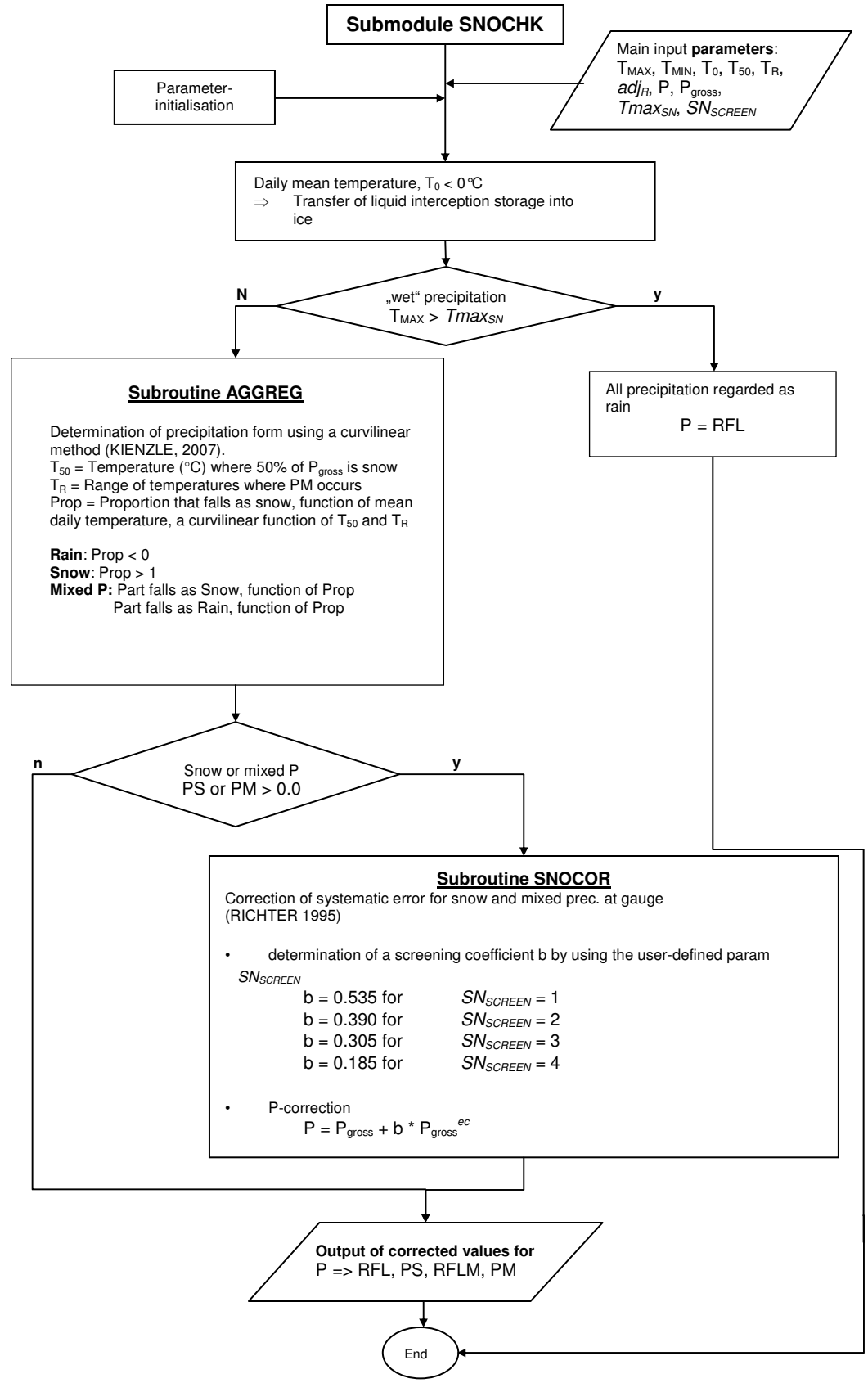

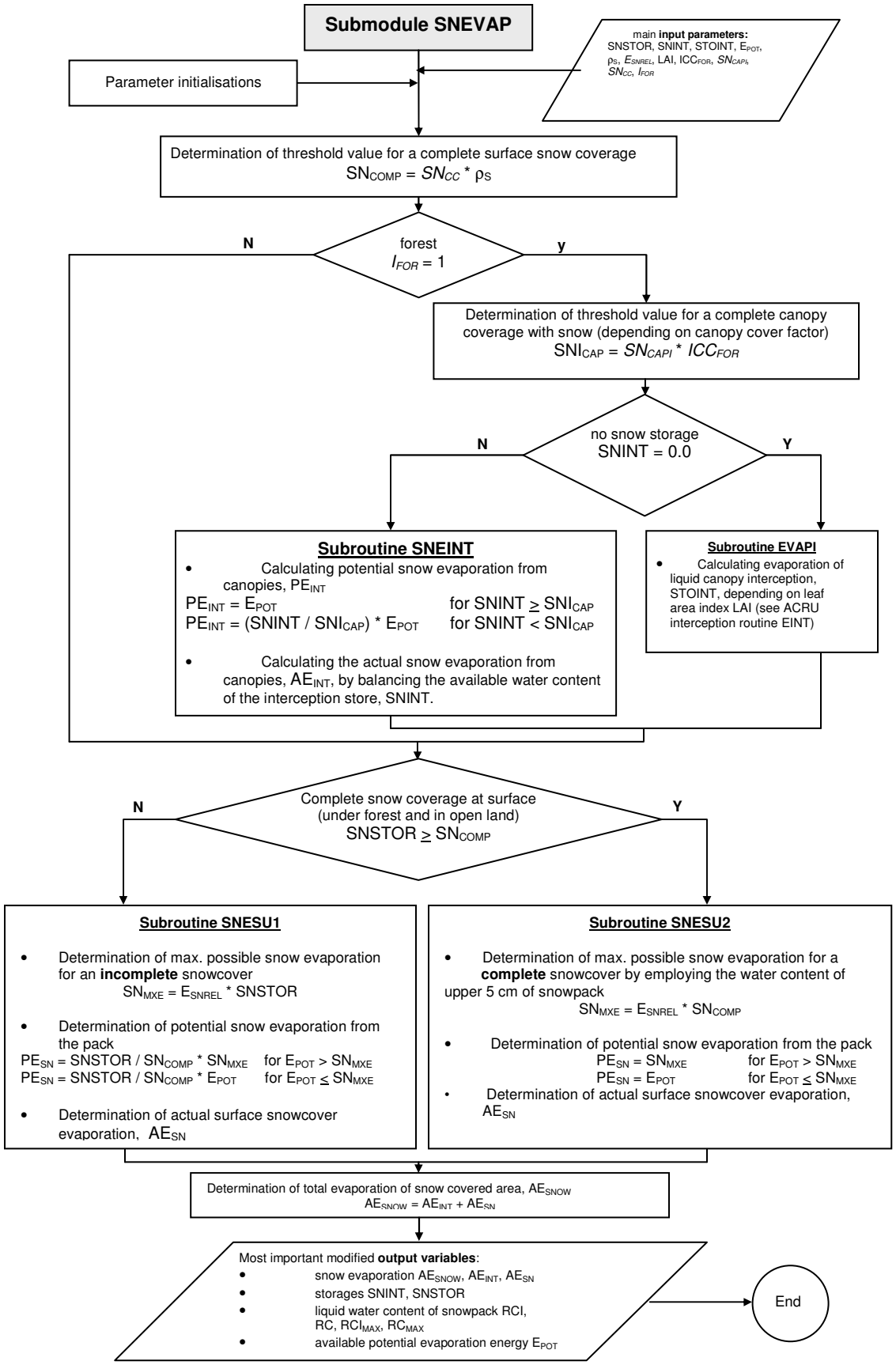
Submodule SNEVAP
main input parameters:
SNSTOR, SNINT, STOINT, E_{POT}, ρ_S, E_{SNREL}, LAI, ICC_{FOR}, SN_{CAPI}, SN_{CC}, I_{FOR}
Parameter initialisations
Determination of threshold value for a complete surface snow coverage
$SN_{COMP} = SN_{CC} * \rho_S$
forest
$I_{FOR} = 1$
N
y
Determination of threshold value for a complete canopy coverage with snow (depending on canopy cover factor)
$SNI_{CAP} = SN_{CAPI} * ICC_{FOR}$
no snow storage
SNINT = 0.0
N
Y
Subroutine SNEINT
Calculating potential snow evaporation from canopies, PE_{INT}
$PE_{INT} = E_{POT}$ for SNINT ≥ SNI_{CAP}
$PE_{INT} = (SNINT / SNI_{CAP}) * E_{POT}$ for SNINT < SNI_{CAP}
Calculating the actual snow evaporation from canopies, AE_{INT}, by balancing the available water content of the interception store, SNINT.
Subroutine EVAPI
Calculating evaporation of liquid canopy interception, STOINT, depending on leaf area index LAI (see ACRU interception routine EINT)
Complete snow coverage at surface (under forest and in open land)
SNSTOR ≥ SN_{COMP}
N
Y
Subroutine SNESU1
Determination of max. possible snow evaporation for an incomplete snowcover
$SN_{MXE} = E_{SNREL} * SNSTOR$
Determination of potential snow evaporation from the pack
$PE_{SN} = SNSTOR / SN_{COMP} * SN_{MXE}$ for $E_{POT} > SN_{MXE}$
$PE_{SN} = SNSTOR / SN_{COMP} * E_{POT}$ for $E_{POT} \leq SN_{MXE}$
Determination of actual surface snowcover evaporation, AE_{SN}
Subroutine SNESU2
Determination of max. possible snow evaporation for a complete snowcover by employing the water content of upper 5 cm of snowpack
$SN_{MXE} = E_{SNREL} * SN_{COMP}$
Determination of potential snow evaporation from the pack
$PE_{SN} = SN_{MXE}$ for $E_{POT} > SN_{MXE}$
$PE_{SN} = E_{POT}$ for $E_{POT} \leq SN_{MXE}$
Determination of actual surface snowcover evaporation, AE_{SN}
Determination of total evaporation of snow covered area, AE_{SNOW}
$AE_{SNOW} = AE_{INT} + AE_{SN}$
Most important modified output variables:
snow evaporation AE_{SNOW}, AE_{INT}, AE_{SN}
storages SNINT, SNSTOR
liquid water content of snowpack RCI, RC, RCI_{MAX}, RC_{MAX}
available potential evaporation energy E_{POT}
End

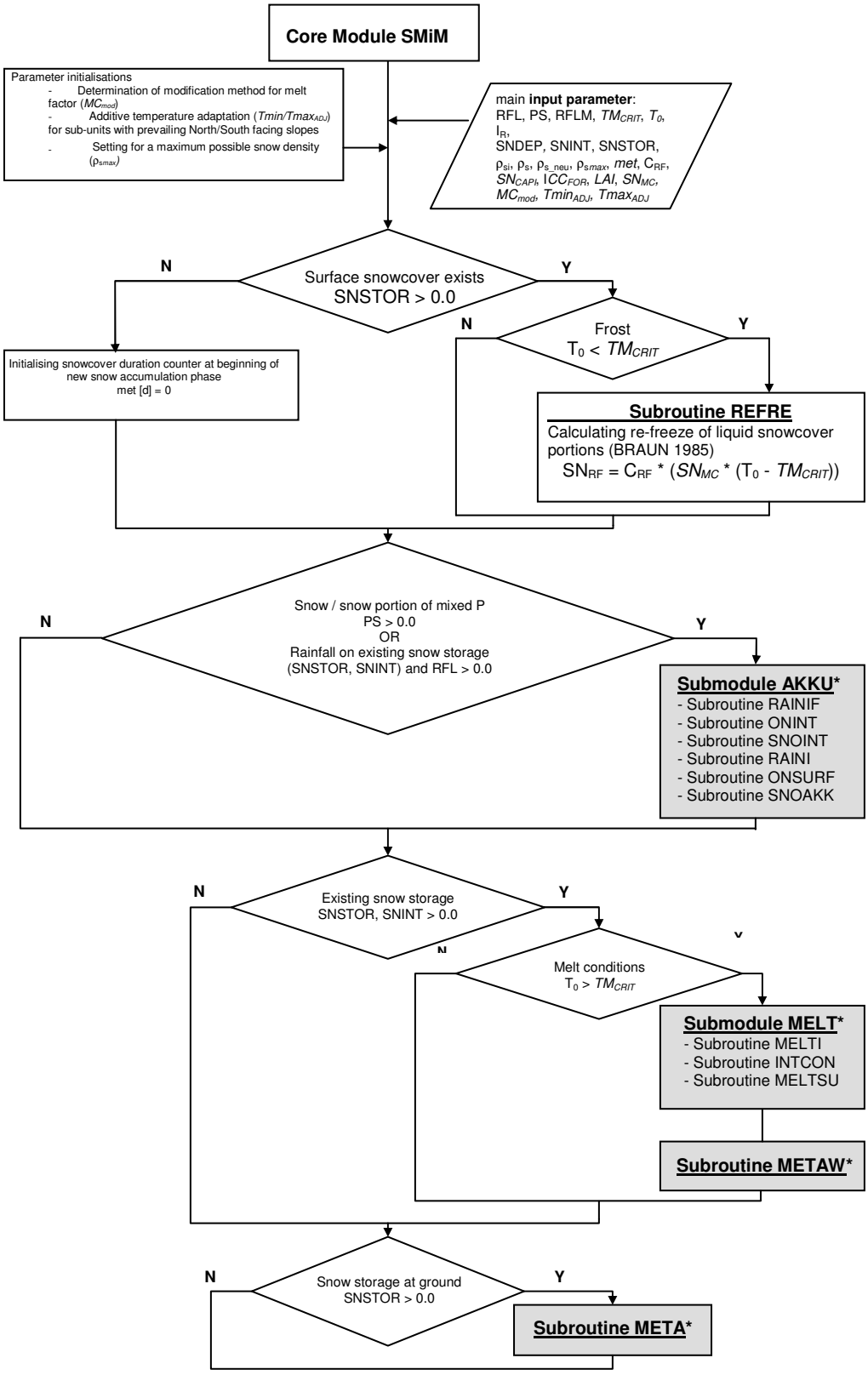
Core Module SMiM
Parameter initialisations
- Determination of modification method for melt factor (MC_{mod})
- Additive temperature adaptation ($Tmin/Tmax_{ADJ}$) for sub-units with prevailing North/South facing slopes
- Setting for a maximum possible snow density (ρ_{smax})
main **input parameter**:
RFL, PS, RFLM, TM_{CRIT}, T_0, I_R,
SNDEP, SNINT, SNSTOR,
ρ_{si}, ρ_s, ρ_{s_neu}, ρ_{smax}, *met*, C_{RF}, SN_{CAPI}, ICC_{FOR}, *LAI*, SN_{MC}, MC_{mod}, $Tmin_{ADJ}$, $Tmax_{ADJ}$
Surface snowcover exists
SNSTOR > 0.0
N
Y
Initialising snowcover duration counter at beginning of new snow accumulation phase
met [d] = 0
Frost
$T_0 < TM_{CRIT}$
N
Y
Subroutine REFRE
Calculating re-freeze of liquid snowcover portions (BRAUN 1985)
$SN_{RF} = C_{RF} * (SN_{MC} * (T_0 - TM_{CRIT}))$
Snow / snow portion of mixed P
PS > 0.0
OR
Rainfall on existing snow storage
(SNSTOR, SNINT) and RFL > 0.0
N
Y
Submodule AKKU*
- Subroutine RAINIF
- Subroutine ONINT
- Subroutine SNOINT
- Subroutine RAINI
- Subroutine ONSURF
- Subroutine SNOAKK
Existing snow storage
SNSTOR, SNINT > 0.0
N
Y
Melt conditions
$T_0 > TM_{CRIT}$
N
Y
Submodule MELT*
- Subroutine MELTI
- Subroutine INTCON
- Subroutine MELTSU
Subroutine METAW*
Snow storage at ground
SNSTOR > 0.0
N
Y
Subroutine META*

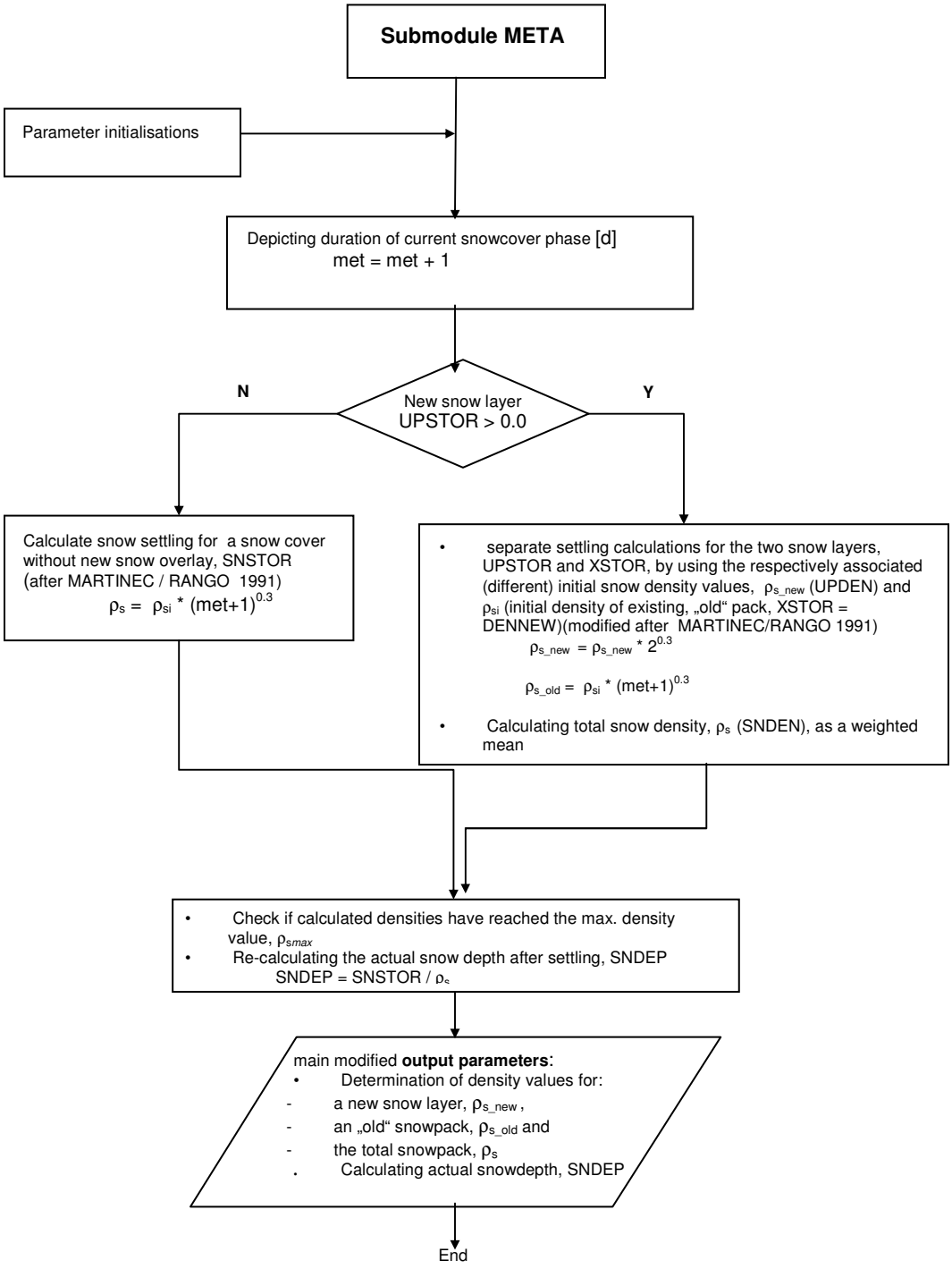
Submodule META
Parameter initialisations
Depicting duration of current snowcover phase [d]
met = met + 1
N
New snow layer
UPSTOR > 0.0
Y
Calculate snow settling for a snow cover without new snow overlay, SNSTOR (after MARTINEC / RANGO 1991)
$\rho_s = \rho_{si} * (met+1)^{0.3}$
• separate settling calculations for the two snow layers, UPSTOR and XSTOR, by using the respectively associated (different) initial snow density values, ρ_{s_new} (UPDEN) and ρ_{si} (initial density of existing, „old" pack, XSTOR = DENNEW)(modified after MARTINEC/RANGO 1991)
$\rho_{s\_new} = \rho_{s\_new} * 2^{0.3}$
$\rho_{s\_old} = \rho_{si} * (met+1)^{0.3}$
• Calculating total snow density, ρ_s (SNDEN), as a weighted mean
• Check if calculated densities have reached the max. density value, ρ_{smax}
• Re-calculating the actual snow depth after settling, SNDEP
SNDEP = SNSTOR / ρ_s
main modified **output parameters**:
• Determination of density values for:
- a new snow layer, ρ_{s_new} ,
- an „old" snowpack, ρ_{s_old} and
- the total snowpack, ρ_s
. Calculating actual snowdepth, SNDEP
End

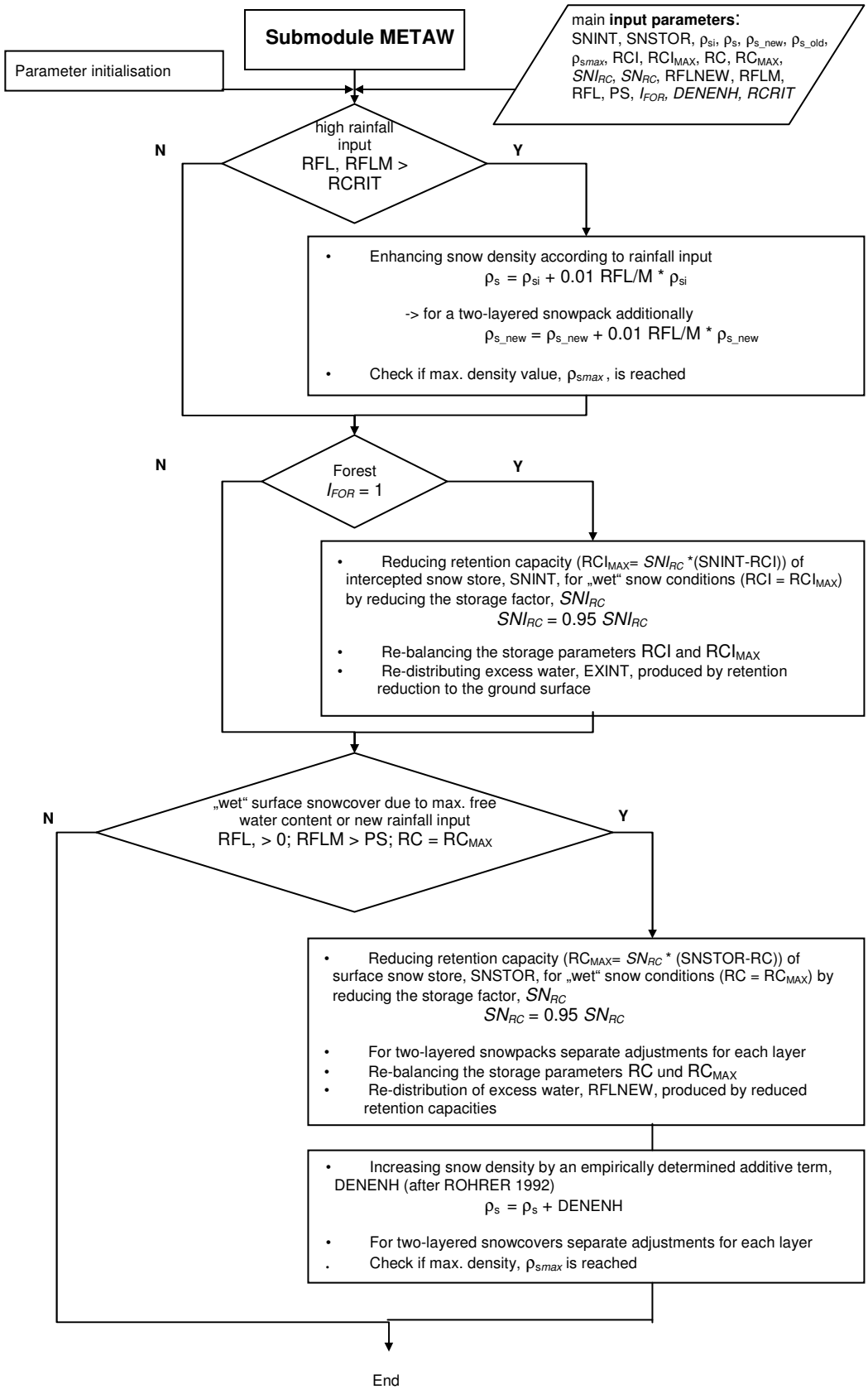
Submodule METAW
Parameter initialisation
main input parameters:
SNINT, SNSTOR, ρsi, ρs, ρs_new, ρs_old, ρsmax, RCI, RCIMAX, RC, RCMAX, SNIRC, SNRC, RFLNEW, RFLM, RFL, PS, IFOR, DENENH, RCRIT
high rainfall input
RFL, RFLM > RCRIT
N
Y
• Enhancing snow density according to rainfall input
ρs = ρsi + 0.01 RFL/M * ρsi
-> for a two-layered snowpack additionally
ρs_new = ρs_new + 0.01 RFL/M * ρs_new
• Check if max. density value, ρsmax , is reached
Forest
IFOR = 1
N
Y
• Reducing retention capacity (RCIMAX= SNIRC *(SNINT-RCI)) of intercepted snow store, SNINT, for „wet“ snow conditions (RCI = RCIMAX) by reducing the storage factor, SNIRC
SNIRC = 0.95 SNIRC
• Re-balancing the storage parameters RCI and RCIMAX
• Re-distributing excess water, EXINT, produced by retention reduction to the ground surface
„wet“ surface snowcover due to max. free water content or new rainfall input
RFL, > 0; RFLM > PS; RC = RCMAX
N
Y
• Reducing retention capacity (RCMAX= SNRC * (SNSTOR-RC)) of surface snow store, SNSTOR, for „wet“ snow conditions (RC = RCMAX) by reducing the storage factor, SNRC
SNRC = 0.95 SNRC
• For two-layered snowpacks separate adjustments for each layer
• Re-balancing the storage parameters RC und RCMAX
• Re-distribution of excess water, RFLNEW, produced by reduced retention capacities
• Increasing snow density by an empirically determined additive term, DENENH (after ROHRER 1992)
ρs = ρs + DENENH
• For two-layered snowcovers separate adjustments for each layer
. Check if max. density, ρsmax is reached
End

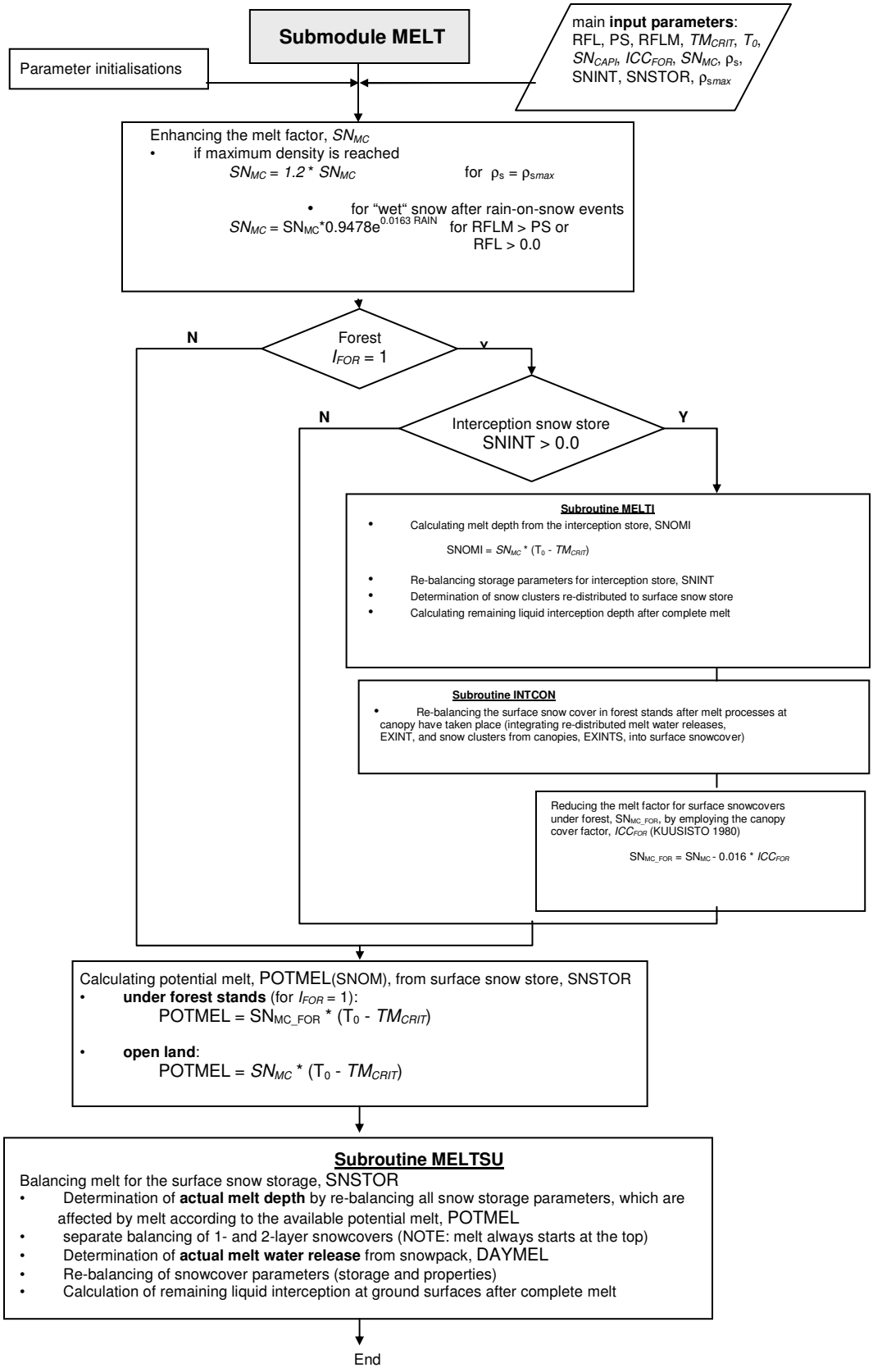
Submodule MELT
Parameter initialisations
main input parameters: RFL, PS, RFLM, TM_{CRIT}, T_0, SN_{CAPI}, ICC_{FOR}, SN_{MC}, ρ_s, SNINT, SNSTOR, ρ_{smax}
Enhancing the melt factor, SN_{MC}
• if maximum density is reached
$SN_{MC} = 1.2 * SN_{MC}$ for $\rho_s = \rho_{smax}$
• for "wet" snow after rain-on-snow events
$SN_{MC} = SN_{MC} * 0.9478e^{0.0163\ RAIN}$ for RFLM > PS or RFL > 0.0
Forest $I_{FOR} = 1$
N
Y
Interception snow store SNINT > 0.0
N
Y
Subroutine MELTI
• Calculating melt depth from the interception store, SNOMI
SNOMI = $SN_{MC} * (T_0 - TM_{CRIT})$
• Re-balancing storage parameters for interception store, SNINT
• Determination of snow clusters re-distributed to surface snow store
• Calculating remaining liquid interception depth after complete melt
Subroutine INTCON
• Re-balancing the surface snow cover in forest stands after melt processes at canopy have taken place (integrating re-distributed melt water releases, EXINT, and snow clusters from canopies, EXINTS, into surface snowcover)
Reducing the melt factor for surface snowcovers under forest, SN_{MC_FOR}, by employing the canopy cover factor, ICC_{FOR} (KUUSISTO 1980)
$SN_{MC\_FOR} = SN_{MC} - 0.016 * ICC_{FOR}$
Calculating potential melt, POTMEL(SNOM), from surface snow store, SNSTOR
• under forest stands (for $I_{FOR} = 1$):
POTMEL = $SN_{MC\_FOR} * (T_0 - TM_{CRIT})$
• open land:
POTMEL = $SN_{MC} * (T_0 - TM_{CRIT})$
Subroutine MELTSU
Balancing melt for the surface snow storage, SNSTOR
• Determination of actual melt depth by re-balancing all snow storage parameters, which are affected by melt according to the available potential melt, POTMEL
• separate balancing of 1- and 2-layer snowcovers (NOTE: melt always starts at the top)
• Determination of actual melt water release from snowpack, DAYMEL
• Re-balancing of snowcover parameters (storage and properties)
• Calculation of remaining liquid interception at ground surfaces after complete melt
End

APPENDIX B

ACRU Parameterization

B.1 MENU File of Parent Modelling System

```
Mode of simulation (point/lumped vs distributed)
    ------------------------------------------------
ICELL
,,,,I
   1

     Distributed model specifications
    ---------------------------------
 ISUBNO MINSUB MAXSUB LOOPBK
,,,,III,,,,III,,,,III,,,,,,I
     5      1      5     0

     Hydrograph routing options
    ---------------------------
 IROUTE DELT
,,,,,,I,FFFF.F
     0 1440.0

     Subcatchment configuration information
    ---------------------------------------
ICELLN IDSTRM PRTOUT
,,,III,,,,III,,,,,,F
    1      2      0
    2      3      0
    3      5      0
    4      5      0
    5      5      0

     Rainfall file organisation
    ---------------------------
IRAINF
AAAAAAAAAAAAAAAAAAAAAAAAAAAAAAAAAAAAAAAAAAAAAAAAAAAAAAAAAAAAAAAAAAAAAAA
AAAAAAAAAAAAAAAAAAAA
C:\ACRU\aHD2020.DAT                                    1
C:\ACRU\aHD2020.DAT                                    2
C:\ACRU\aHD2020.DAT                                    3
C:\ACRU\aHD2020.DAT                                    4
C:\ACRU\aHD2020.DAT                                    5

     Rainfall information
```

FORMAT PPTCOR MAP
,,,,,,F,,,,,,F,,IIIII
1 1 435
1 1 435
1 1 435
1 1 435
1 1 435

Monthly rainfall adjustment factors, CORPPT(i)

JAN FEB MAR APR MAY JUN JUL AUG SEP OCT NOV DEC
,F.FF,F.FF,F.FF,F.FF,F.FF,F.FF,F.FF,F.FF,F.FF,F.FF,F.FF,F.FF
1.03 1.49 1.19 1.46 1.18 0.85 0.99 1.01 1.00 1.33 0.96 0.99 1
0.98 1.48 1.19 1.39 1.20 0.84 1.04 1.01 1.06 1.22 1.17 1.05 2
1.01 1.51 1.17 1.28 1.17 0.82 1.03 0.97 1.02 1.20 1.16 1.12 3
1.06 1.62 1.23 1.29 1.24 0.84 1.09 0.98 1.14 1.12 1.09 1.24 4
1.06 1.62 1.23 1.22 1.23 0.82 1.09 0.95 1.13 1.11 1.23 1.29 5

Availability of observed streamflow data

IOBSTQ IOBSPK IOBOVR
,,,,,I,,,,,,I,,,,,,I
0 0 0 1
0 0 0 2
0 0 0 3
0 0 0 4
1 0 0 5

Dynamic file option

DNAMIC
F
0 1
0 2
0 3
0 4
0 5

Dynamic file organisation

IDYNFL

General heading of simulation

HEAD
AAAAAAAAAAAAAAAAAAAAAAAAAAAAAAAA
Response Unit 1 1
Response Unit 2 2
Response Unit 3 3
Response Unit 4 4
Response Unit 5 5

Locational information

CLAREA	ELEV	ALAT	ALONG	IHEMI	IQUAD	
FFFFF.FF	FFFF.F	FF.FF	FF.FF	,,,,I	,,,I	
60.03	1565.0	49.75	113.8	1	2	1
61.31	1410.3	49.75	113.8	1	2	2
55.89	1468.1	49.75	113.8	1	2	3
46.42	1258.0	49.75	133.8	1	2	4
30.43	1234.0	49.75	133.8	1	2	5

Period of record for simulation

IYSTRT	IYREND	
,,IIII	,,IIII	
1961	1990	1
1961	1990	2
1961	1990	3
1961	1990	4
1961	1990	5

Simulation printout options

WRIDY	WRIMO	
,,,,F	,,,,F	
0	1	1
0	1	2
0	1	3
0	1	4
0	1	5

Statistical output options (I)

SUMMRY	ICOMPR	
,,,,FF	,,,,,I	
0	0	1
0	0	2
0	0	3
0	0	4

```
   0     0                                        5

    Statistical output options (II)
    -------------------------------
 ICOMPV LOGVAL
,,,,,,I,,,,,,I
    0     0                                       1
    0     0                                       2
    0     0                                       3
    0     0                                       4
    0     0                                       5

    Monthly means of daily max temperature, TMAX(i)
    -----------------------------------------------
  JAN   FEB   MAR   APR   MAY   JUN   JUL   AUG   SEP   OCT   NOV   DEC
,FFF.F,FFF.F,FFF.F,FFF.F,FFF.F,FFF.F,FFF.F,FFF.F,FFF.F,FFF.F,FFF.F,FFF.F
  -1.5   2.4   6.3  11.8  17.7  23.6  27.5  26.8  20.6  15.5   6.1   0.9     1
  -1.5   2.4   6.3  11.8  17.7  23.6  27.5  26.8  20.6  15.5   6.1   0.9     2
  -1.5   2.4   6.3  11.8  17.7  23.6  27.5  26.8  20.6  15.5   6.1   0.9     3
  -1.5   2.4   6.3  11.8  17.7  23.6  27.5  26.8  20.6  15.5   6.1   0.9     4
  -1.5   2.4   6.3  11.8  17.7  23.6  27.5  26.8  20.6  15.5   6.1   0.9     5

    Monthly means of daily min temperature, TMIN(i)
    -----------------------------------------------
  JAN   FEB   MAR   APR   MAY   JUN   JUL   AUG   SEP   OCT   NOV   DEC
,FFF.F,FFF.F,FFF.F,FFF.F,FFF.F,FFF.F,FFF.F,FFF.F,FFF.F,FFF.F,FFF.F,FFF.F
 -13.5  -9.0  -5.5  -0.7   4.9  10.1  12.6  11.8   6.5   1.8  -5.7 -10.8     1
 -13.5  -9.0  -5.5  -0.7   4.9  10.1  12.6  11.8   6.5   1.8  -5.7 -10.8     2
 -13.5  -9.0  -5.5  -0.7   4.9  10.1  12.6  11.8   6.5   1.8  -5.7 -10.8     3
 -13.5  -9.0  -5.5  -0.7   4.9  10.1  12.6  11.8   6.5   1.8  -5.7 -10.8     4
 -13.5  -9.0  -5.5  -0.7   4.9  10.1  12.6  11.8   6.5   1.8  -5.7 -10.8     5

#    Reference potential evaporation control variables
    -------------------------------------------------
EQPET
,,FFF
  104     IPNF = 1 if Penman                       1
  104                                              2
  104                                              3
  104                                              4
  104                                              5

    Evaporation input availability control flags
    --------------------------------------------
  IEIF  ILRF  IWDF  IRHF  ISNF  IRDF  IPNF
,,,,,I,,,,,I,,,,,I,,,,,I,,,,,I,,,,,I,,,,,I
```

0	1	1	1	1	0	1	1
0	1	1	1	1	0	1	2
0	1	1	1	1	0	1	3
0	1	1	1	1	0	1	4
0	1	1	1	1	0	1	5

Means of monthly totals of pan evaporation, E(i)

JAN	FEB	MAR	APR	MAY	JUN	JUL	AUG	SEP	OCT	NOV	DEC	
,FFF.F	FFF.F	FFF.F	FFF.F	FFF.F	FFF.F	FFF.F	FFF.F	FFF.F	FFF.F	FFF.F	FFF.F	
00.0	00.0	000.0	000.0	000.0	000.0	000.0	000.0	000.0	000.0	00.0	00.0	1
00.0	00.0	000.0	000.0	000.0	000.0	000.0	000.0	000.0	000.0	00.0	00.0	2
00.0	00.0	000.0	000.0	000.0	000.0	000.0	000.0	000.0	000.0	00.0	00.0	3
00.0	00.0	000.0	000.0	000.0	000.0	000.0	000.0	000.0	000.0	00.0	00.0	4
00.0	00.0	000.0	000.0	000.0	000.0	000.0	000.0	000.0	000.0	00.0	00.0	5

Temperature adjustment for altitude

TELEV	LRREG	
FFFF.F	,,,,II	
1031.0	0	1
1031.0	0	2
1031.0	0	3
1031.0	0	4
1031.0	0	5

Mean lapse rates for min and max temperatures

TMAXLR	TMINLR	
FFFF.FF	FFFF.FF	
-6.20	-6.20	1
-6.20	-6.20	2
-6.20	-6.20	3
-6.20	-6.20	4
-6.20	-6.20	5

Mean daily windspeed (m/s)

WNDSPD	
,,FF.F	
5.4	1
5.4	2
5.4	3
5.4	4
5.4	5

Windspeed region number

LINWIN
,,,III

0	1
0	2
0	3
0	4
0	5

Monthly means of daily windrun (km/day), WIND(i)

JAN	FEB	MAR	APR	MAY	JUN	JUL	AUG	SEP	OCT	NOV	DEC	
,FFF.F,	FFF.F,	FFF.F,	FFF.F,	FFF.F,	FFF.F,	FFF.F,	FFF.F,	FFF.F,	FFF.F,	FFF.F,	FFF.F	
581.0	510.0	473.0	452.0	439.0	407.0	378.0	355.0	409.0	500.0	558.0	604.0	1
581.0	510.0	473.0	452.0	439.0	407.0	378.0	355.0	409.0	500.0	558.0	604.0	2
581.0	510.0	473.0	452.0	439.0	407.0	378.0	355.0	409.0	500.0	558.0	604.0	3
581.0	510.0	473.0	452.0	439.0	407.0	378.0	355.0	409.0	500.0	558.0	604.0	4
581.0	510.0	473.0	452.0	439.0	407.0	378.0	355.0	409.0	500.0	558.0	604.0	5

Monthly means of daily average relative humidity, RH(i)

JAN	FEB	MAR	APR	MAY	JUN	JUL	AUG	SEP	OCT	NOV	DEC	
,FF.F,	FF.F,	FF.F,	FF.F,	FF.F,	FF.F,	FF.F,	FF.F,	FF.F,	FF.F,	FF.F,	FF.F	
60.8	58.1	61.9	55.2	53.2	64.3	54.7	55.0	56.4	56.8	60.4	57.4	1
60.8	58.1	61.9	55.2	53.2	64.3	54.7	55.0	56.4	56.8	60.4	57.4	2
60.8	58.1	61.9	55.2	53.2	64.3	54.7	55.0	56.4	56.8	60.4	57.4	3
60.8	58.1	61.9	55.2	53.2	64.3	54.7	55.0	56.4	56.8	60.4	57.4	4
60.8	58.1	61.9	55.2	53.2	64.3	54.7	55.0	56.4	56.8	60.4	57.4	5

Penman equation control variables

ALBEDO	ICONS	ISWAVE	
,,F.FF,	,,,,I,	,,,,I	
.14	1	0	1
.20	1	0	2
.20	1	0	3
.20	1	0	4
.26	1	0	5

Monthly means of daily hours of sunshine, ASSH(i)

JAN	FEB	MAR	APR	MAY	JUN	JUL	AUG	SEP	OCT	NOV	DEC	
,FF.F,	FF.F,	FF.F,	FF.F,	FF.F,	FF.F,	FF.F,	FF.F,	FF.F,	FF.F,	FF.F,	FF.F	
3.5	5.4	6.1	7.3	8.1	9.0	10.2	8.1	6.2	5.3	3.7	3.5	1
3.5	5.4	6.1	7.3	8.1	9.0	10.2	8.1	6.2	5.3	3.7	3.5	2

```
 3.5  5.4  6.1  7.3  8.1  9.0 10.2  8.1  6.2  5.3  3.7  3.5              3
 3.5  5.4  6.1  7.3  8.1  9.0 10.2  8.1  6.2  5.3  3.7  3.5              4
 3.5  5.4  6.1  7.3  8.1  9.0 10.2  8.1  6.2  5.3  3.7  3.5              5
```

"A" coefficient in Penman equation, ACONS(i)

```
 JAN  FEB  MAR  APR  MAY  JUN  JUL  AUG  SEP  OCT  NOV  DEC
,F.FF,F.FF,F.FF,F.FF,F.FF,F.FF,F.FF,F.FF,F.FF,F.FF,F.FF,F.FF
 .27  .27  .28  .24  .24  .25  .24  .21  .23  .23  .22  .24              1
 .27  .27  .28  .24  .24  .25  .24  .21  .23  .23  .22  .24              2
 .27  .27  .28  .24  .24  .25  .24  .21  .23  .23  .22  .24              3
 .27  .27  .28  .24  .24  .25  .24  .21  .23  .23  .22  .24              4
 .27  .27  .28  .24  .24  .25  .24  .21  .23  .23  .22  .24              5
```

"B" coefficient in Penman equation, BCONS(i)

```
 JAN  FEB  MAR  APR  MAY  JUN  JUL  AUG  SEP  OCT  NOV  DEC
,F.FF,F.FF,F.FF,F.FF,F.FF,F.FF,F.FF,F.FF,F.FF,F.FF,F.FF,F.FF
 .51  .55  .57  .56  .58  .54  .52  .49  .52  .52  .51  .50              1
 .51  .55  .57  .56  .58  .54  .52  .49  .52  .52  .51  .50              2
 .51  .55  .57  .56  .58  .54  .52  .49  .52  .52  .51  .50              3
 .51  .55  .57  .56  .58  .54  .52  .49  .52  .52  .51  .50              4
 .51  .55  .57  .56  .58  .54  .52  .49  .52  .52  .51  .50              5
```

Monthly means of daily incoming radiation, RADMET(i)

```
 JAN  FEB  MAR  APR  MAY  JUN  JUL  AUG  SEP  OCT  NOV  DEC
,FF.F,FF.F,FF.F,FF.F,FF.F,FF.F,FF.F,FF.F,FF.F,FF.F,FF.F,FF.F
 3.8  7.5 13.2 17.9 21.2 20.7 24.1 19.6 13.5  9.0  5.0  3.1              1
 4.1  7.9 13.7 18.3 21.6 21.0 24.5 20.1 14.0  9.4  5.3  3.3              2
 4.2  8.0 13.8 18.4 21.7 21.1 24.6 20.2 14.1  9.5  5.4  3.4              3
 4.0  7.8 13.6 18.4 21.7 21.1 24.6 20.2 14.0  9.3  5.2  3.2              4
 4.0  7.8 13.6 18.4 21.7 21.1 24.6 20.1 14.0  9.3  5.2  3.2              5
```

Penman equation option for either S-tank or A-pan equivalent evaporation

---

```
SAPANC
,,,,,I
   1          1=APAN                                  1
   1                                                  2
   1                                                  3
   1                                                  4
   1                                                  5
```

Smoothed mean monthly A-pan/S-pan ratios, SARAT(i)

```
 JAN FEB MAR APR MAY JUN JUL AUG SEP OCT NOV DEC
,F.FF,F.FF,F.FF,F.FF,F.FF,F.FF,F.FF,F.FF,F.FF,F.FF,F.FF,F.FF
 1.36 1.37 1.35 1.32 1.28 1.27 1.26 1.25 1.26 1.27 1.30 1.34          1
 1.36 1.37 1.35 1.32 1.28 1.27 1.26 1.25 1.26 1.27 1.30 1.34          2
 1.36 1.37 1.35 1.32 1.28 1.27 1.26 1.25 1.26 1.27 1.30 1.34          3
 1.36 1.37 1.35 1.32 1.28 1.27 1.26 1.25 1.26 1.27 1.30 1.34          4
 1.36 1.37 1.35 1.32 1.28 1.27 1.26 1.25 1.26 1.27 1.30 1.34          5

     Pan adjustment option
    ----------------------
PANCOR
,,,,,F
    1                                                    1
    1                                                    2
    1                                                    3
    1                                                    4
    1                                                    5

     Monthly pan adjustment factors, CORPAN(i)
    -----------------------------------------
 JAN FEB MAR APR MAY JUN JUL AUG SEP OCT NOV DEC
,F.FF,F.FF,F.FF,F.FF,F.FF,F.FF,F.FF,F.FF,F.FF,F.FF,F.FF,F.FF
 1.00 1.00 1.00 1.00 1.00 1.00 1.00 1.00 1.00 1.00 1.00 1.00          1
 1.00 1.00 1.00 1.00 1.00 1.00 1.00 1.00 1.00 1.00 1.00 1.00          2
 1.00 1.00 1.00 1.00 1.00 1.00 1.00 1.00 1.00 1.00 1.00 1.00          3
 1.00 1.00 1.00 1.00 1.00 1.00 1.00 1.00 1.00 1.00 1.00 1.00          4
 1.00 1.00 1.00 1.00 1.00 1.00 1.00 1.00 1.00 1.00 1.00 1.00          5

#    Level of soils information
    ---------------------------
PEDINF
,,,,,F
    1                                                    1
    1                                                    2
    1                                                    3
    1                                                    4
    1                                                    5

     Soils texture information
    --------------------------
 ITEXT
,,,,II
    8                                                    1
    8                                                    2
    8                                                    3
    7                                                    4
```

7 5

Soil physics based infiltration/soil water redistribution option

---

REDIST
,,,,,F
0 1
0 2
0 3
0 4
0 5

Rainfall intensity distribution type

IRDIST
,,,,,I
2 1
2 2
2 3
2 4
2 5

Soils information (adequate)

DEPAHO DEPBHO WP1 WP2 FC1 FC2 PO1 PO2 ABRESP BFRESP
,FF.FF,,FF.FF,.FFF,.FFF,.FFF,.FFF .FFF,.FFF,,FF.FF,,FF.FF
.15 .42 .160 .194 .369 .348 .404 .467 .50 .85 1
.16 .16 .135 .171 .298 .336 .440 .465 .52 .85 2
.15 .23 .160 .114 .330 .255 .449 .453 .50 .90 3
.15 .24 .153 .169 .331 .341 .432 .466 .49 .85 4
.15 .24 .142 .161 .314 .320 .427 .464 .52 .85 5

Shrink-swell soils option

ICRACK
,,,,,I
0
0
0
1
1

Initial values of soil water retention constants

SMAINI SMBINI

```
,FFF.FF,FFF.FF
  50.00  50.00                                          1
  50.00  50.00                                          2
  50.00  50.00                                          3
  50.00  50.00                                          4
  50.00  50.00                                          5

     Option for statistical analysis of soil water regime
     ----------------------------------------------------
SWLOPT
,,,,,F
     1                                                  1
     1                                                  2
     1                                                  3
     1                                                  4
     1                                                  5

     Soil water content thresholds for A horizon, SWLAM(i)
     -----------------------------------------------------
   1      2      3      4      5      6
,,F.FFF,,F.FFF,,F.FFF,,F.FFF,,F.FFF,,F.FFF
   .018   .050   .100   .150   .200   .300                 1
   .018   .050   .100   .150   .200   .300                 2
   .018   .050   .100   .150   .200   .300                 3
   .018   .050   .100   .150   .200   .300                 4
   .018   .050   .100   .150   .200   .300                 5

     Soil water content thresholds for B horizon, SWLBM(i)
     -----------------------------------------------------
   1      2      3      4      5      6
,,F.FFF,,F.FFF,,F.FFF,,F.FFF,,F.FFF,,F.FFF
   .018   .050   .100   .150   .200   .300                 1
   .018   .050   .100   .150   .200   .300                 2
   .018   .050   .100   .150   .200   .300                 3
   .018   .050   .100   .150   .200   .300                 4
   .018   .050   .100   .150   .200   .300                 5

#    Level of land cover information
     -------------------------------
LCOVER
,,,,,I
     1                                                  1
     1                                                  2
     1                                                  3
     1                                                  4
     1                                                  5
```

Land cover number information

CROPNO
,,,FFFFFFF

0	1
0	2
0	3
0	4
0	5

Determination of canopy interception loss

INTLOS
,,,,,I

3	1
3	2
3	3
3	4
3	5

Leaf area index information

LAIND
,,,,,I

1	1
1	2
1	3
1	4
1	5

Monthly means of crop coefficients, CAY(i)

JAN	FEB	MAR	APR	MAY	JUN	JUL	AUG	SEP	OCT	NOV	DEC	
,F.FF	F.FF	F.FF	F.FF	F.FF	F.FF	F.FF	F.FF	F.FF	F.FF	F.FF	F.FF	
.50	.50	.50	.72	.90	1.05	1.15	1.15	1.01	.87	.63	.50	1
.50	.50	.55	.60	.76	1.05	1.13	1.13	1.00	.88	.62	.50	2
.50	.50	.52	.60	.76	1.10	1.15	1.14	1.02	.95	.62	.50	3
.50	.50	.50	.50	.79	1.08	1.13	0.93	0.84	.60	.50	.50	4
.50	.50	.50	.50	1.08	1.16	1.10	0.61	0.59	.55	.50	.50	5

Monthly means of leaf area index, ELAIM(i)

JAN	FEB	MAR	APR	MAY	JUN	JUL	AUG	SEP	OCT	NOV	DEC	
,F.FF	F.FF	F.FF	F.FF	F.FF	F.FF	F.FF	F.FF	F.FF	F.FF	F.FF	F.FF	
1.26	1.26	1.26	1.53	2.34	3.00	2.91	2.86	2.20	1.63	1.26	1.26	1

.24	.24	.24	.89	1.43	1.63	1.42	1.29	1.09	1.11	.24	.24	2
.08	.08	.08	.79	1.29	1.42	1.20	1.06	0.92	1.03	.08	.08	3
.00	.00	.00	.44	.81	1.98	2.30	1.78	.50	.59	.00	.00	4
.00	.00	.00	.00	.20	3.00	4.15	3.05	.00	.00	.00	.00	5

Fraction of active root system in topsoil horizon, ROOTA(i)

JAN	FEB	MAR	APR	MAY	JUN	JUL	AUG	SEP	OCT	NOV	DEC	
,F.FF	F.FF	F.FF	F.FF	F.FF	F.FF	F.FF	F.FF	F.FF	F.FF	F.FF	F.FF	
.80	.80	.80	.75	.70	.60	.60	.60	.60	.70	.75	.80	1
.90	.90	.90	.85	.75	.68	.68	.68	.68	.73	.83	.90	2
1.00	1.00	1.00	.95	.80	.75	.75	.75	.75	.75	.90	1.00	3
1.00	1.00	1.00	.95	.80	.75	.75	.75	.75	.75	.90	1.00	4
1.00	1.00	1.00	.95	.80	.75	.75	.75	.75	.75	.90	1.00	5

Effective total rooting depth

EFRDEP	
FFF.FF	
.00	
.00	
.00	
.00	
.00	

Total evaporation control variables

EVTR	FPAW	
,,,,F	,,,F	
2	0	1
2	0	2
2	0	3
2	0	4
2	0	5

Fraction of PAW at which plant stress sets in

CONST	
FF.FF	
.25	1
.25	2
.25	3
.25	4
.25	5

Critical leaf water potential

CRLEPO CRLEPO
FFFFF.F FFFFF.F
-800.0 -1000.0 1
-800.0 -1000.0 2
-800.0 -1000.0 3
-800.0 -1100.0 4
-800.0 -1200.0 5

Option for enhanced wet canopy evaporation

FOREST
,,,,,F
1 1
0 2
0 3
0 4
0 5

Mean temperature threshold (øC) for active growth to take place

---

TMPCUT
,,FF.F
2.0 1
2.0 2
2.0 3
2.0 4
2.0 5

Unsaturated soil moisture redistribution

IUNSAT
,,,,,I
1 1
1 2
1 3
1 4
1 5

Streamflow simulation control variables

QFRESP COFRU SMDDEP IRUN ADJIMP DISIMP STOIMP
,FF.FF,,,F.FFF,FFF.FF,,,,I,,F.FFF,,F.FFF,,,F.FF

.08	.050	.40	1	.003	.000	2.00	1
.05	.035	.25	1	.003	.000	2.00	2
.05	.030	.25	1	.003	.000	2.00	3
.03	.030	.25	1	.000	.000	1.00	4
.03	.030	.25	1	.000	.000	1.00	5

Coefficient of initial abstraction, COIAM(i)

JAN	FEB	MAR	APR	MAY	JUN	JUL	AUG	SEP	OCT	NOV	DEC	
,F.FF	F.FF	F.FF	F.FF	F.FF	F.FF	F.FF	F.FF	F.FF	F.FF	F.FF	F.FF	
.10	.10	.10	.15	.30	.35	.35	.35	.35	.35	.30	.15	1
.03	.03	.03	.05	.25	.25	.25	.25	.25	.20	.10	.05	2
.03	.03	.03	.05	.25	.25	.25	.25	.25	.20	.10	.05	3
.03	.03	.03	.05	.15	.20	.20	.20	.20	.15	.10	.05	4
.03	.03	.03	.05	.15	.20	.20	.20	.20	.15	.10	.05	5

B.2 ACRUSNOW MENU File

- ISNOW: variable that specifies whether snow modelling is incorporated into model application -> Yes or No=1 or 2 (I1)
1
- ISNOTP: specifies which method is applied for determination of precipitation form -> 1, 2 or 3 (I1)
4
- IPSCOR: specifies which method is applied for correction of systematic error of snow and mixed precipitation -> 1,2 or 3 (I1)
0
- ISCREE: indicates degree of screening at rainfall station 1,2,3 or 4 (I1)
4
- TPCRIT(I)[°C]: critical (base) temperature indicating transformation from rain and snow precipitation (12(F5.1,1x))
10.0 10.0 6.0 5.0 2.5 2.5 2.5 2.5 2.5 2.5 3.5 3.5
- TRANGE [°C]: Temperature Range within which a proportion of precip falls as rain
7.0 7.0 10.0 10.0 9.0 2.0 0.0 0.0 6.0 12.0 12.0 9.0
- ADJ(I): adjustment factor for rain portion of mixed precipitation (12(4.2,1x))
1.00 1.00 1.00 1.00 1.00 1.00 1.00 1.00 1.00 1.00 1.00 1.00
- TMAXSN(I): maximum temperature for snow generation; if TMAXD.gt.TMAXSN all precipitation is regarded as rain °C (12(F5.1,1x))
7.5 9.0 9.0 9.0 7.5 7.5 7.5 7.5 10.0 10.0 10.0 7.5
- IEXP: specifies subcatchments with inclined surface (for temperature adjustment on inclined surface) -> 0 (No) or 1 (Yes) (I1)
0
- TMNADJ(I) (for sloping catchments only): minimum temperature adjustment value for sloping surfaces °C (12(F5.1,1x))
0.0 0.0 0.0 0.0 0.0 0.0 0.0 0.0 0.0 0.0 0.0 0.0
- TMXADJ(I) (for sloping catchments only): maximum temperature adjustment value for sloping surfaces °C (12(F5.1,1x))

0.0 0.0 0.0 0.0 0.0 0.0 0.0 0.0 0.0 0.0 0.0 0.0
- IFOR: specification whether the subcatchment under consideration is under forest (1=yes,0=no)(I1)
0
- ICC(I)[%] (for forest catchments only): monthly values for canopy coverage (12(I3,1x))
50 50 50 50 60 75 80 80 70 55 50 50
- SNCAPI (for forest catchments only): canopy interception capacity for snow (F4.2)
0.20
- CORPS(I) monthly systematic error correction values for snow precipitation
if IPSCOR.eq. 1 => adjustment factor decimal]; if IPSCOR .eq. 2 => additive term [mm] (12(F5.2,1x))
1.30 1.30 1.30 1.30 1.30 1.30 1.30 1.30 1.30 1.30 1.30 1.30
- SNORC: initial fraction of liquid water retention capacity of new snow pack (e.g. 0.10 = 10%)(F4.2)
0.10
- SNIRC: initial fraction of liquid water retention capacity of intercepted snow (e.g. 0.05 = 5%)(F4.2)
0.05
- TMCRIT(I)[°C]: critical temperature for onset of melt (12(F5.1,1x))
0.0 0.0 0.0 0.0 0.0 0.0 0.0 0.0 0.0 0.0 0.0 0.0
- MCMOD: indicator for continuous daily modification of melt coefficient SNOMC -> Yes (1) or NO (0) (I1)
1
- SNOMC(I)[mm/°C*d]: melt factor for open areas (12(F4.2,1x))
3.00 3.00 5.00 2.00 2.00 2.00 2.00 2.00 2.00 3.00 3.00 3.00
- SNEREL(I) [fraction]: portion of snow stores upper 5 cm WE that can be evaporated at max (12(F5.3,1x))
0.025 0.025 0.030 0.040 0.045 0.050 0.050 0.050 0.045 0.040 0.035 0.030
- SNCC: complete surface snow coverage factor (F5.2) 75.00

APPENDIX C

ACRU Input Variable Directory

ABRESP = Fraction of "saturated" soil water to be redistributed daily from the topsoil into the subsoil when the topsoil is above its drained upper limit.

e.g. 0.1 is slow, typical of clays
0.8 is fast, typical of sands
Default value = 0.5

ACONS(I) = Locally determined monthly values of the a-constant for estimation of incoming radiation flux densities from sunshine duration information (If *ICONS* = NO, *EQPET* = 103 or 104).

ADJIMP = Fraction of the catchment occupied by adjunct impervious areas, i.e. areas joined (connected) directly to a watercourse, from which precipitation contributes directly to quickflow. The precipitation falling on the adjunct impervious area has no effect on the soil moisture budget of the remaining catchment area.

ALAT = Latitude of the centre of the catchment/subcatchment (degrees and minutes of a degree).

ALBEDO = Reflection coefficient of incoming shortwave radiation fluxes, required when EQ*PET* = 103 or 104. Depends on surface cover, season,wetness. To estimate *Er* *ALBEDO* = Default value = 0.07 (=7%) because A-pan equivalent is required.

ALONG = Longitude of the centre of the catchment/subcatchment (degree and minutes of a degree).

ALPHA = Runoff erosivity constant ("*sy*) in M.U.S.L.E.

ALTH = Altitude (m above sea level) of highest elevation upstream of simulation site

ALTIR = Altitude (m above sea level) of nearest receiving water body (stream, lake, wetland, drainage canal etc.), that is situated downstream of simulation site.

ALTIS = Altitude (m above sea level) of centre of the simulation site.

ARCAP = Variable to specify whether or not a predetermined surface area : storage volume relationship exists for use in the reservoir yield analysis *ARCAP* = 0 area : volume relationship is available; variables *RESCON*, *RESEXP* are therefore to be specified > 0 no area : volume relationship is available; variables *RESCON, RESEXP* are therefore to be calculated internally in *ACRU* from other input information and selected default reservoir shapes.

ASSH(I) = Mean daily sunshine duration (hours and fractions) for each month, required when *EQPET* = 104 or 107.

BCONS(I) = Locally determined monthly values of the b-constant for estimation of incoming radiation flux densities from sunshine duration information (If *ICONS* = NO, *EQPET* = 103 or 104).

BETA = Runoff erosivity exponent ($*sy*) in M.U.S.L.E.

BFRESP = Fraction of "saturated" soil water to be redistributed daily from the subsoil into the intermediate/groundwater store when the subsoil is above its drained upper limit.
e.g. 0.1 is slow, typical of clays
0.8 is fast, typical of sands
Default value = 0.5

CAY(I) = Average monthly crop coefficients, *Kcm* , for the pervious land cover of catchment/subcatchment (i.e. the proportion of water "consumed" by a plant under conditions of maximum evaporation in relation to that evaporated by an A-pan in a given period).

CLAREA = Area of the catchment/subcatchment (km2).

CORPAN(I) = Monthly adjustment factors to be applied to evaporation pan data set to correct for screening and systematic errors (if *PANCOR* = YES). e.g. If the pan value has to be corrected up by 10% in January then *CORPAN(1)* = 1.10.

CORPPT(I) = Rainfall adjustment factors, given month-by-month, by which the daily point rainfall input data are adjusted, to give a more representative catchment/subcatchment rainfall (If *PPTCOR* = 1 or 2). e.g. (a) If *PPTCOR* = 1 and if the catchment's rainfall is >station's rainfall by 8% in March then *CORPPT(3)* = 1.08, or (b) if *PPTCOR* = 2 and if the measured rainfall on
each day with rain in May is consistently lower at the station than the actual rainfall by 2 mm, then
CORPPT(5) = -2.0.

CRLEPO = Critical leaf water potential of the vegetation type, input in negative kPa (if *FPAW* = YES). *CRLEPO* for maize : = -1700 kPa for grass : = -1000 kPa.

DEPAHO = Thickness (m) of the topsoil of the soil profile.

DEPBHO = Thickness (m) of the subsoil of the soil profile.

DEPIMP = Depth of impervious layer (m), i.e. the bottom of the aquifer, below simulation site.

DEPROT = Maximum depth of (tap) roots (mm), which extend beyond the Bhorizon into the intermediate zone.

DISIMP = Fraction of the catchment occupied by impervious areas which are not adjacent to a watercourse (e.g. house roofs discharging onto lawn).Precipitation falling on this impervious area thus does not contributes directly to streamflow, but is assumed to re-infiltrate on the remaining pervious portion of the catchment. The precipitation falling on disjunct impervious areas thus have an effect on the soil moisture budget of the remaining catchment area.

DISTA = Distance (m) between centre of simulation site and highest elevation upstream of simulation site.

DISTR = Distance (m) between centre of simulation site and nearest receiving water body.

DNAMIC = NO no dynamic input file to be used (i.e. *IDYNFL* left blank) = YES dynamic input file is to be invoked (i.e.
assign file name to *IDYNFL*).

EFRDEP = Effective root depth (m), defaulted to (*DEPAHO+DEPBHO*). If an

EFRDEP < (*DEPAHO+DEPBHO*), this overrides the total soil depth used in soil water budgeting.

ELAIM(I) = Monthly mean value of leaf area index (if *LAIND* = 1).

ELAMD1..3 = Stress coefficients (lambda values) for the phenological (growth) stages used in the *ACRU* maize yield model, i.e. a weighting coefficient to account for the relative importance of *Et/Etm* during each growth stage.

ELEV = Average altitude (m) above mean sea level of the catchment/subcatchment.

EQPET = Variable to specify which method is to be used to derive reference potential evaporation (*Er*), where the reference is daily A-pan equivalent evaporation.

EQPET = 100 The expert system on reference potential evaporation will decide, on day-by-day basis, which is the best method to estimate *Er* , based on the input information available on that day

EQPET > 100 The user has the option to choose manually by which method *Er* is to be derived, thus "over-riding" the expert system
= 101 Daily observed A-pan equivalent evaporation (unscreened)
= 102 Monthly totals of daily A-pan equivalent evaporation (unscreened)

= 103 PENMAN (1948) equation - daily input
= 104 PENMAN (1948) equation – monthly input
= 105 HARGREAVES & SAMANI (1982) equation - daily input with sunshine calibration
= 106 HARGREAVES & SAMANI (1985) equation - daily input using temperature data only
= 107 HARGREAVES & SAMANI (1982) equation - monthly input with sunshine calibration
= 108 HARGREAVES & SAMANI (1985) equation - monthly input using temperature values only
= 109 LINACRE (1991) equation – daily temperature input
= 110 LINACRE (1991) equation – monthly temperature input
= 111 LINACRE (1984) equation – daily temperature input
= 112 LINACRE (1984) equation – monthly temperature input
= 113 LINACRE (1977) equation – monthly temperature input
= 114 BLANEY & CRIDDLE (1950) equation - monthly temperature input
= 115 THORNTHWAITE (1948) equation - monthly temperature input.

EVTR = Option for estimation of total evaporation as an entity or by soil water evaporation (*Es*) and plant transpiration (*Et*) computed separately.

EVTR = 1 Es + Et are calculated as an entity = 2 Es + Et are calculated separately.

FC1 = Soil water content (m.m-1) at drained upper limit for the topsoil.

FC2 = Soil water content (m.m-1) at drained upper limit for the subsoil.

FCIZ = Soil water content (m.m-1) at drained upper limit (field capacity) for the intermediate zone.

FOREST = Variable to specify whether or not to simulate wet canopy evaporation at an enhanced rate, which occurs under forest conditions, and to inform *ACRU* that the *EUCDYGEN* dynamic file generator has been used to create the dynamic file used in the *Eucalyptus grandis* timber yield model.

FOREST = 0 wet canopy evaporation at potential rate (for short vegetation) = 1 enhanced wet canopy evaporation if forest covers > 50 % of (sub)catchment = 2 *Eucalyptus grandis* timber yield model is selected, including enhanced wet canopy evaporation (dynamic file created by *EUCDYGEN* dynamic file generator).

FORMAT = Option to specify the format by which the daily climatic and other data are read into the program.

FORMAT = COMPOSITE multi-variable format which can contain a range of daily climatic and other data = SINGLE single variable format by which only daily rainfall

(or alternatively, only daily streamflow, if *ISTRMF*=) data are read in.
FPAW = Option to select method to detect onset of plant stress. *FPAW* = YES use *CRLEPO* to detect onset of plant stress = NO use *CONST* to detect onset of plant stress.

HEAD = General heading/title for the particular catchment, subcatchment, location or simulation run in order to identify the run.

ICELL = Option to specify the mode of simulation, i.e. whether the model is to simulate at a point, for a lumped catchment, or operate in distributed mode as a series of cell-linked subcatchments.
ICELL = NO operate in lumped catchment/point location mode = YES operate in distributed catchment mode.

ICELLN = The number of the subcatchment under consideration when the model is operated in distributed mode (NB: The numbering has to be sequential, increasing downstream).

ICONS = Variable to specify whether default constant values (constants *ACONS(I)* and *BCONS(I)*) are to be used in the Penman equation for potential evaporation when solar radiation is estimated from sunshine data. *ICONS* = NO locally determined constants to be used = YES default values for constants to be used.

ICRACK = Option to account for cracking soils (*ICRACK*#3), based on the clay contents of the soil. *ICRACK* = 0 cracking soils not taken into consideration > 0 cracking soils are accounted for.

IDOMR = Option to invoke abstractions from a river for purposes other than for irrigation (e.g. for domestic or industrial use). *IDOMR* = NO no abstractions (other than for irrigation) from the river = YES abstractions from a river take place (other than for irrigation).

IDSTRM = The number of the subcatchment immediately downstream of the subcatchment under consideration, when the model is operated in distributed mode.

IEIF = Control flag, to indicate the availability of mean monthly A-pan equivalent reference evaporation. *IEIF* = NO mean monthly A-pan equivalent reference potential evaporation values
not available = YES mean monthly A-pan equivalent reference potential evaporation values are available.

IGWATR = Option to request the simulation of shallow groundwater components, i.e. the simulation of the water budget of the intermediate zone, including transpiration via tap roots, water table fluctuation and water table drawdown. This routine has been developed to be applied in areas with a homogeneous aquifer and with deep sandy soils (as in Northeastern Kwazulu-Natal). *IGWATR* = NO no shallow groundwater simulation
IGWATR = YES shallow groundwater simulation required.

IHEMI = Indicator whether the catchment/subcatchment is in the northern or southern hemisphere. *IHEMI* = NORTH Northern hemisphere = SOUTH Southern hemisphere.

ILRF = Control flag, to indicate whether an altitudinal correction of temperature is required. *ILRF* = NO altitudinal correction of temperature not required = YES altitudinal correction of temperature required.

INCELL = Variable to specify whether, when irrigation takes place, it is applied within the (sub)catchment under consideration or not. *INCELL* = NO irrigation is applied outside of the (sub)catchment = YES irrigation is applied within the (sub)catchment.

INTLOS = Option to select method of determining plant canopy interception loss.*INTLOS* = 1 interception loss determined using *VEGINT(I)*= 2 interception loss determined event-byevent by the Von Hoyningen-Huene equation using *ELAIM(I)* = 3 interception loss determined indirectly by the Von Hoyningen-Huene equation using *CAY* if *ELAIM(I)* values are not available.
IOBOVR = Option to use observed streamflow data (if available, i.e. when *IOBSTQ* = YES) as streamflow input to the downstream subcatchment instead of using simulated inflow to the downstream subcatchment. This allows for the self-correction of streamflow as the simulation cascades downstream. *IOBOVR* = NO simulated streamflow values "flow" into the downstream subcatchment = YES observed streamflow values "flow" into the downstream subcatchment.

IOBSPK = Variable which specifies availability of observed daily values of peak discharge *IOBSPK* = NO no observed values are available = YES observed values are available (*FORMAT*=COMPOSITE).

IOBSTQ = Variable which specifies availability of observed daily values of streamflow volume. *IOBSTQ* = NO no observed values are available = YES observed values are available (*FORMAT*=COMPOSITE or *FORMAT*=SINGLE).

IPNF = Control flag, to indicate whether the Penman equation should be invoked. *IPNF* = NO Penman equation not invoked = YES Penman equation invoked.

IQUAD = Indicator whether the catchment/subcatchment is to the east or west of Greenwich *IQUAD* = EAST longitude east of Greenwich = WEST longitude west of Greenwich.

IRAINF = File name, including path, assigned to the daily hydrometeorological or rainfall (only) data input file relevant to the particular catchment/subcatchment, i.e. the file name may refer to either an *ACRU* single format file or an *ACRU* composite format file.

IRANK = Selection of variable on which extreme value analysis is to be undertaken using the Annual Maximum Series. *IRANK* = 1 maximum daily rainfall (mm) = 2 maximum daily observed streamflow depth (mm) = 3 maximum daily simulated streamflow depth

(mm)= 4 maximum daily observed peak discharge (m3.s-1)= 5 maximum daily simulated peak discharge (m3.s-1).

IRDF = Control flag, to indicate the availability of mean monthly radiation flux densities . *IRDF* = NO radiation flux density information is not *IRDF* = YES radiation flux density information is available.

IRDIST = Rainfall intensity distribution type 1, 2, 3 or 4 as delineated for southern Africa (cf. *ACRU* Theory Chapter 12; Section 6.16 of *ACRU* User Manual).

IRHF = Control flag, to indicate the availability of mean monthly relative humidity information. *IRHF* = NO relative humidity information is not available = YES relative humidity information is available.

IRRPED = Option to specify that, in addition to soil textural information, soil water retention values for the drained upper limit, permanent wilting point and saturation are available.

IRRPED = NO soil water retention values are not available = YES values for the irrigated soil's permanent wilting point, drained upper limit and saturation are available. If *IRRPED* = NO values for the irrigated soil's permanent wilting point, drained upper limit and saturation are derived from the irrigated soil's textural class using information preprogrammed in the *Menubuilder*.
IRSPLY = Variable to specify from which catchment number (*ICELLN*) irrigation water is supplied when operating in the "loopback" mode (*LOOPBK* = YES)

IRUN = Variable to request the exclusion or inclusion of baseflow from the simulation of streamflow. *IRUN* = NO baseflow excluded from the simulated streamflow (i.e. streamflow = stormflow only) = YES baseflow included in streamflow (i.e. simulated streamflow = stormflow + baseflow). Default input = YES, i.e. 1.

ISNF = Control flag, to indicate the availability of mean monthly sunshine duration information. *ISNF* = NO sunshine duration information is not available *ISNF* = YES sunshine duration information is available.

ISTRMF = File name assigned to the observed daily streamflow input file for a particular catchment/subcatchment. (NB: applicable only if a separate streamflow data file exists, in which case *FORMAT* = SINGLE).

ISUBNO = Total number of subcatchments making up the catchment.

ISWAVE = Specification whether incoming shortwave radiation input is available from observations or has to be estimated from sunshine duration information in the Penman monthly potential evaporation equation.

ISWAVE = NO adjusted mean daily radiation flux densities are available from observation for each month (*RADMET(I)*) = YES radiation input has to be estimated in the program by using sunshine duration information.

ITEXT = Soil texture classes for which soil water retention constants, redistribution rates and other information are preprogrammed in the *Menubuilder*.
ITEXT = 1 clay
= 2 loam
= 3 sand
= 4 loamy sand
= 5 sandy loam
= 6 silty loam
= 7 sandy clay loam
= 8 clay loam
= 9 silty clay loam
= 10 sandy clay
= 11 silty clay.

IUNSAT = Request to include redistribution of unsaturated soil water (both downwards and upwards, i.e. capillary action) in the soil water budgeting routines. *IUNSAT* = NO unsaturated soil water redistribution not requested. = YES unsaturated soil water redistribution to be included.

IWDF = Control flag, to indicate the availability of mean monthly windspeed data. *IWDF* = NO windspeed data are not available = YES windspeed data are available.

IYREND = The year, on the first day of which, the simulation run will terminate. A blank will end the simulation in the last month of available input data in the file.

IYSTRT = The first year of a rainfall/hydrometeorological data series to be used in a simulation run. A blank will start the simulation in the first month of available input data in the file.

IZTEXT = Soil texture classes for the intermediate zone. The height of the associated capillary fringe is computed from this information by the *Menubuilder*. *IZTEXT* = 0 default to texture of the surface soil
(*ITEXT*)
= 1 clay
= 2 loam
= 3 sand
= 4 loamy sand
= 5 sandy loam
= 6 silty loam
= 7 sandy clay loam
= 8 clay loam
= 9 silty clay loam

= 10 sandy clay
= 11 silty clay

LAG = Option to specify which method is to be used to estimate catchment lag, a variable required for peak discharge computations. *LAG* = 1 lag is calculated using the original SCS Equation = 2 lag is calculated using the Schmidt/Schulze equation = 3 lag is calculated from the catchment time of concentration (*TCON*).

LAIND = Option to indicate what leaf area index (LAI) information is available for the land use/crop in question. *LAIND* = 0 no LAI information is available = 1 monthly LAI information available and specified in *ELAIM(I)* = 2 daily LAI information, *ELAID(K)*, available and specified in the daily hydrometeorological input file (*FORMAT* = COMPOSITE, *IRAINF* =).

LCOVER = Option to specify whether manually input or default values are to be used with regard to land cover information in the *Menubuilder*. *LCOVER* = 0 default values to be used = 1 actual values of *CAY(I)*, *ROOTA(I)*, *ELAIM(I)* (optional) and *VEGINT(I)* to be given.

LENGTH = Length of the growing season (days) for a crop (if *CROP* = 1 or *CROP* = 3).

LINWIN = Wind coefficient for the Linacre (1977) reference potential evaporation equation, required when *EQPET* = 113. In southern Africa this coefficient can be input by specifying a wind region number, with wind regions delineated by Dent, Schulze and Angus (1988). Monthly wind coefficients are preprogrammed into *ACRU* for each mapped region in southern Africa. *LINWIN* = 0 wind region unknown, e.g. when simulating outside of southern Africa (default wind coefficient = 15 is used) *LINWIN* = 1 - 7 select wind region for southern Africa from map.

LRREG = Adiabatic lapse rate region number. Southern Africa has been delineated into 12 lapse rate regions by Schulze and Maharaj (1994). Monthly lapse rates for maximum and minimum temperatures are preprogrammed into *ACRU* for each mapped region in southern Africa. *LRREG* = 0 if simulating outside of southern Africa, but a lapse rate is required (i.e. *ILRF* =1)

LRREG = 1 - 12 if simulating in southern Africa and a regional lapse rate is required (*ILRF* = 1).

LYSIM = Option to simulate the water budget of an internally drained area, including that of a lysimeter. NB: The stormflow generated when this "lysimeter" option is used, is re-infiltrated. *LYSIM* = NO stormflow is generated and flows out of (sub)catchment = YES stormflow is re-infiltrated into soil and no stormflow flows out of (sub)catchment or lysimeter.

MAP = Mean Annual Precipitation (mm) for (sub)catchment.

MAXSUB = Number of the last subcatchment (*ICELLN*) to be processed in a particular run. e.g. If only the first 3 subcatchments of a catchment with 8 subcatchments (*ISUBNO* = 8) are to be processed, then *MAXSUB* = 3.

MINSUB = Number of the first subcatchment (*ICELLN*) to be processed in a particular run. e.g. If the first 3 subcatchments of a catchment with 8 subcatchments (*ISUBNO* = 8) are to be excluded, then *MINSUB* = 4.

PANCOR = Option to request monthly pan evaporation adjustment factors. *PANCOR* = 0 no adjustment factors to be applied = 1 adjustment factor to be applied to all evaporation values, by multiplication with monthly factors to be given in *CORPAN(I)* *PANCOR* = 2 adjustment factor applied to estimated evaporation values only and not to observed values, when the evaporation data set contains both observed and estimated values.

PEAK = Option to request the estimation of peak discharge. *PEAK* = NO no peak discharge estimate required *PEAK* = YES peak discharge estimate required.

PEDDEP = Default values to approximate soil horizon thicknesses (in m, if *PEDINF* = NO). Depth classes for use in the *ACRU Menubuilder*:

PEDINF = Adequacy of soils information (i.e. whether soil water retention and soil horizon thickness information is available or if only soil textural classes and default depths are to be used to generate soils input). *PEDINF* = NO inadequate soils information is available (i.e. only *ITEXT* and *PEDDEP* need to be input) = YES adequate soils information is available (i.e. values of *WP1, WP2, FC1, FC2, PO1, PO2, DEPAHO, DEPBHO, ABRESP* and *BFRESP* must be given).

PO1 = Soil water content (m.m-1) at saturation (i.e. porosity) for the topsoil.

PO2 = Soil water content (m.m-1) at saturation (i.e. porosity) for the subsoil.

PPTCOR = Option to denote that the point rainfall data from the station which was selected requires adjustment in order to represent the (sub)catchment areal rainfall more realistically. If *PPTCOR* is requested, daily rainfall values are converted by a factor *CORPPT(I)*, which can vary month-by-month. *PPTCOR* = 0 no correction to be applied = 1 adjustment to be applied by multiplication of a factor *CORPPT(I)* = 2 adjustment by addition or subtraction of a constant value *CORPPT(I)* because of a systematic error in the raingauge recording.

QFRESP = Stormflow response fraction for the catchment/subcatchment, i.e. the fraction of the total stormflow (#1.0) that will run off from the catchment/subcatchment on the same day as the rainfall event.

RADMET(I) = Mean daily shortwave radiation flux densities (MJ.m-2) for each month (if *ISWAVE* = NO, *EQPET* = 104).

RH(I) = Monthly means of daily average relative humidity (%), required when *EQPET* = 104

ROOTA(I) = Fraction of effective root system in the topsoil horizon, specified month-by-month.

SAPANC = Option to indicate whether S-tank or A-pan equivalent evaporation estimates are required from the Penman equation (if *IPNF*=YES). *SAPANC* = NO S-tank equivalent evaporation
estimates required = YES A-pan equivalent evaporation estimates required.

SARAT(I) = Smoothed mean monthly A-pan/S-tank evaporation ratios, required when *EQPET* = 103 or 104.

SLOPE = Average slope (%) of catchment/subcatchment (if *LAG* = 1 or 2).

SMAINI = Soil water content of the topsoil at the start of the simulation, expressed as a percentage of plant available water capacity (PAWC), e.g. 100 if at drained upper limit, 0 if at permanent wilting point.

SMBINI = Soil water content of the subsoil at the start of the simulation, expressed as a percentage of PAWC.

SMDDEP = Effective (critical) depth of the soil (m) from which stormflow generation takes place. *SMDDEP* = 0 effective depth is not known and is defaulted to be the thickness of the topsoil horizon (*DEPAHO*) > 0 effective depth is as specified (m).

STOIMP = Surface storage capacity (i.e. depression storage, or initial abstraction) of impervious surface, which needs to be filled before stormflow commences. For example, it could be assumed that tarmac has a storage of (say) 1 mm, after which stormflow from the impervious surface commences. The storage is dynamic and is depleted as a result of evaporative demand.

SWLAM(I) = SWC thresholds for the topsoil, used to define class intervals in order to perform a frequency analysis of the SWC in each interval (if *SWLOPT* = YES).

SWLBM(I) = SWC thresholds for the subsoil, used to define class intervals in order to perform a frequency analysis of the SWC in each interval (if *SWLOPT* = YES).

SWLOPT = Option for the frequency analysis of Soil Water Contents (SWC) of top- and subsoil horizons to be undertaken. *SWLOPT* = NO no frequency analysis is performed. = YES frequency analysis of SWC performed.

TCON = Time of concentration (h) (if *LAG* = 3).

TELEV = Altitude (m) of the base temperature station, values from which will undergo a temperature : altitude adjustment (using regional lapse rates) to account for the (sub)catchment temperatures being different to those of the base station (required if *ILRF* = 1).

TMAX(I) = Monthly means of daily maximum temperatures (EC), adjusted if necessary for slope/aspect. NB : altitude correction for temperature is optional (cf. *ILRF* flag).

TMAXLR = Mean regional lapse rate (+/-EC.1000m-1) for maximum temperature. Where no regional lapse rates are known, default is -6.2EC.1000m-1 altitude. Required if *LRREG* = 0. The lapse rate is usually a negative value, indicating a decrease in temperature with altitude.

TMIN(I) = Monthly means of daily minimum temperatures (EC), adjusted if necessary for slope/aspect. NB : altitude correction for temperature is optional (cf. *ILRF* flag).

TMINLR = Mean regional lapse rate (+/-EC.1000m-1) for minimum temperature. Where no regional lapse rates are known, default is -6.2EC.1000m-1 altitude. The lapse rate is usually a negative value, indicating a decrease in temperature with altitude. Required if *LRREG* = 0.

TMPCUT = Threshold mean daily temperature (oC), above which active transpiration takes place.

VEGINT(I) = Interception loss (mm.rainday-1) by vegetation, given month-by month.

WIND(I) = Monthly means of the daily windrun (km.day-1), required when *EQPET* = 104, 109, 110, 111 or 112 (if *IWDF* = YES, i.e. 1)

WNDSPD = Mean daily windspeed in m.s-1, required when *EQPET* = 109, 110, 111 or 112 (if *IWDF* = NO i.e. 0). Typically 1.6 m.s-1. *WNDSPD* > 0 if windspeed (m.s-1) is known = 0 value of windspeed is not known and a default value of 1.6 m.s-1 is to be used.

WP1 = Soil water content (m.m-1) at permanent wilting point for the topsoil.

WP2 = Soil water content (m.m-1) at permanent wilting point for the subsoil.